The structure of the proton….

…….and its relevance for LHC physics

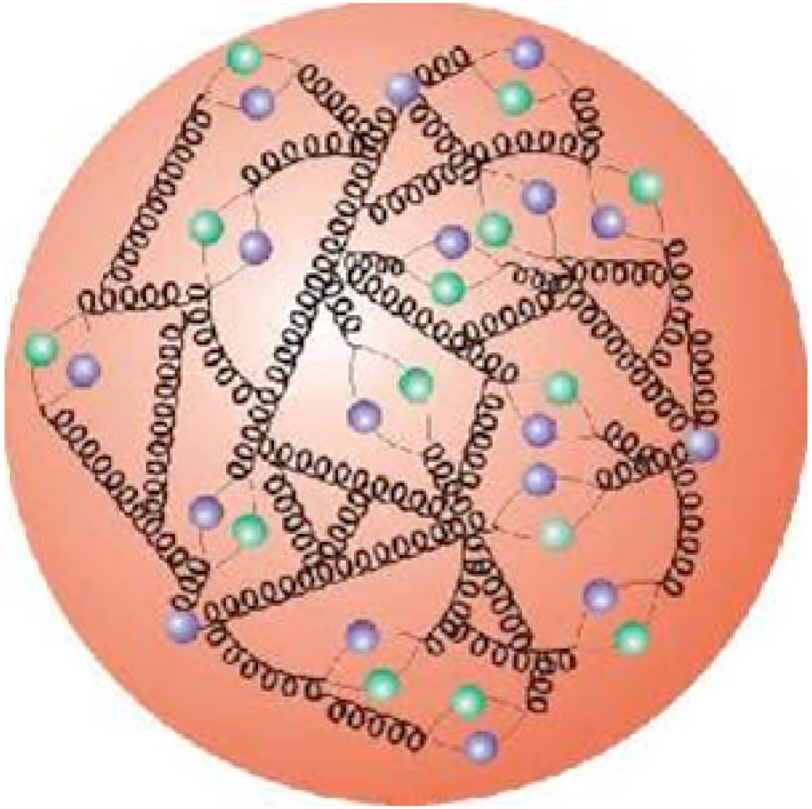

Alghero 6/6/2008 Gigi.Rolandi@cern.ch

Acknowledgments : E. Perez, A. Martin, A de Roeck.

LHC is cooling down

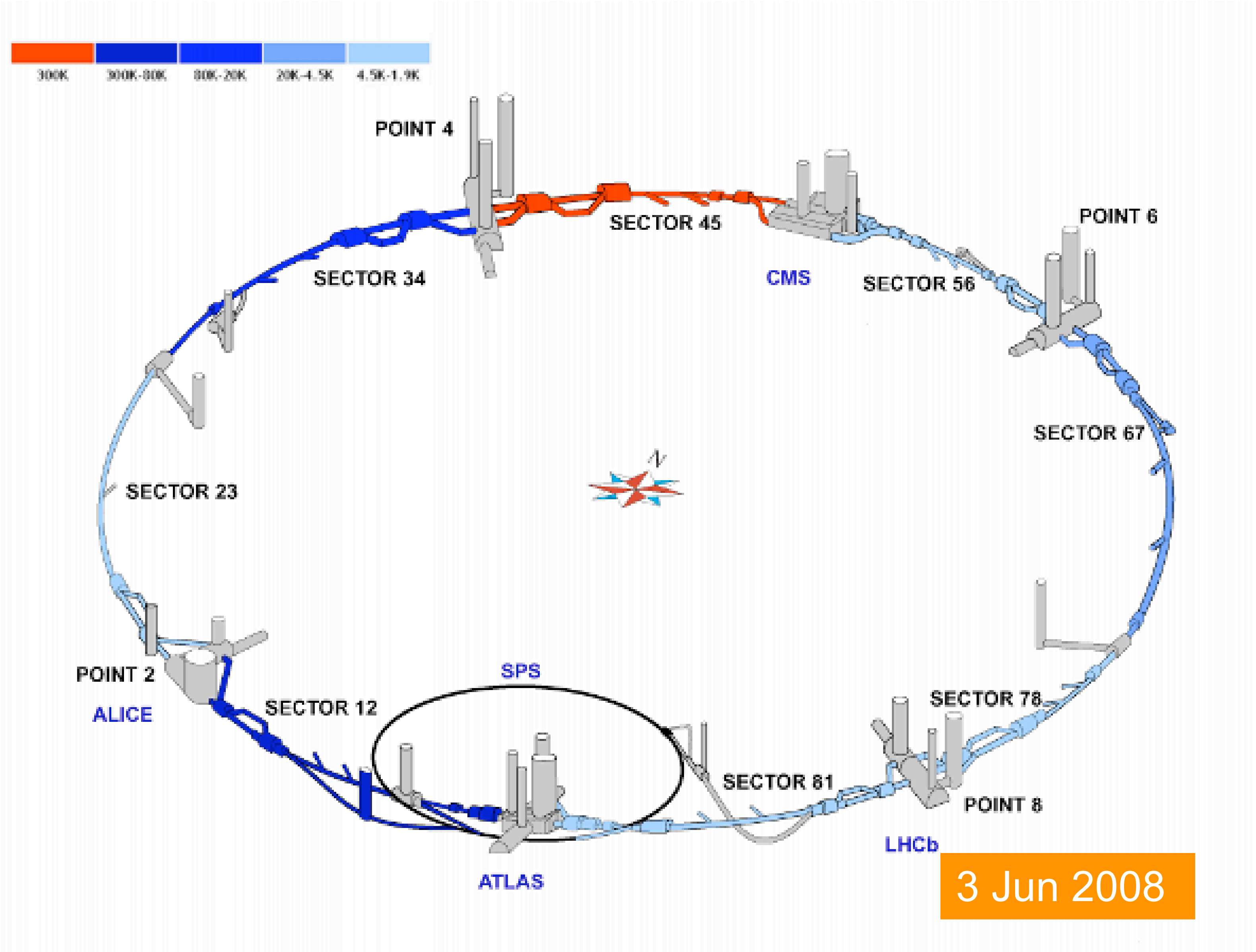

3 Jun 2008

LHC Schedule

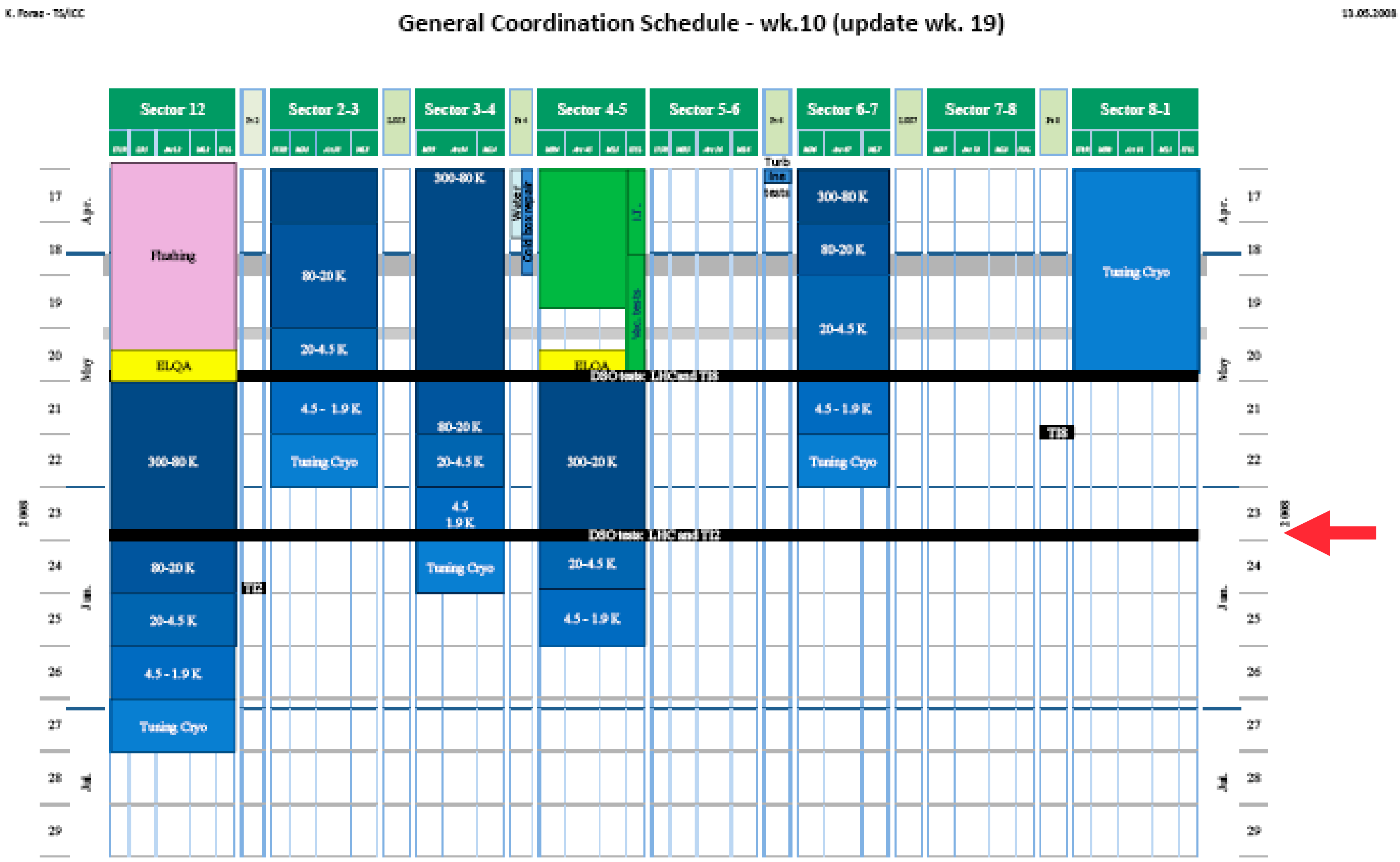

CMS with Beam pipe installed

Factorization in pp collisions

$$\sigma_{hh\to Hx} = PDF(x_a,Q^2)PDF(x_b,Q^2)\otimes\sigma_{ab\to q\bar{q}}\otimes D_{q\to H}(z_q,Q^2)$$

Cross section in hadronic collisions

Parton Distribution Functions
x_a , x_b= momentum fraction of partons a and x in the hadrons

Partonic cross section

Fragmentation of quark q in hadron H

Hard processes in pp collisions can be computed with pQCD techniques and factorization theorems

Partonic cross section is calculable in pQCD

Parton distribution functions and fragmentations functions are non perturbative processes (long distances, large time scales) and cannot be computed with pQCD. However pQCD predicts their evolution with Q^2

How well do we know the proton ?

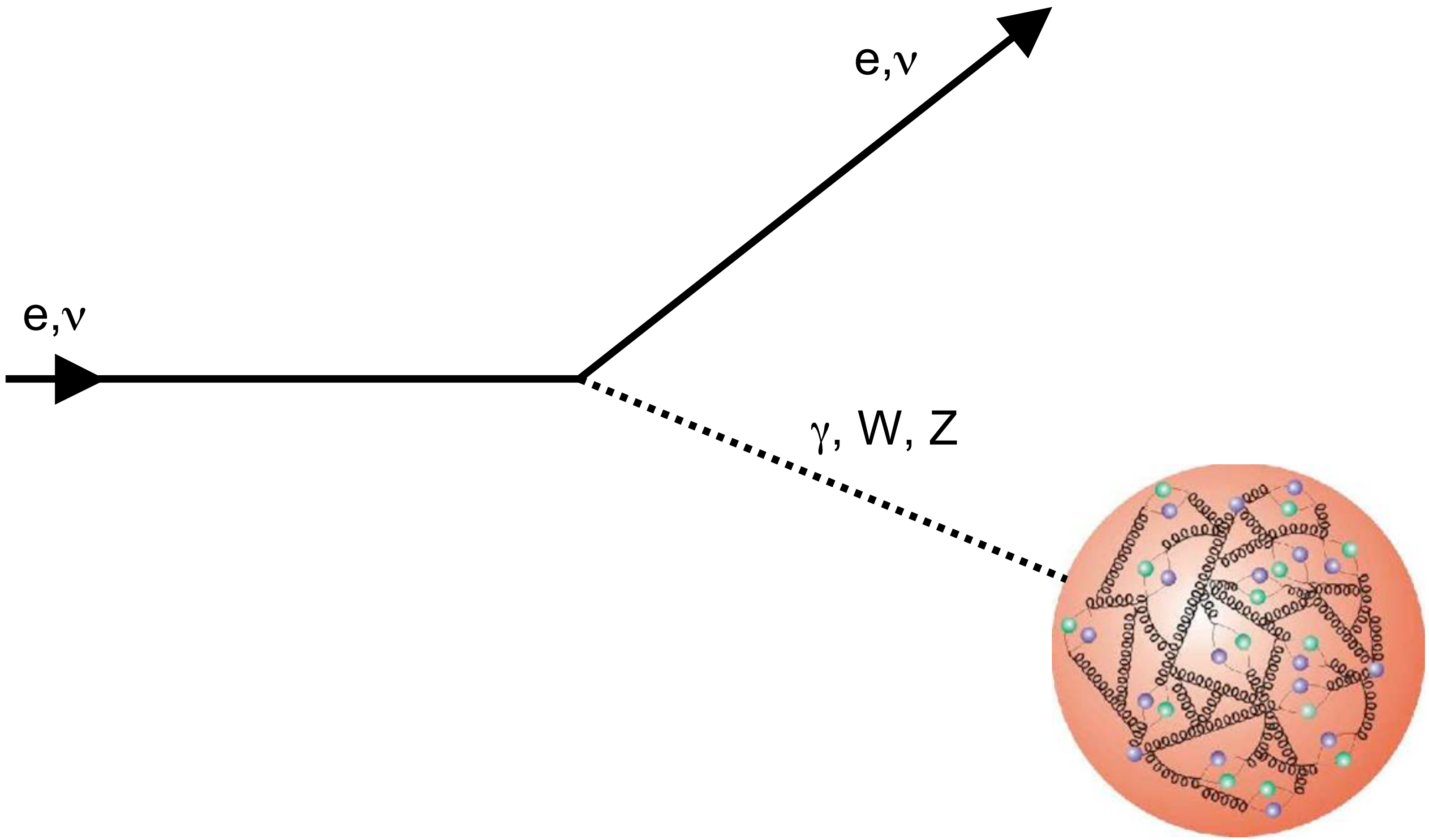

Probing the nucleon

Scattering of a "pointlike" (e.g. lepton) probe on a target : used for long to underpin the target contents.

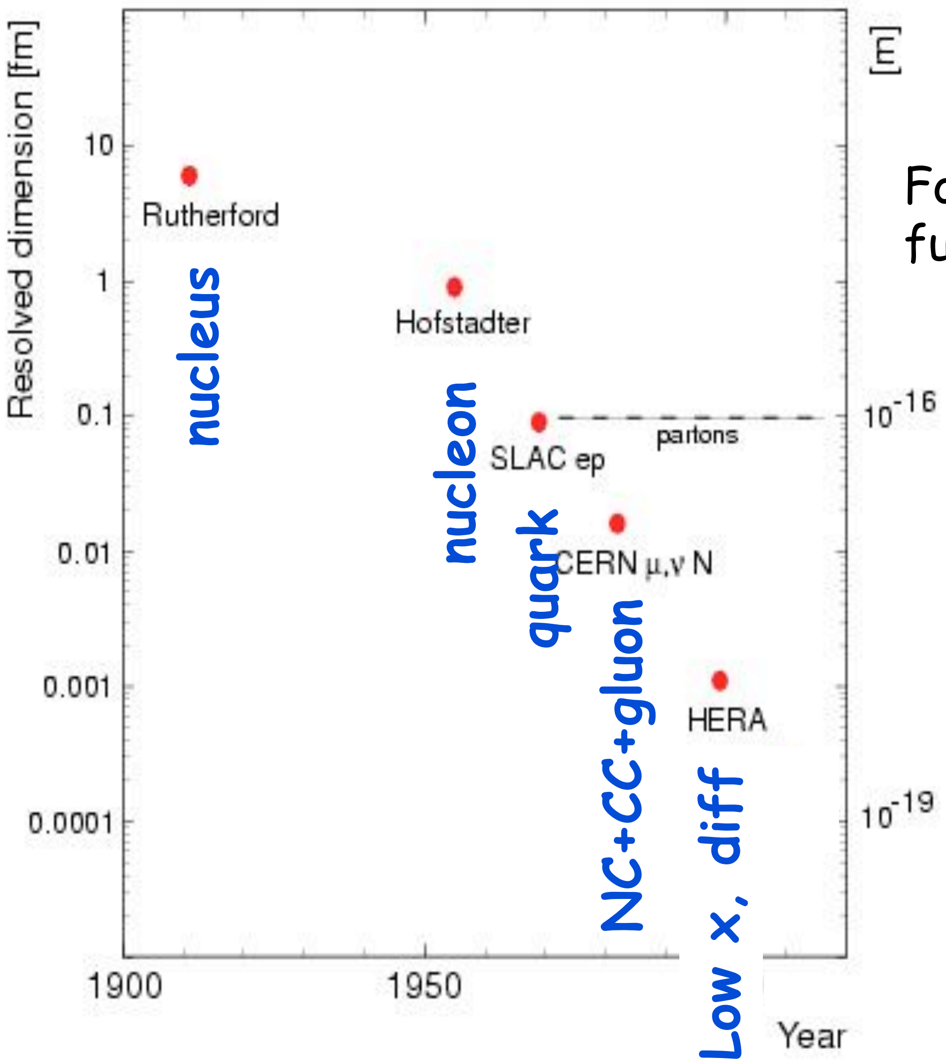

$G_E, G_M(Q^2) \rightarrow W_1, W_2(\omega) \rightarrow F_i(x,Q^2)$

Form factors, Bjorken scaling, structure functions.

Deep inelastic scattering of a lepton off a nucleon (nuclei) is the golden process to study the parton distribution functions.

Other processes also bring important constraints, as will be seen later.

Elastic scattering on a point-like particle

M>>m,E

$$Q^2 = 4E_0 E' \sin^2\theta/2$$

E_0=E'=E

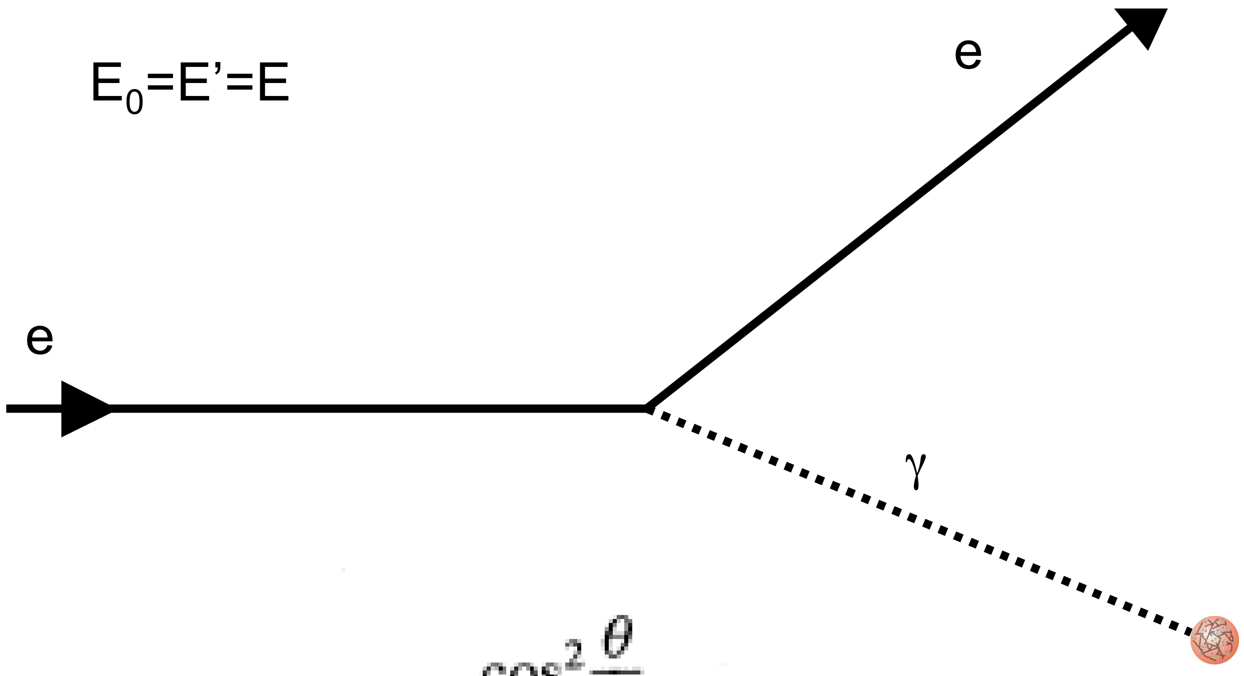

$1/Q^2 \gg (1\ \text{Fermi})^2$

$$\sigma_{\text{Mott}} = \frac{e^4}{4E^2} \frac{\cos^2\frac{\theta}{2}}{\sin^4\frac{\theta}{2}} .$$

Elastic Scattering on a finite proton

$$E' = \frac{E}{1 + (2E/Mc^2)\sin^2(\theta/2)}$$

$$Q^2 = 4E_0 E' \sin^2\theta/2$$

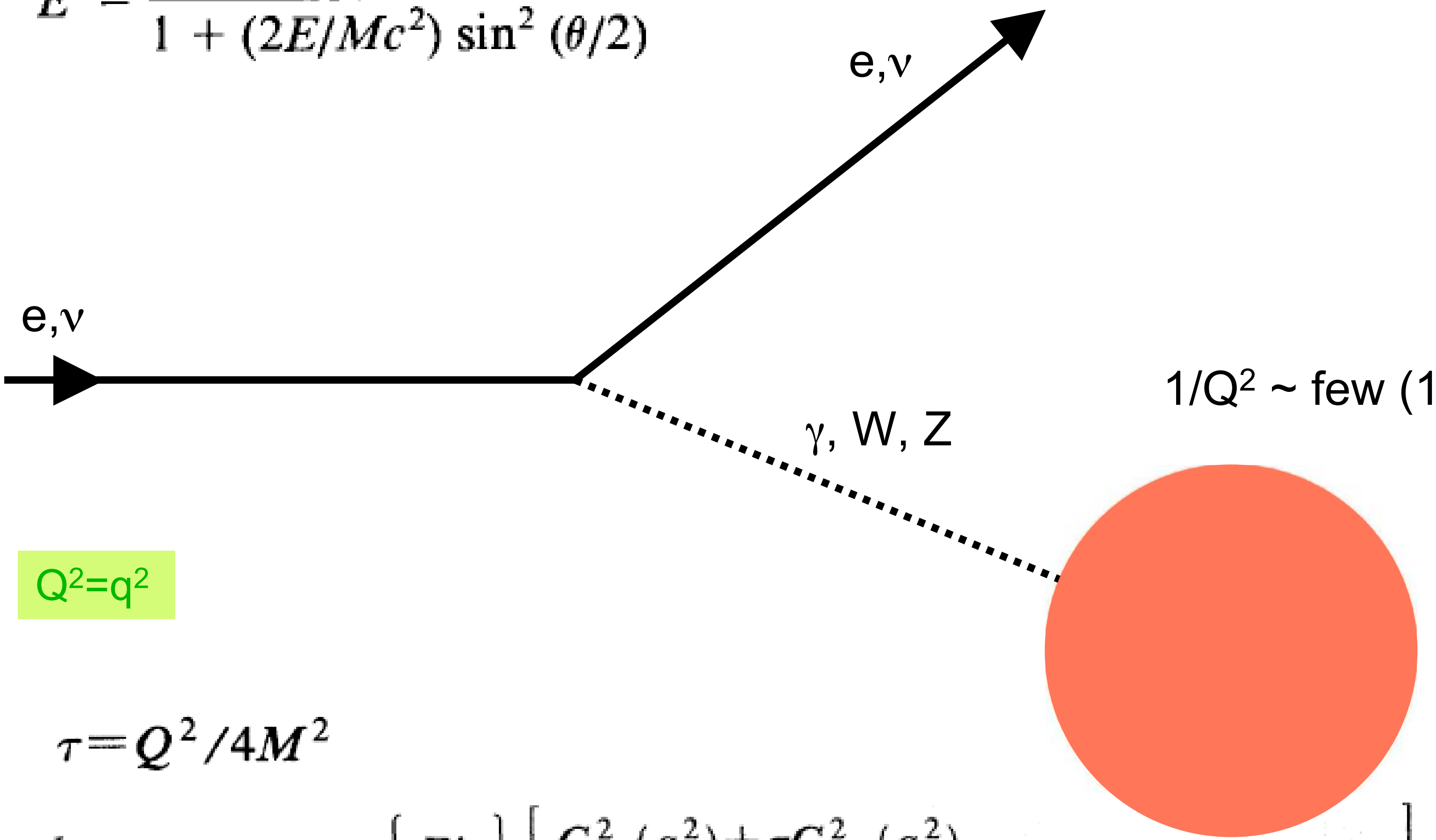

$Q^2=q^2$

$$\tau = Q^2/4M^2$$

$$\frac{d\sigma}{d\Omega}(E) = \sigma_M(E)\left[\frac{E'}{E}\right]\left[\frac{G_{Ep}^2(q^2)+\tau G_{Mp}^2(q^2)}{1+\tau} + 2\tau G_{Mp}^2 \tan^2(\theta/2)\right]$$

Electron-proton elastic scattering

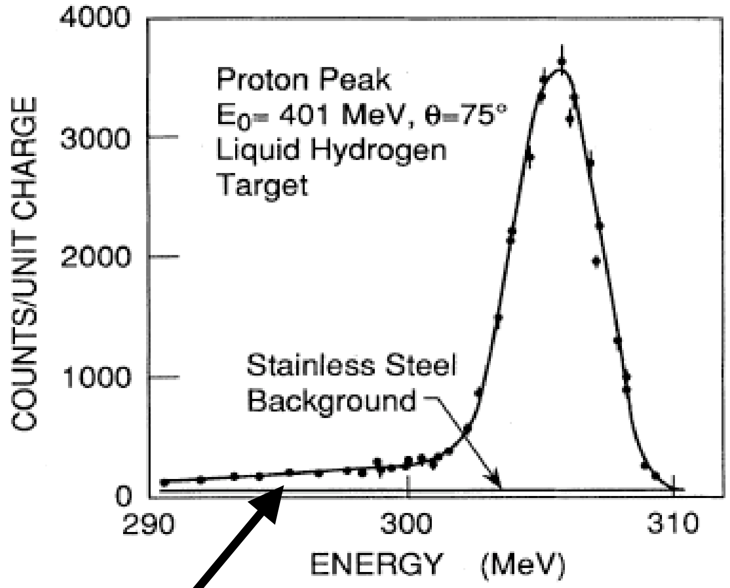

Radiative tail

Angle or Energy --> Q^2

1955- HEPL 550 MeV

1 free variable

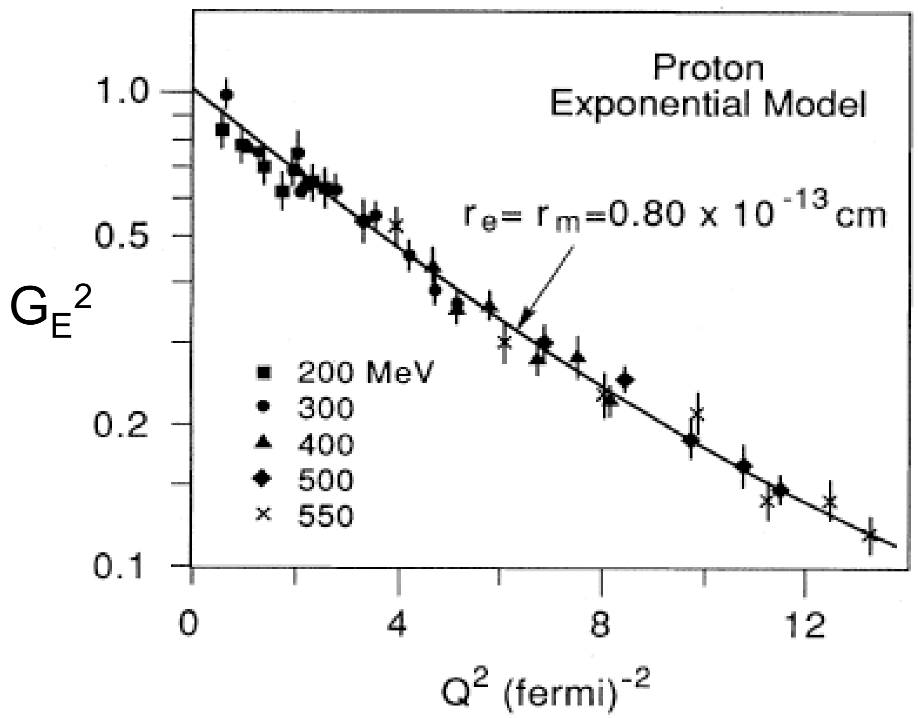

Quasi-elastic scattering on deuterium

1965

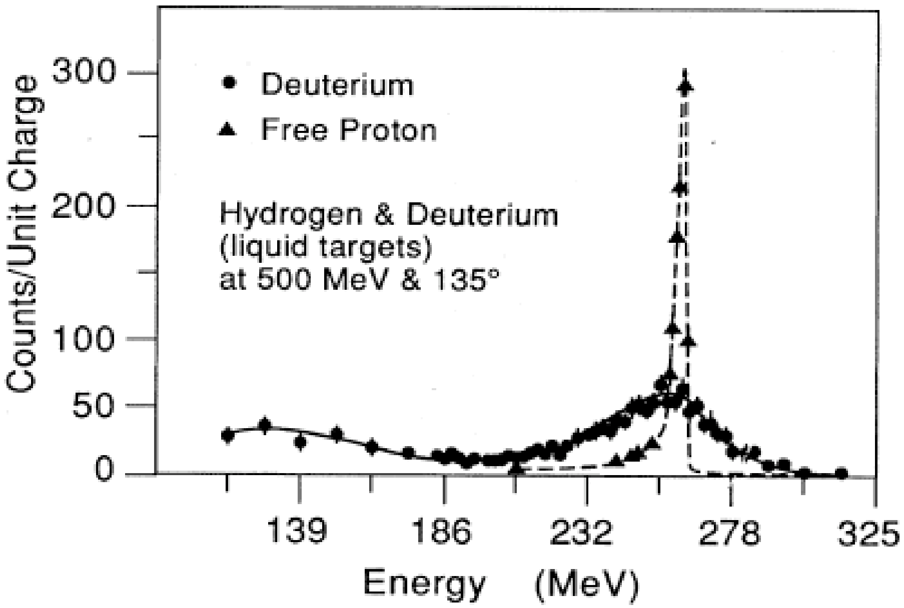

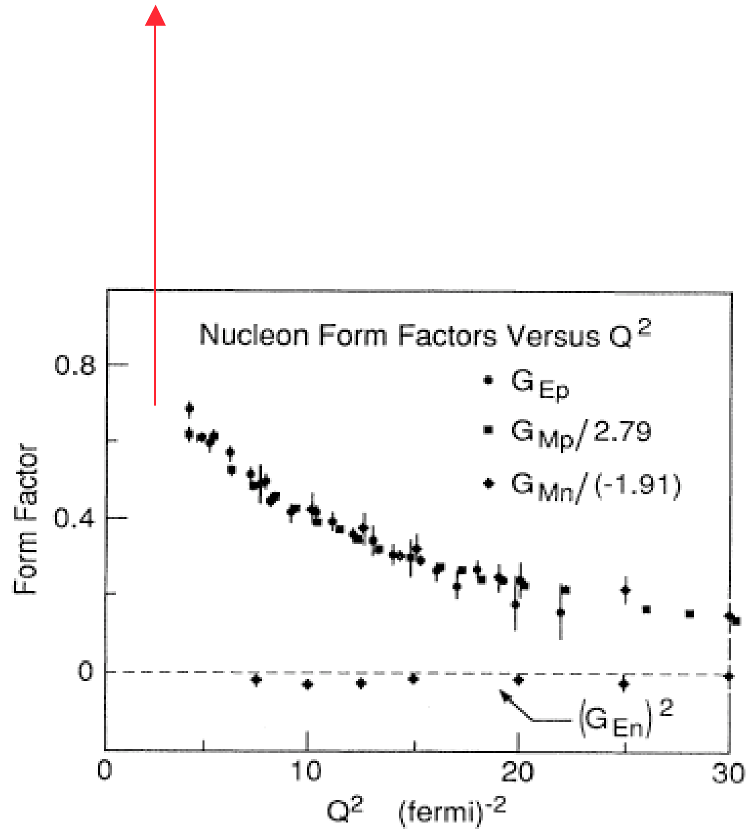

Elastic scattering compared to Mott

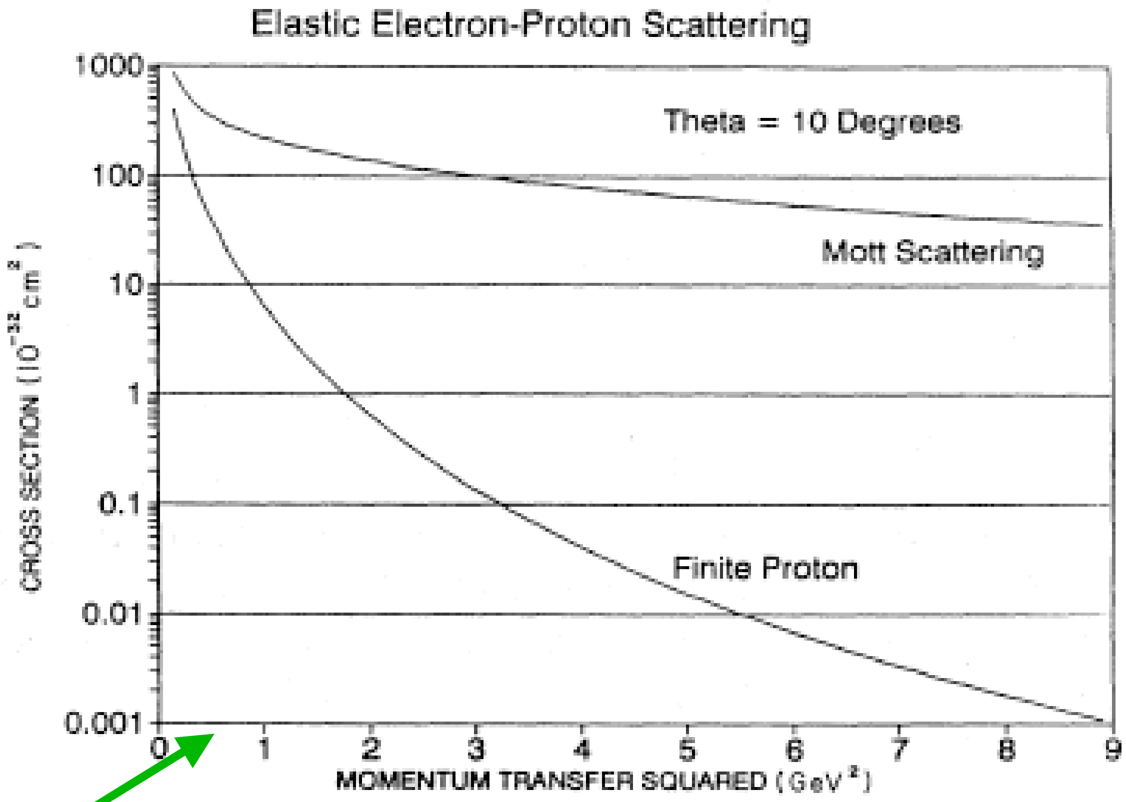

500 MeV beam

…astic scattering cross sections for electrons from a "point" proton and for the actual proton. The differences are attributable to the finite size of the proton.

Electron Scattering on Nuclei

$$E' = \frac{E}{1 + (2E/Mc^2)\sin^2(\theta/2)}$$

$$Q^2 = 4E_0E'\sin^2\theta/2$$

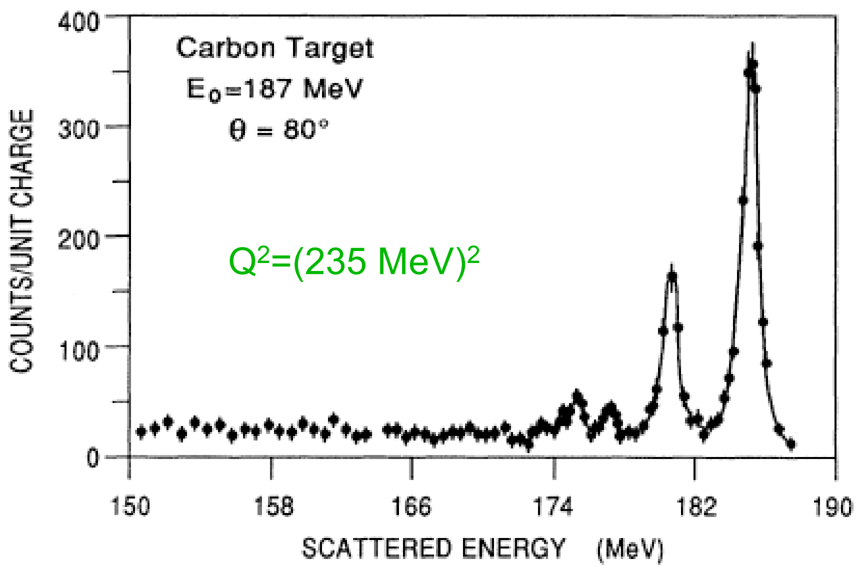

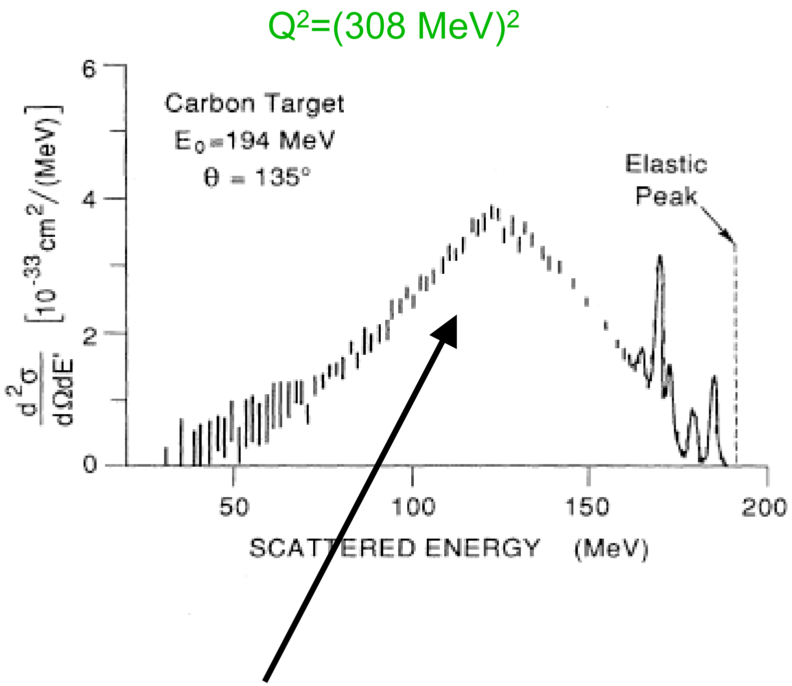

E=187 MeV

Scattering on protons:

Inelastic e-p scattering

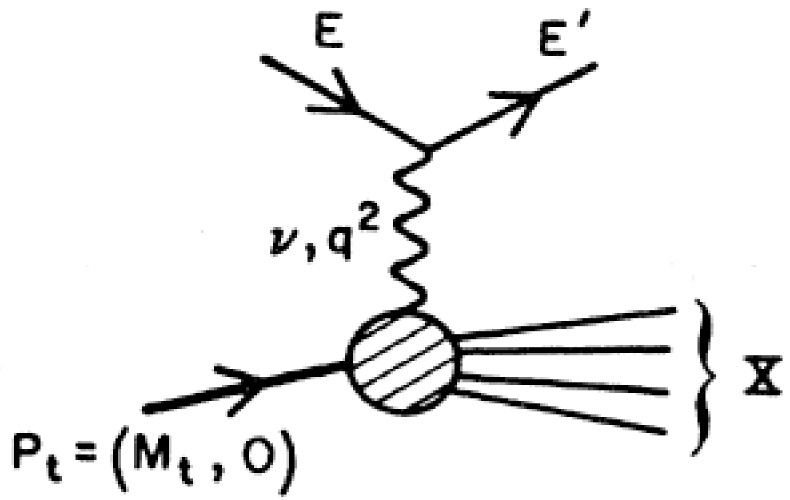

In the inelastic scattering the mass of the system X changes after the scattering. It can be computed as “missing” mass from the Electron kinematics variables

$$Q^2 = 4E_0 E' \sin^2\theta/2$$

$W^2=(p_1+p_2-p_3)^2$

$$W^2 = (2M\nu + M^2 - q^2)$$

$$\nu = E - E' \neq q^2/(2M)$$

This equality holds only for elastic scattering

Inelastic e-p scattering

$$\frac{d^2\sigma}{d\Omega\, dE'}(E,E',\theta)$$
$$=\sigma_M[W_2(\nu,q^2)+2W_1(\nu,q^2)\tan^2(\theta/2)]\ .$$

This is a structure similar to the elastic cross section, but the form factors depend now on 2 variables and E' and theta are now independent variables

By investigating models that satisfy current algebra Bjorken had conjectured that in the limit of infinite ν and q^2 the ratio $\omega=2M\nu/q^2$ stays finite and the functional dependence of W_1 and W_2 simplifies to

$$2MW_1(\nu,q^2)=F_1(\omega)\ ,$$
$$\nu W_2(\nu,q^2)=F_2(\omega)\ .$$

$\omega^{-1}=x=q^2/2M\nu$

Stanford Linear Accelerator Center

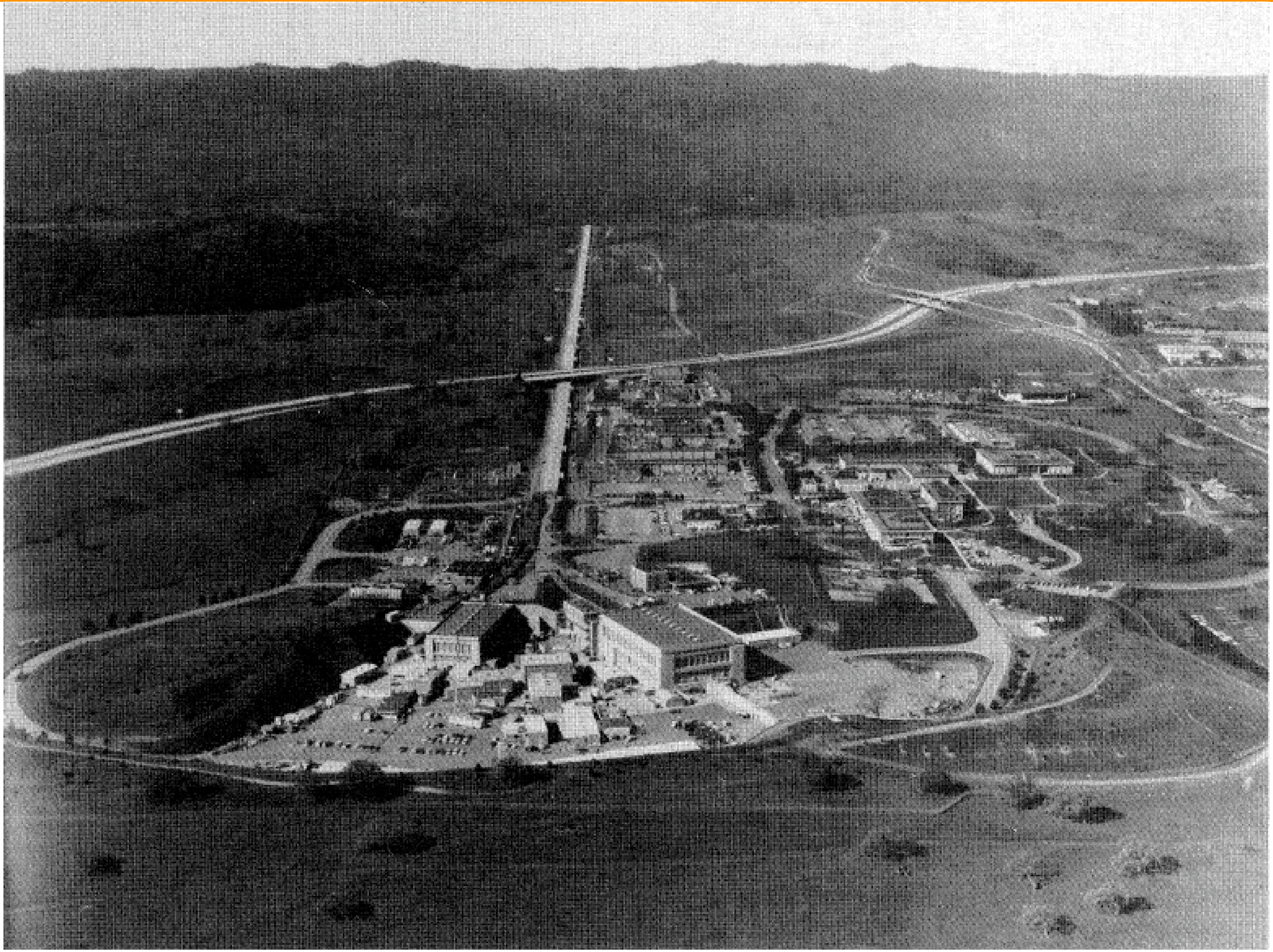

The spectrometers

In order to cover a range of scattering angles it was our intention to build the spectrometer so that it could be rotated around the target from an external control room (Fig. 13, plan). We needed frames which would hold hundreds of tons of magnets and counters in precise alignment while they were moved about the end station.

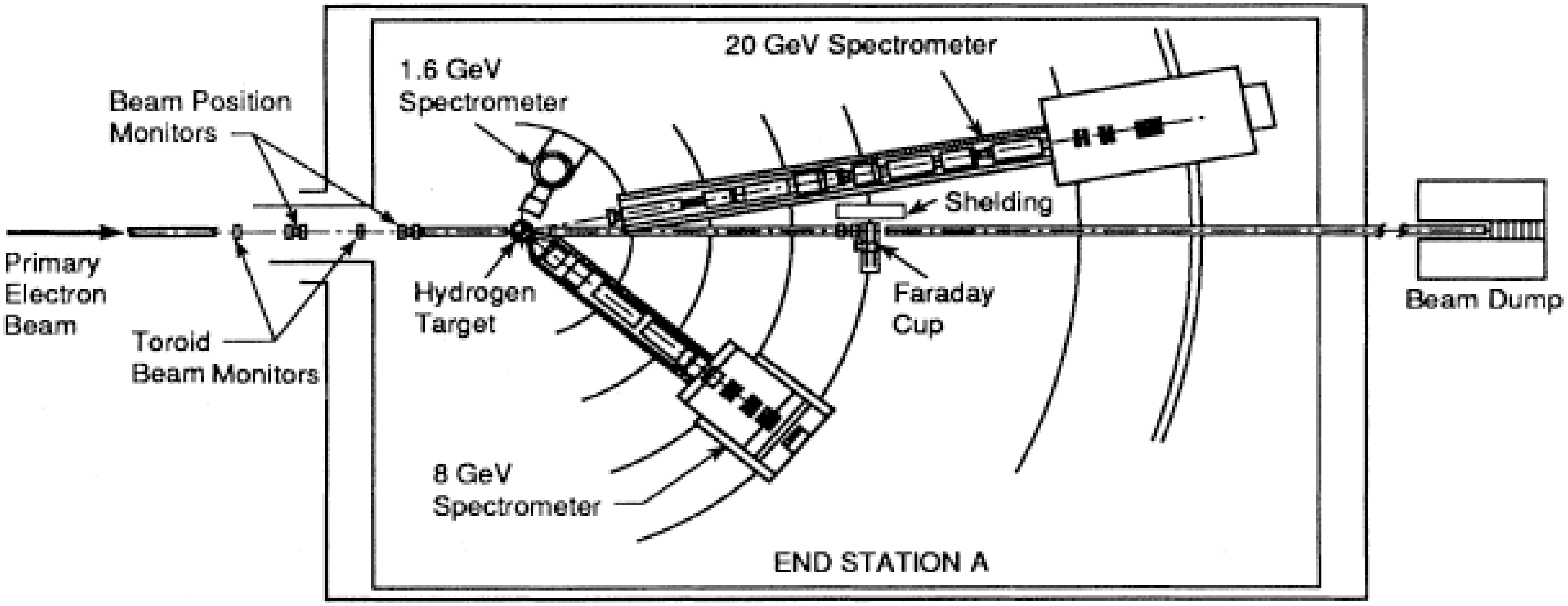

The spectrometer

Scattering in the horizontal plane and bending in the vertical plane allows to separate the two measurements

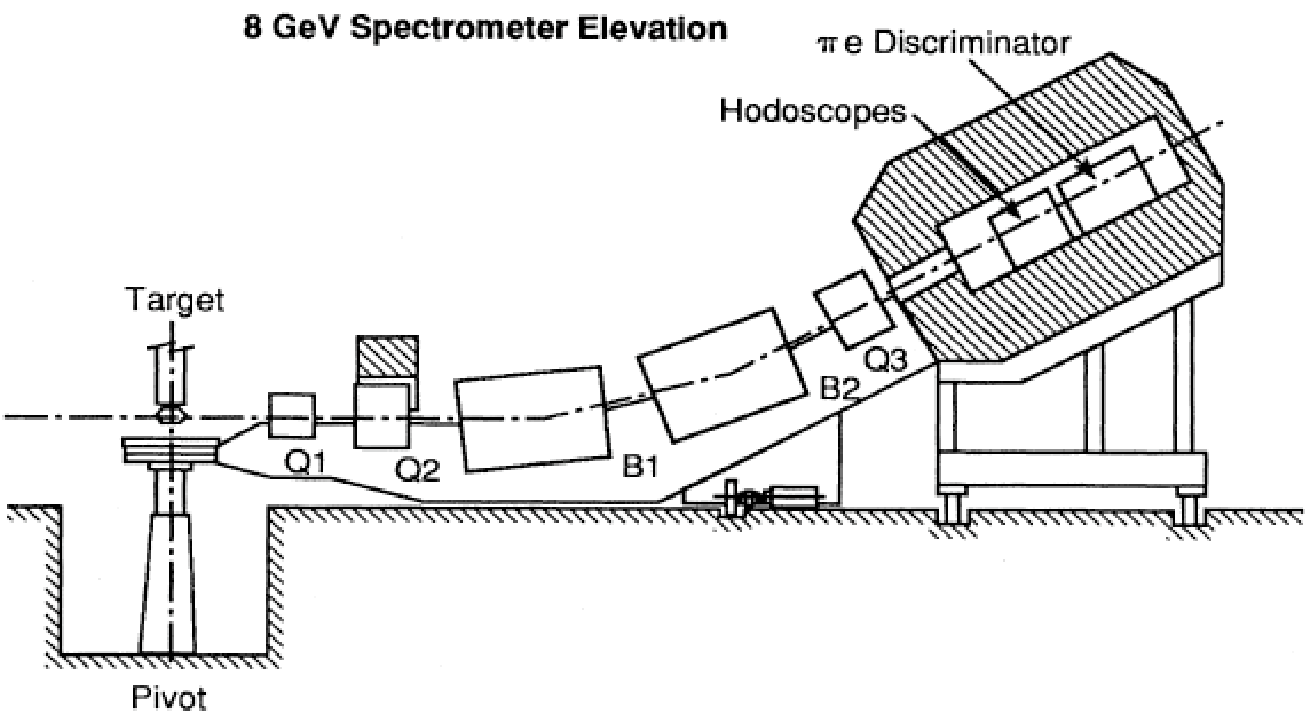

The spectrometers

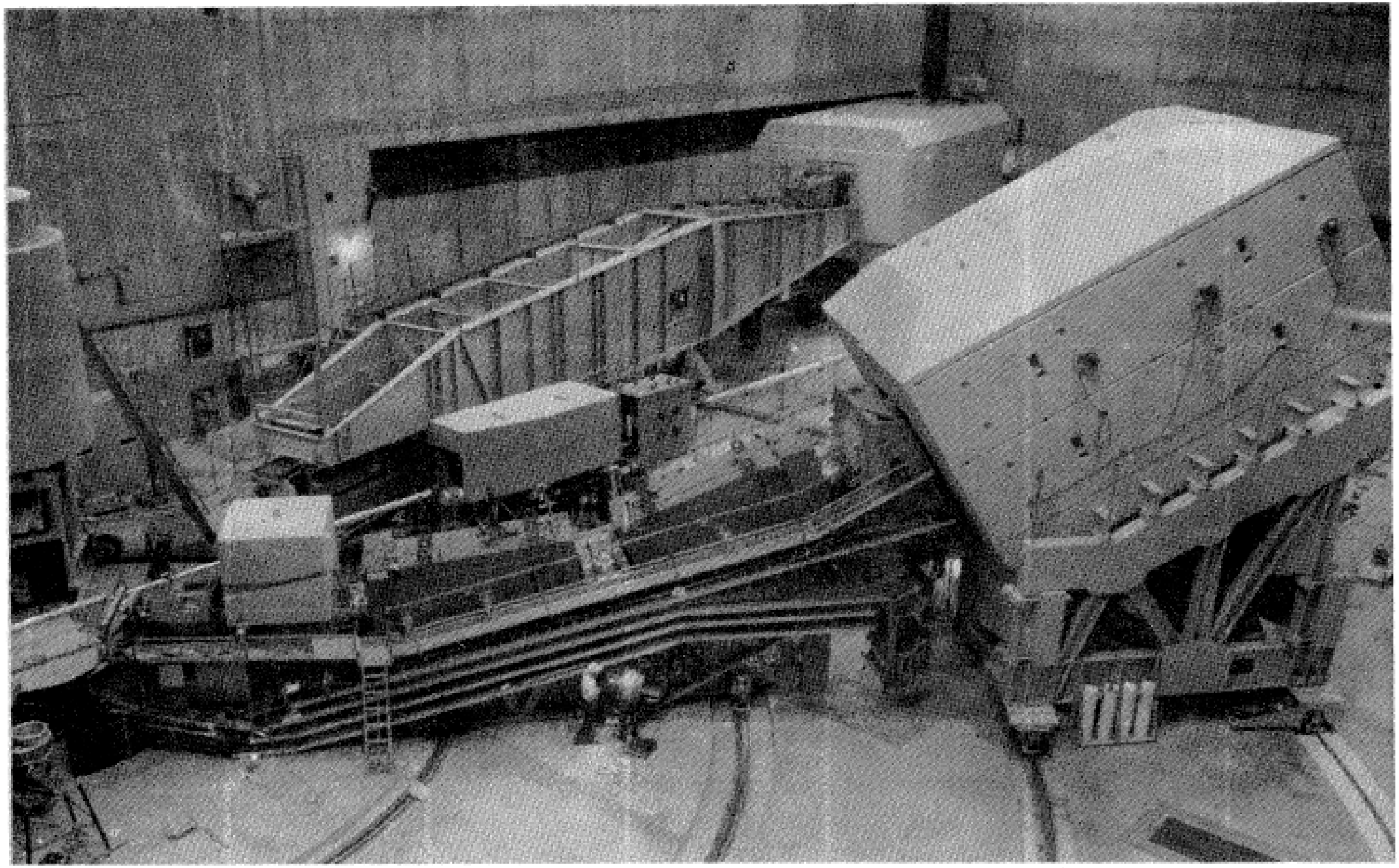

1967 SLAC has electron beams at 20 GeV

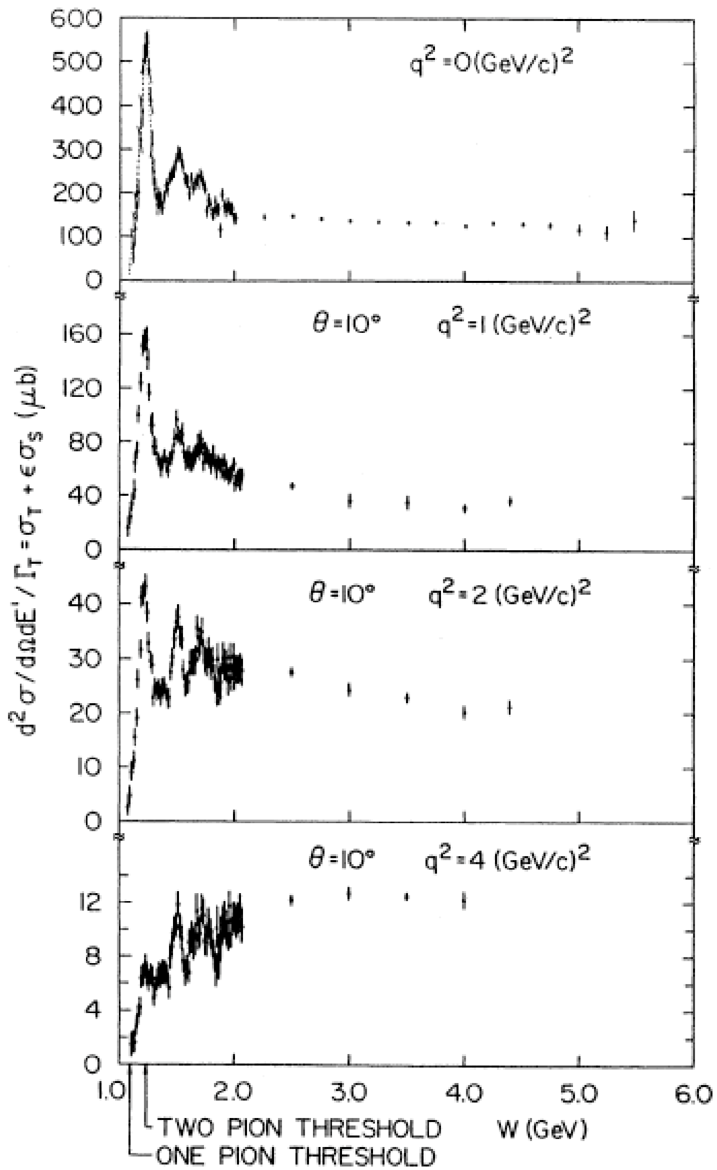

At low Q^2 both the elastic peak and the resonance excitations were large, with little background from non resonance continuum. As Q^2 increased, the resonance cross section decreased rapidly, with the continuum scattering becoming dominant.

SLAC has electron beams at 20 GeV

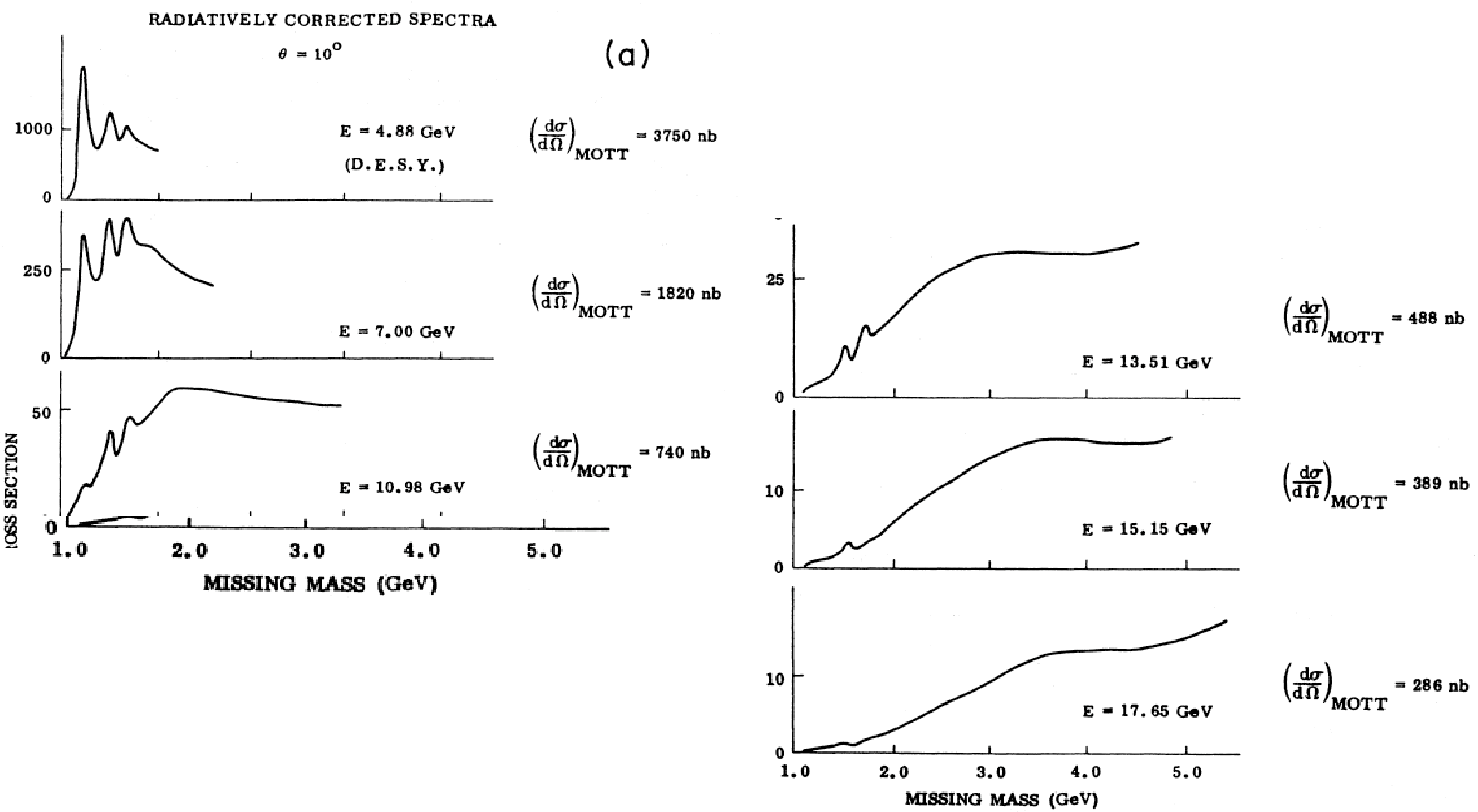

Main features of the inelastic scattering results

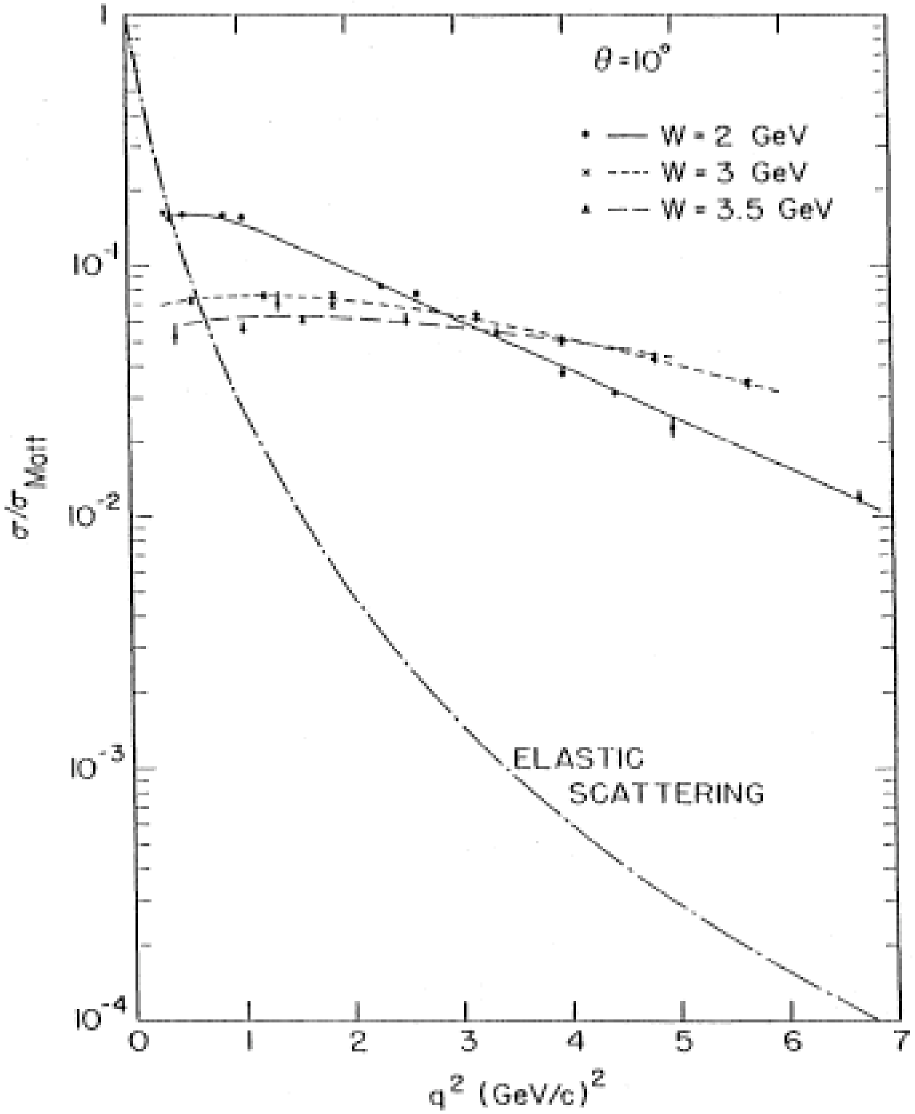

Weak q2 dependence:

$$Q^2 = 4E_0 E' \sin^2\theta/2$$

$$W^2 = (2M\nu + M^2 - q^2)$$

$$\sigma_{\text{Mott}} = \frac{e^4}{4E^2} \frac{\cos^2\dfrac{\theta}{2}}{\sin^4\dfrac{\theta}{2}} .$$

Striking features of the data

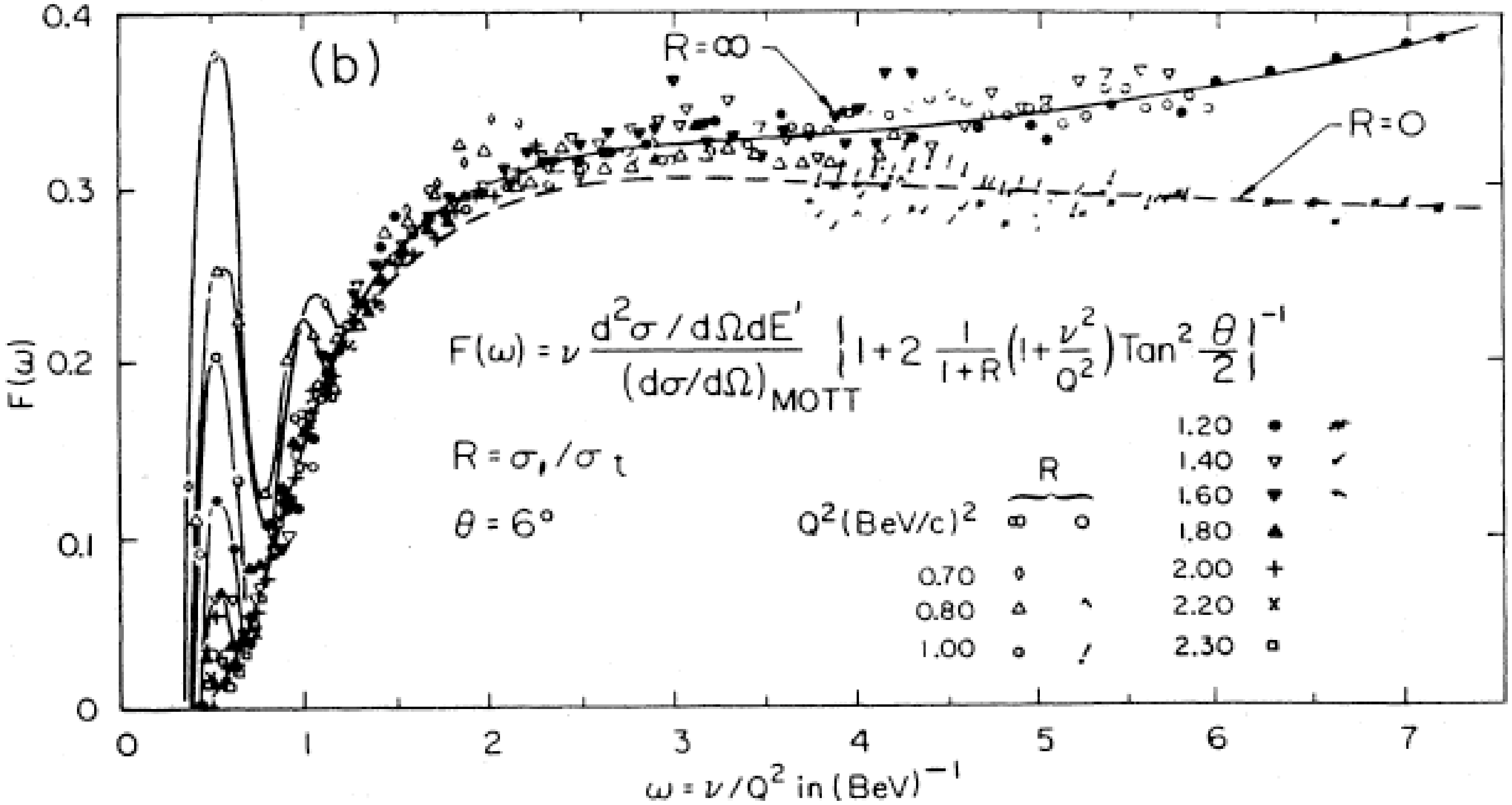

Explanation in the framework of the quark model

$x = q^2/2M\nu \dashrightarrow x = -q^2/qp$

We observe that the elastic scattering of the proton is the specific case of the inelastic scattering where x = 1. So the inelastic structure functions of the proton are related to elastic structure function just by multiplying by a delta $\delta(x-1)$

Comparing the inelastic cross section

$$\frac{d\sigma}{dE'\,d\Omega} = \left(\frac{\alpha\hbar}{2E\sin^2(\theta/2)}\right)^2 [2W_1\sin^2(\theta/2) + W_2\cos^2(\theta/2)]$$

With the elastic cross section

$$\frac{d\sigma}{d\Omega} = \left(\frac{\alpha\hbar}{4ME\sin^2(\theta/2)}\right)^2 \frac{E'}{E}[2K_1\sin^2(\theta/2) + K_2\cos^2(\theta/2)]$$

Quark model -2

We get:

$$W_{1,2}(q^2, x) = -\frac{K_{1,2}(q^2)}{2Mq^2}\,\delta(x-1)$$

Moreover, if we treat the proton as a point-like charge and spin 1/2, the $K_{1,2}$ have a very simple expression:

$$K_1 = -q^2 \quad \text{and} \quad K_2 = (2Mc)^2$$

Using these formula we can write directly the structure functions for scattering off a quark of flavor i as :

$$W_1^i = \frac{Q_i^2}{2m_i}\,\delta(x_i - 1), \qquad W_2^i = -\frac{2m_i c^2 Q_i^2}{q^2}\,\delta(x_i - 1)$$

Where m_i is the mass of the quark and p_i is its momentum and

$$x_i = -\frac{q^2}{2q\cdot p_i}$$

Quark model -3

We make now an assumption: $p_i = z_i p$, i.e. we can write each component of the quark momentum vector as a fraction z_i of the proton momentum vector.

With this assumption: $x_i = \frac{x}{z_i}$ and then

$$W_1^i = \frac{Q_i^2}{2M}\delta(x - z_i), \qquad W_2^i = -\frac{2x^2Mc^2}{q^2}Q_i^2\,\delta(x - z_i)$$

Quark model - 4

Assuming now $f_i(z_i)$ as the probability for the ith quark to carry momentum fraction z:

$$W_1 = \sum_i \int_0^1 \frac{Q_i^2}{2M} \delta(x - z_i) f_i(z_i) dz_i = \frac{1}{2M} \sum_i Q_i^2 f_i(x)$$

$$W_2 = \sum_i \int_0^1 \left(-\frac{2x^2Mc^2}{q^2}\right) Q_i^2 \, \delta(x - z_i) f_i(z_i) dz_i = -\frac{2Mc^2}{q^2} x^2 \sum_i Q_i^2 f_i(x)$$

Thus

$$MW_1 = \frac{1}{2} \sum_i Q_i^2 f_i(x) \equiv F_1(x)$$

$$-\frac{q^2}{2Mc^2x} W_2 = x \sum_i Q_i^2 f_i(x) \equiv F_2(x)$$

And comparing the two expressions

$$F_2(x) = 2xF_1(x)$$

Callan-Gross relation

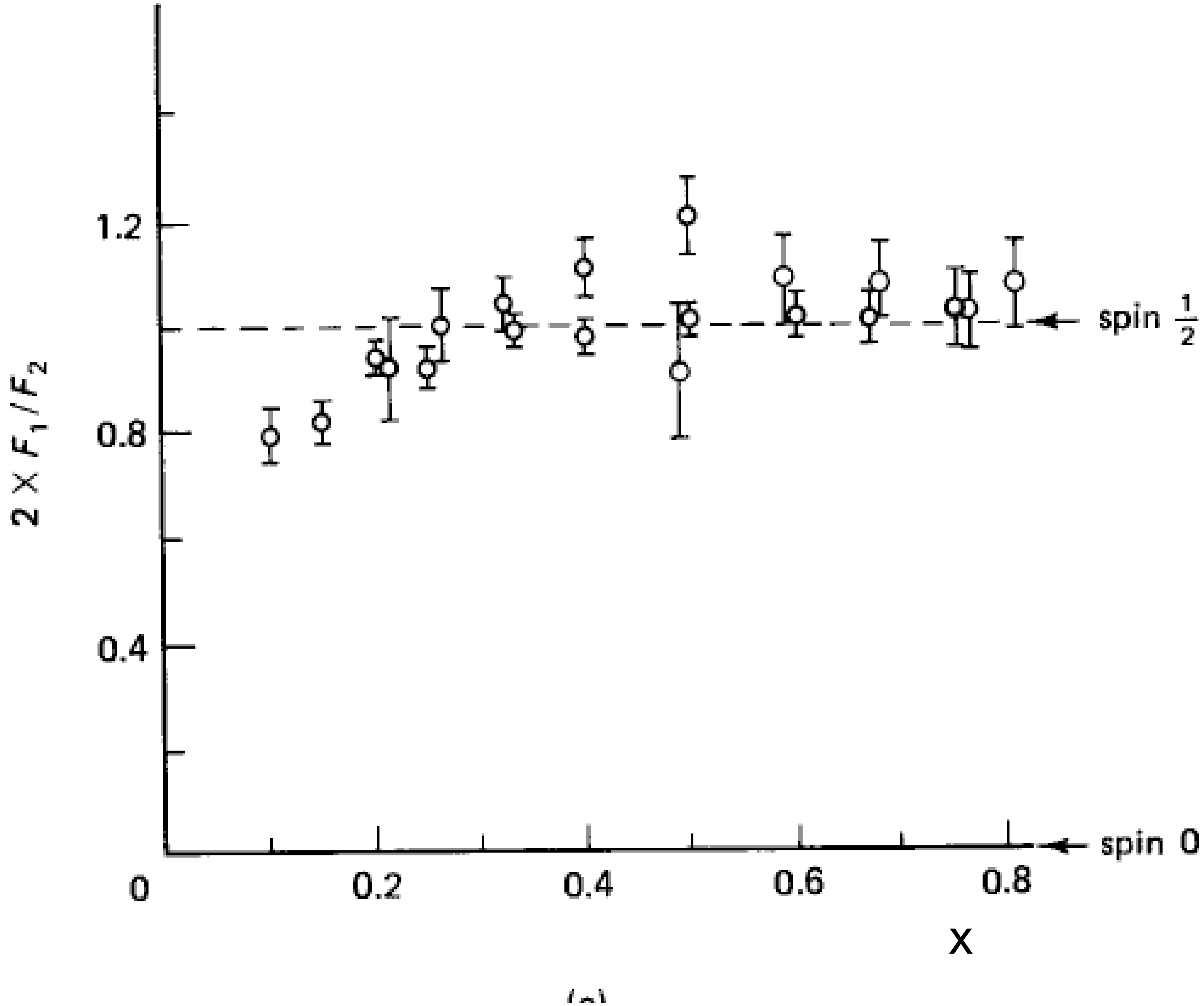

The structure functions of p and n

Neutrons cross sections were extracted from the measured deuteron cross sections using a procedure to eliminate the effect of the fermi motions. The measured PROTON cross sections were kinematically smeared over the fermi momentum , using a model. Subtracting the smeared proton cross sections from the measured deuteron cross sections, one obtains the smeared neutron cross sections, that are eventually unfolded into unsmeared neutron cross sections.

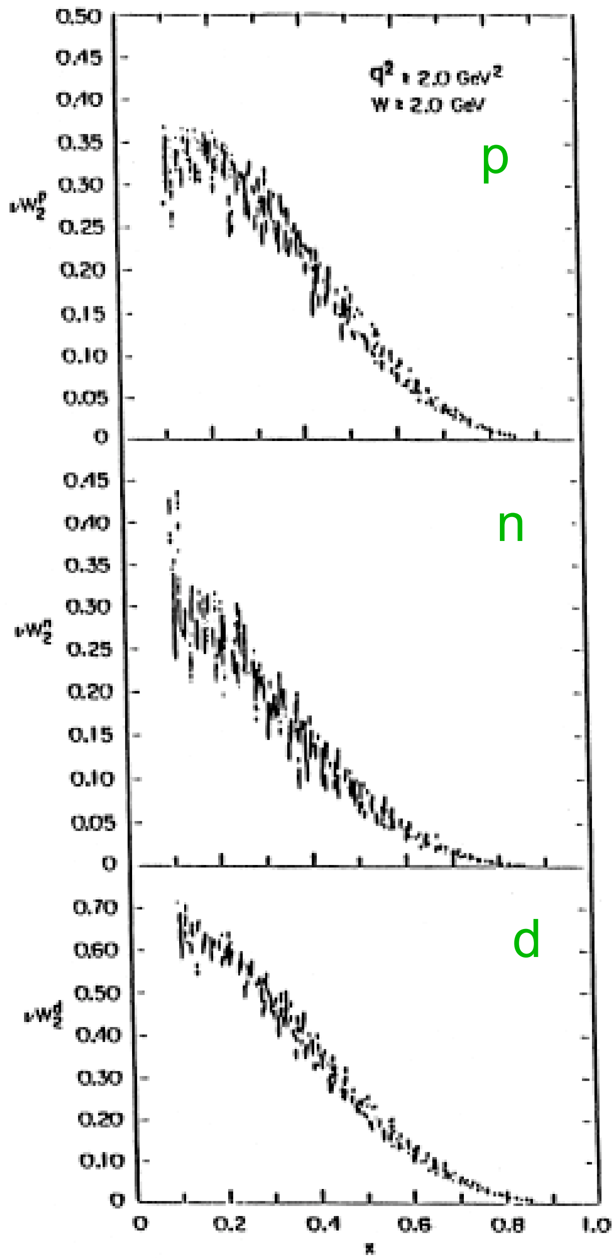

The structure functions of p and n

p,n,d structure functions show the same behavior

The value of R were the same in p,n,d

The ratio of the neutron to proton cross section falls with x

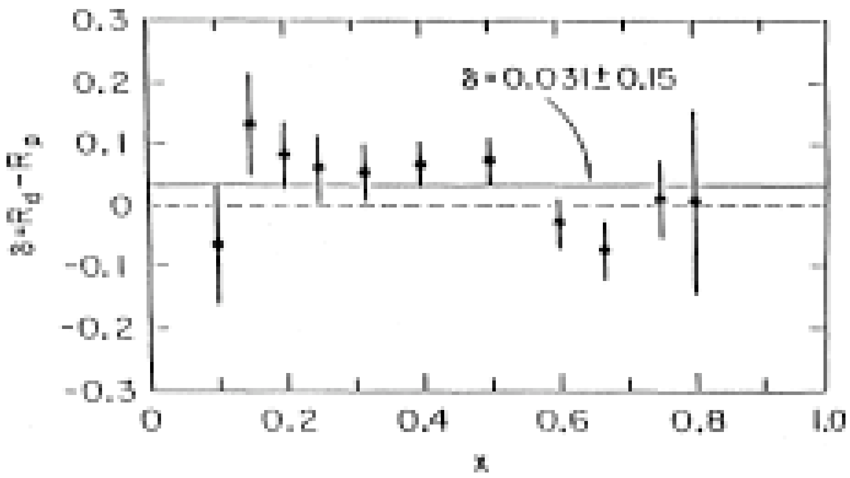

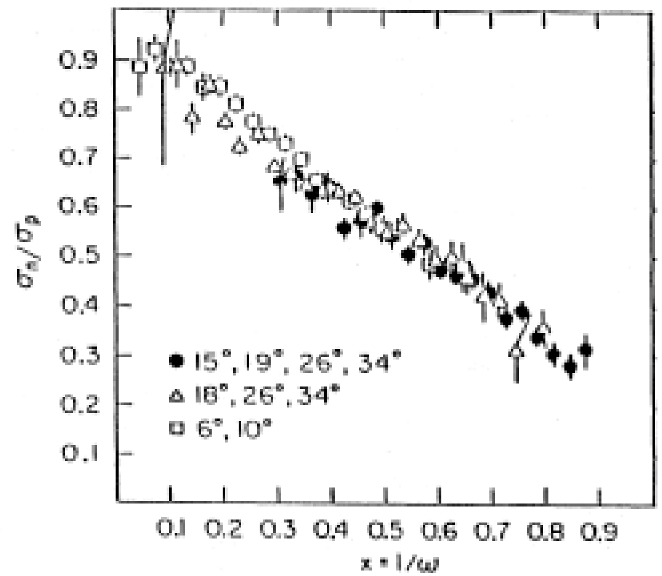

Sigma proportional to $\sum_i Q_i^2 f_i(x)$

Average momentum carried by quarks

If $u_p(x)$ and $d_p(x)$ are defined as the probability density of momentum x carried by the u ad d quark of the proton, then the F_2 distribution is given by:

$$F_2^p(x) = \nu W_2^p(x)$$
$$= x[Q_u^2(u_p(x) + \bar{u}_p(x))$$
$$+ Q_d^2(d_p(x) + \bar{d}_p(x))] ,$$

Using the isospin symmetry one gets

$$\frac{1}{2}\int_0^1 [F_2^p(x) + F_2^n(x)]dx = \frac{Q_u^2 + Q_d^2}{2}\int_0^1 x[u_p(x) + \bar{u}_p(x) + d_p(x) + \bar{d}_p(x)]dx$$

Average momentum carried by quarks

The integral on the right hand side of the expression is equal to 1 if the quarks u and d carry the whole momentum of nucleon

$$\frac{Q_u^2+Q_d^2}{2}=\frac{1}{2}\left[\frac{4}{9}+\frac{1}{9}\right]=\frac{5}{18}=0.28 \ .$$

While the integral of F2 performed numerically on the proton and neutron data gives

$$\frac{1}{2}\int[F_2^p(x)+F_2^n(x)]dx=0.14\pm0.005$$

Only 1/2 of the proton momentum is carried by the u and d quarks, the rest is carried by components of the proton that are not interacting with the electron !

First Neutrino results from CERN (Gargamelle)

Neutrino deep inelastic scattering produces complementary results since the charged current neutrino interaction is independent of the quark charges, but “sees” the same quark momentum distribution

$$\frac{\frac{1}{2}\int[F_2^{ep}(x)+F_2^{en}(x)]dx}{\frac{1}{2}\int[F_2^{\nu p}(x)+F_2^{\nu n}(x)]dx}=\frac{Q_u^2+Q_d^2}{2}$$

Here the denominator is the F2 distribution of the neutrino interaction on an ISOSCALAR target. By combining the neutrino and antineutrino results , the Gargamelle group was able to show

$$\begin{aligned}\frac{1}{2}&\left[\int F_2^{\nu p}(x)+F_2^{\nu n}(x)dx\right]\\&=\int x[u_p(x)+\bar{u}_p(x)+d_p(x)+\bar{d}_p(x)]dx\\&=0.49\pm0.07\ ,\end{aligned}$$

Comparison of Neutrino and electron F2

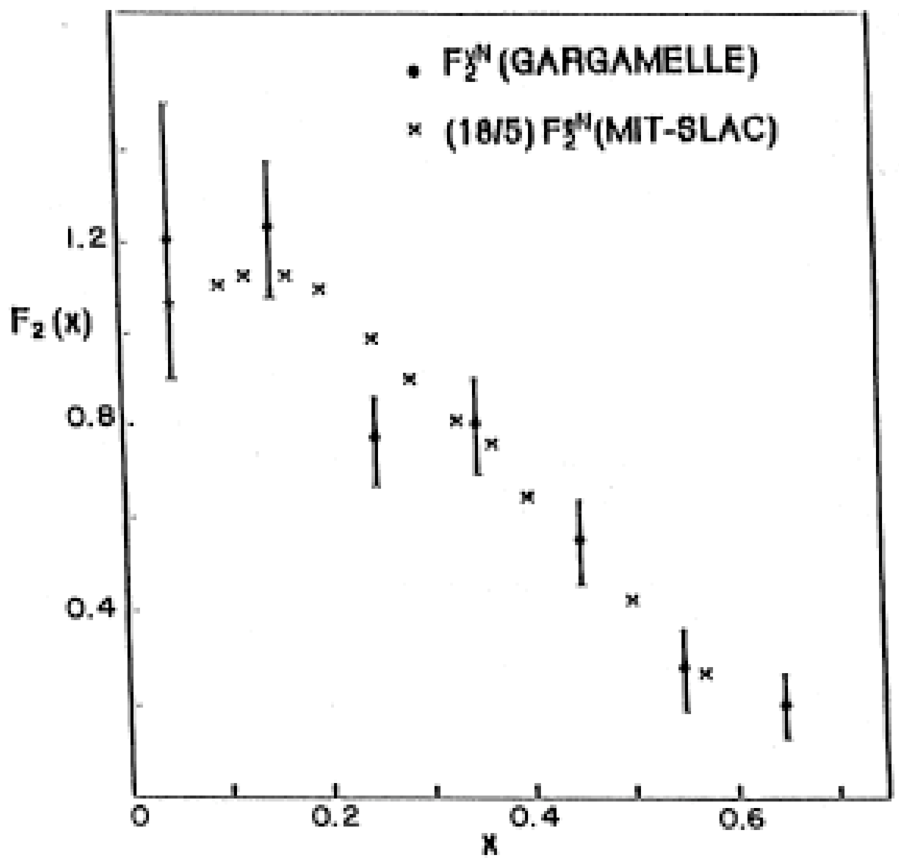

1974

A crucial element in accepting the quark model as THE theory for the proton was the general acceptance of QCD (Gross, Wilczek and Politzer). Which eliminated the last paradox: why the quarks are not free ?

The infrared slavery mechanism of QCD provided a reason to accept quarks are physical constituents without demanding the existence of free quarks. The asymptotic freedom also provided explanation of scaling, but logarithmic deviations were foreseen. These were seen experimentally only later in muon and neutrino scattering at CERN and FNAL.

e-nucleus scatt.

$$W^2 = (p+q)^2$$
$$= M^2 + 2p.q + q^2$$

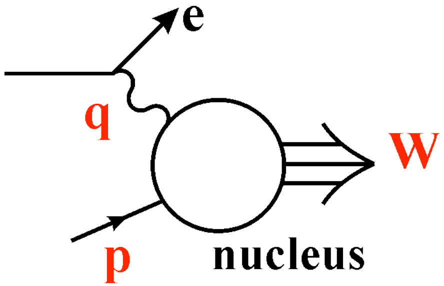

$(Q^2 \equiv -q^2)$

$\lambda = 1/Q$

$\boxed{Q^2R^2 \ll 1}$

elastic
W=M

$$x_N \equiv \frac{Q^2}{2p.q} = 1$$

$$\left.\frac{Q^2}{2M\nu}\right|_{lab.}$$

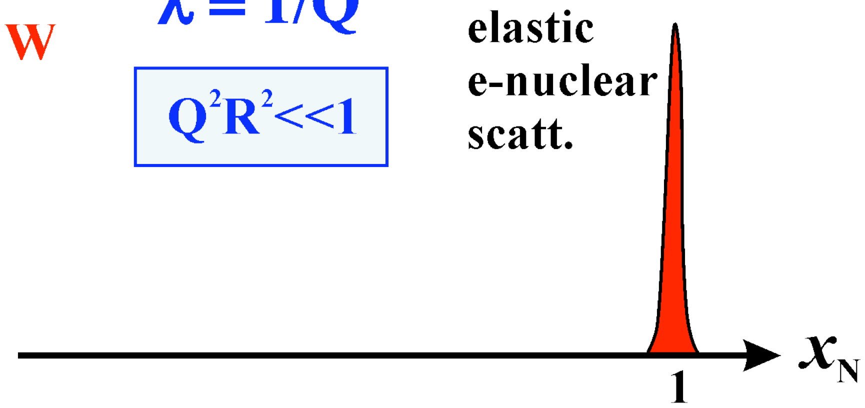

e-nucleus scatt.

$$W^2 = (p+q)^2$$
$$= M^2 + 2p.q + q^2$$

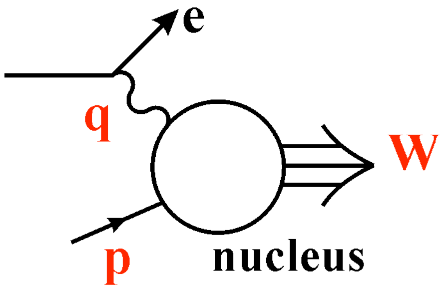

$(Q^2 \equiv -q^2)$

$\lambda = 1/Q$

$\boxed{Q^2R^2 \ll 1}$

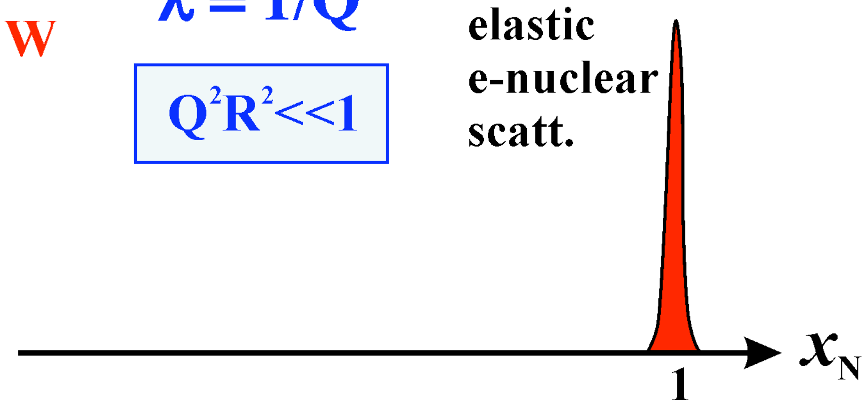

elastic
W=M

$$x_N \equiv \frac{Q^2}{2p.q} = 1$$

$$\left.\frac{Q^2}{2M\nu}\right|_{lab.}$$

$\boxed{Q^2R^2 \sim 1}$

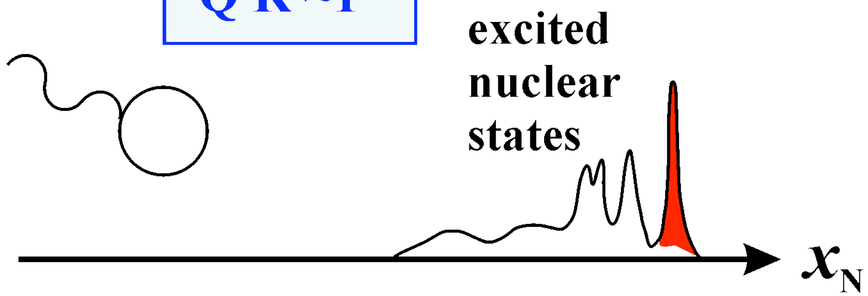

excit^{ns}
W>M

$$x_N < 1$$

e-nucleus scatt.

$$W^2 = (p+q)^2$$
$$= M^2 + 2p.q + q^2$$

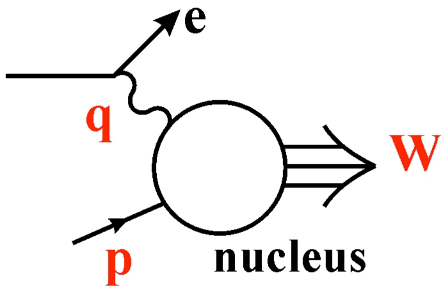

$\lambda = 1/Q$

$(Q^2 \equiv -q^2)$

elastic W=M

$$x_N \equiv \frac{Q^2}{2p.q} = 1$$

$$\left.\frac{Q^2}{2M\nu}\right|_{\text{lab.}}$$

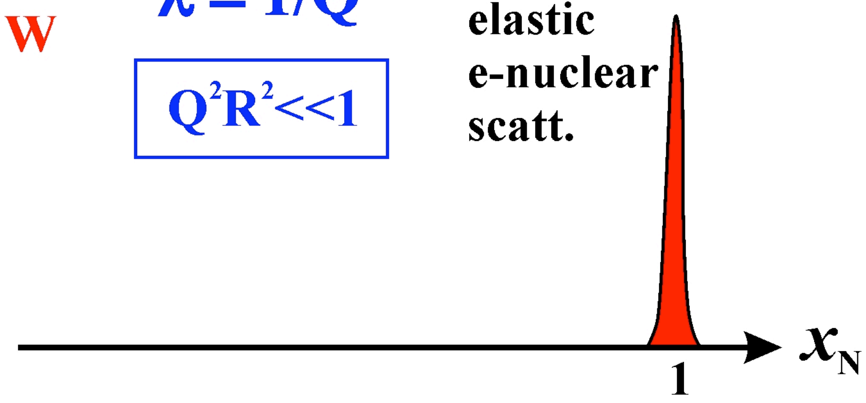

excit^{ns} W>M

$$x_N < 1$$

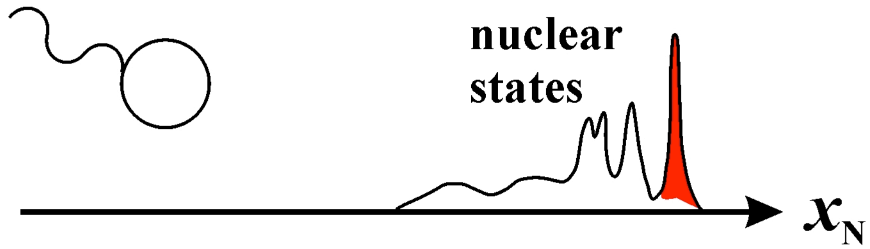

e-proton scatt:

$$x_N = \frac{m_p}{M} \left.\frac{Q^2}{2m_p\nu}\right|_{\text{lab.}} = \frac{1}{A}$$

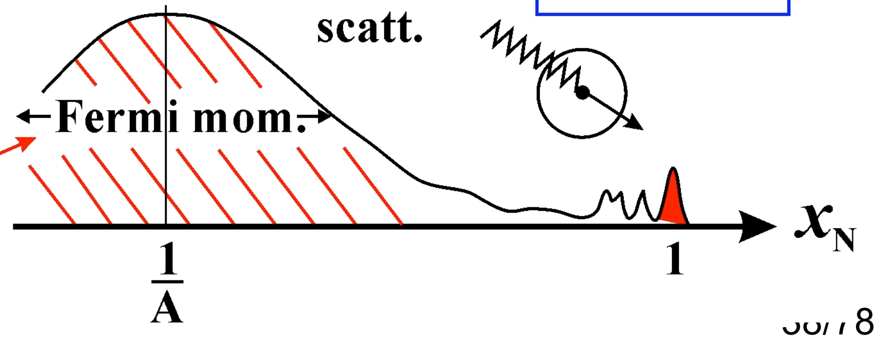

$\sigma \sim Z\sigma_{ep}$

shift: A=N+Z

e-p scattering

$$W^2 = (p+q)^2$$
$$= M^2 + 2p.q + q^2$$
$$(Q^2 \equiv -q^2)$$

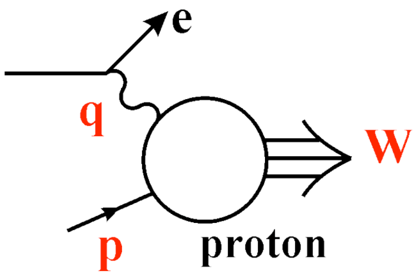

$\lambda >> R$

$Q^2R^2 << 1$

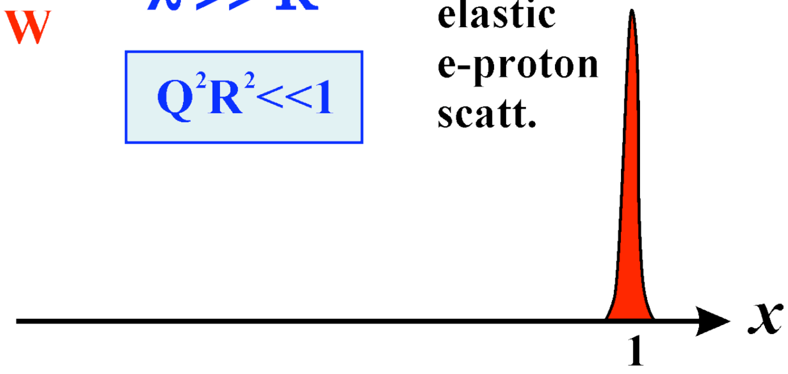

elastic
W=M

$$x \equiv \frac{Q^2}{2p.q} = 1$$

now
$M = m_p$
$R = R_p$

$Q^2R^2 \sim 1$

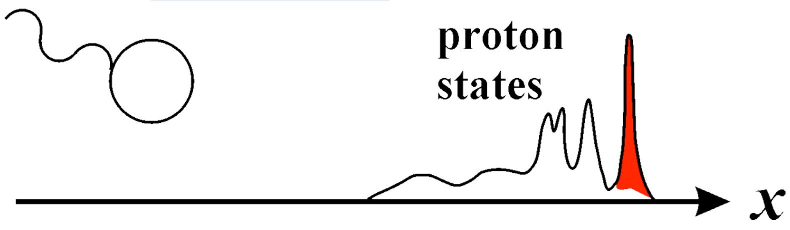

excit^{ns}
W>M

$$x < 1$$

$Q^2R^2 >> 1$

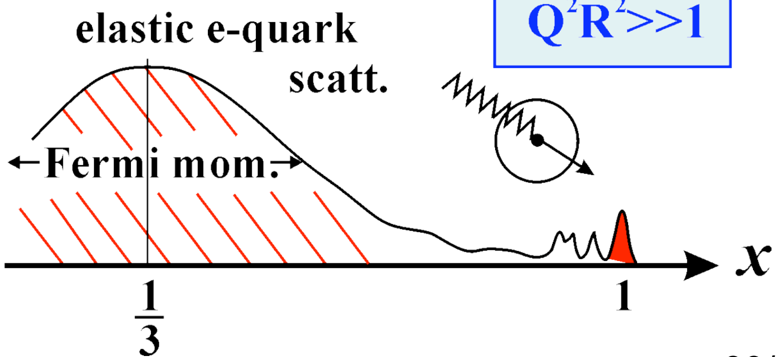

e-quark
scatt:

$$x = \frac{1}{3}\left(\frac{Q^2}{2p_q.q}\right) = \frac{1}{3}$$

$$p_q \sim \frac{1}{3}p$$

Replay : e - proton scatt.

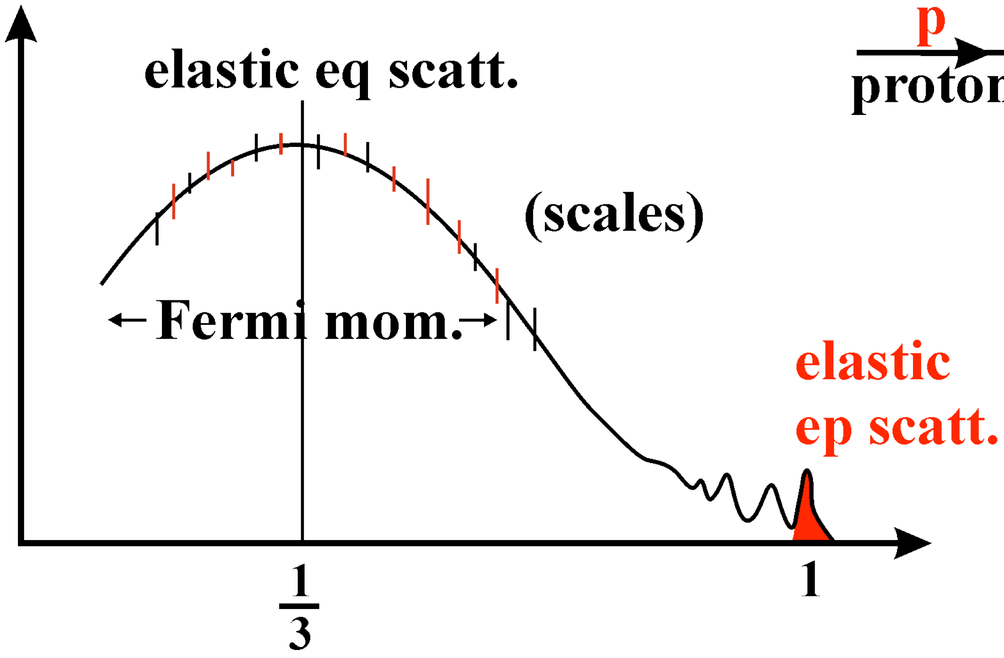

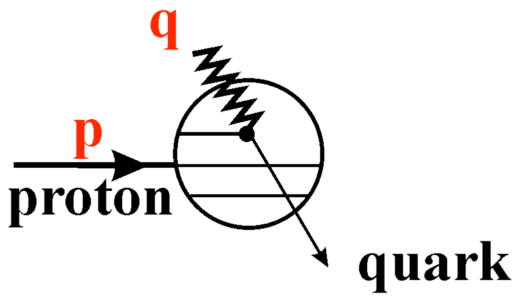

$$x = \frac{Q^2}{2p.q}$$

Bjorken scaling variable

Replay : e - proton scatt.

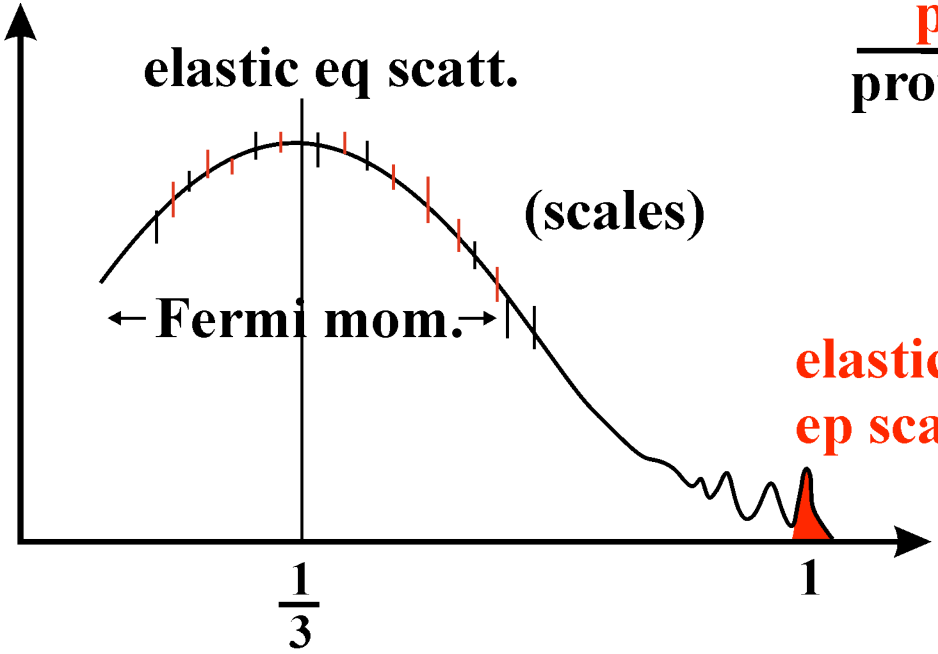

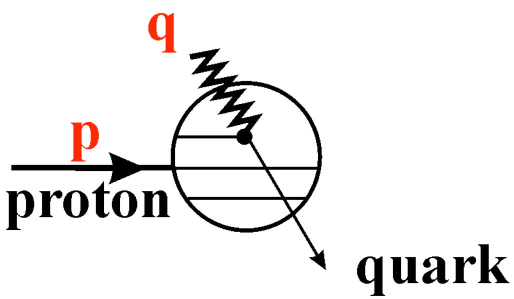

$$x = \frac{Q^2}{2p.q}$$

Bjorken scaling variable

Increase Q further

Another replay ?

peak at $x = \frac{1}{12}$?

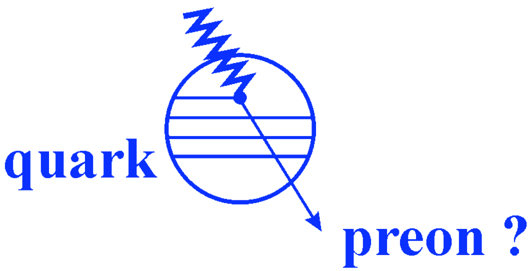

No evidence of q substructure

Instead of finding q substructure

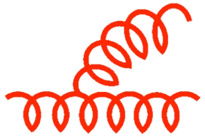

find QCD

(**compare QED** )

eg.

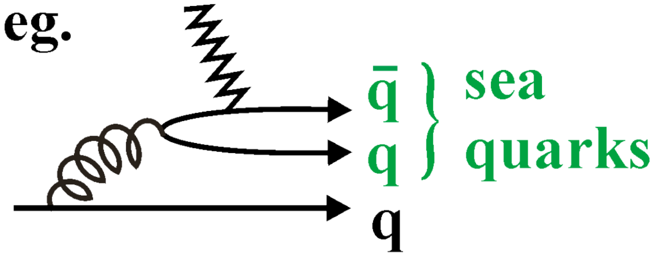

Consequence :
as Q^2 increases, more and more partons are involved.
Each parton, on average, must have smaller x.

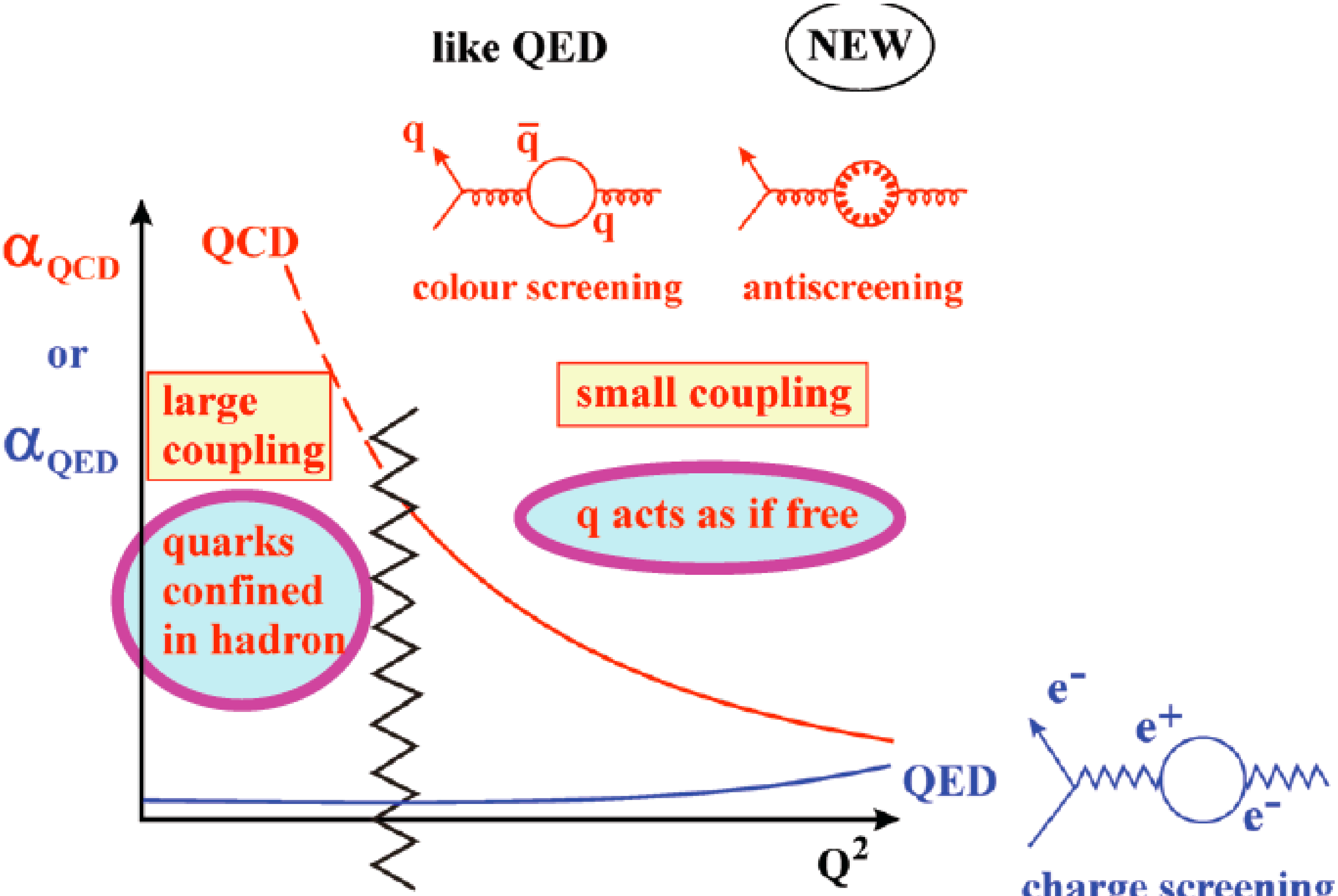

(pQCD predicts running, but not absolute value, of α_{QCD})

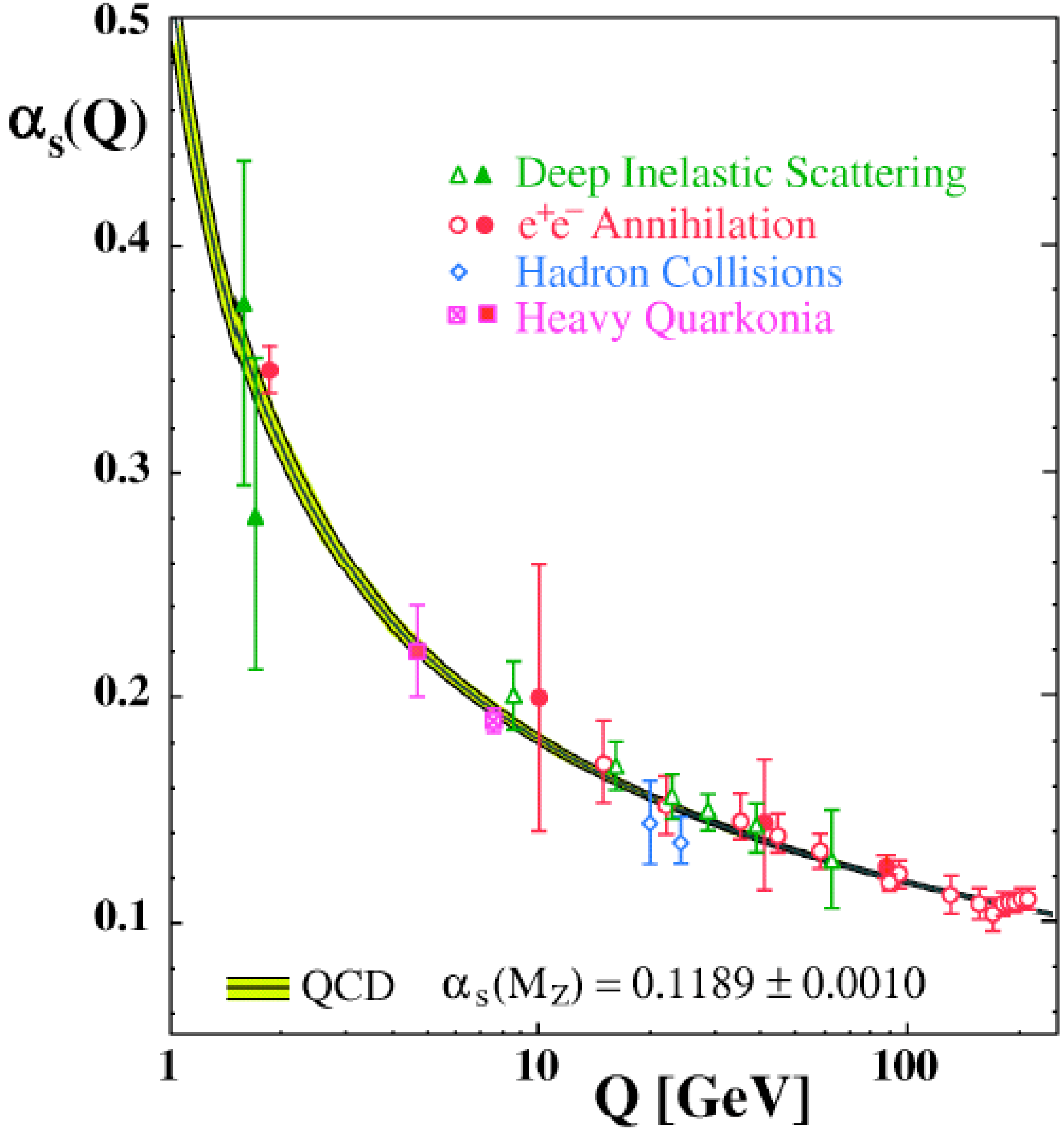
0.5
0.4
0.3
0.2
0.1
αs(Q)
Deep Inelastic Scattering
e+e− Annihilation
Hadron Collisions
Heavy Quarkonia
QCD αs(MZ) = 0.1189 ± 0.0010
1
10
100
Q [GeV]

As Q^2 increases, each parton has, on average, smaller x

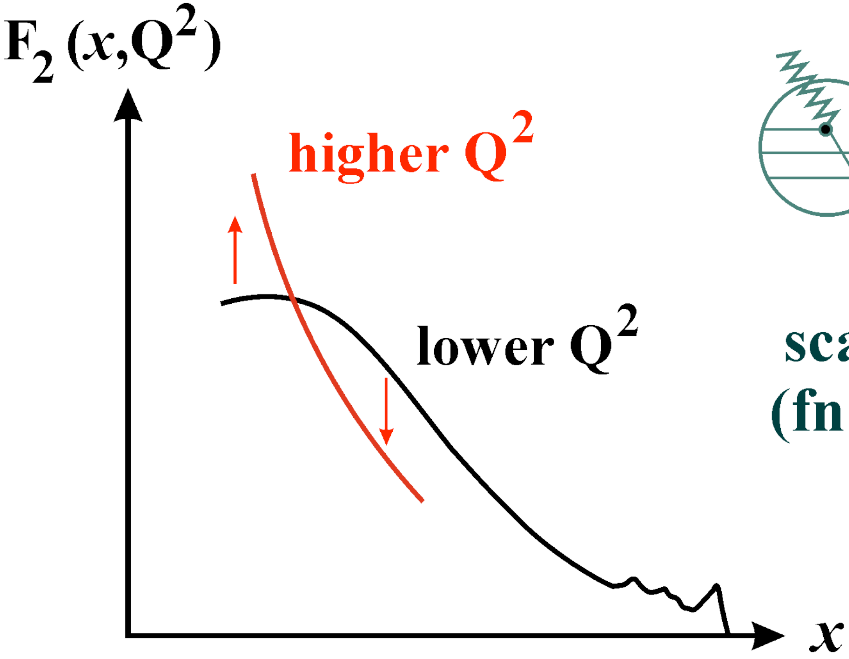

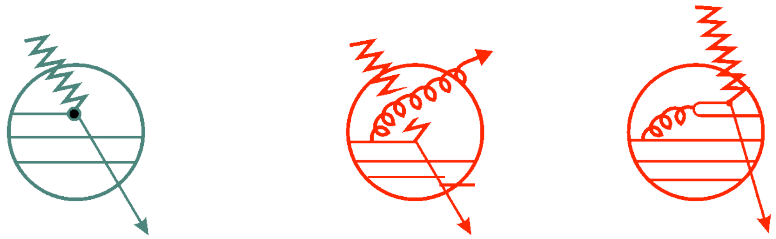

scaling part (fn of x only) $+ \alpha_s P \log \frac{Q^2}{\mu^2}$

QCD scaling violations (x,Q^2)

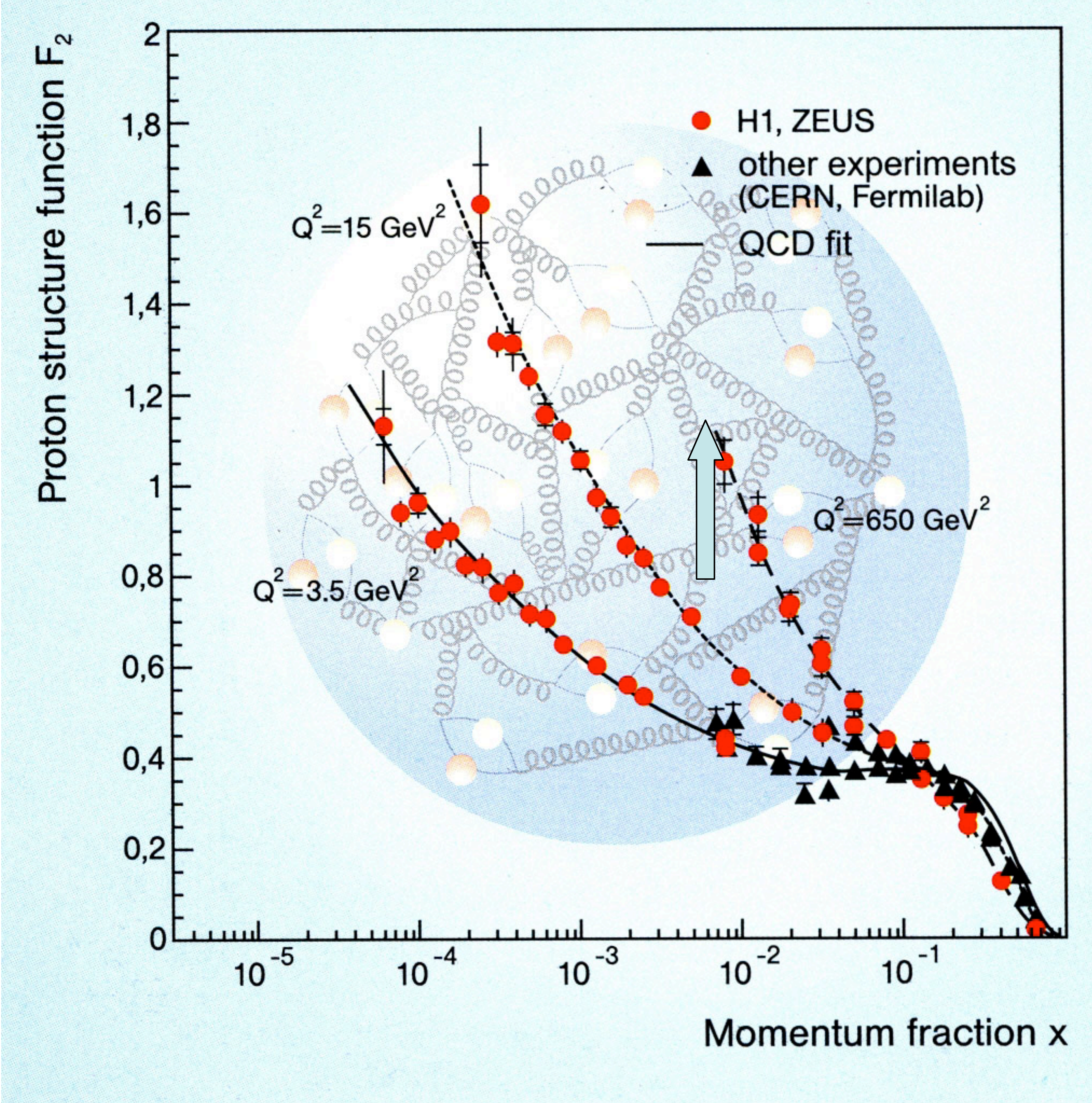
Proton structure function F_2
H1, ZEUS
other experiments (CERN, Fermilab)
QCD fit
Q^2=15 GeV^2
Q^2=650 GeV^2
Q^2=3.5 GeV^2
Momentum fraction x

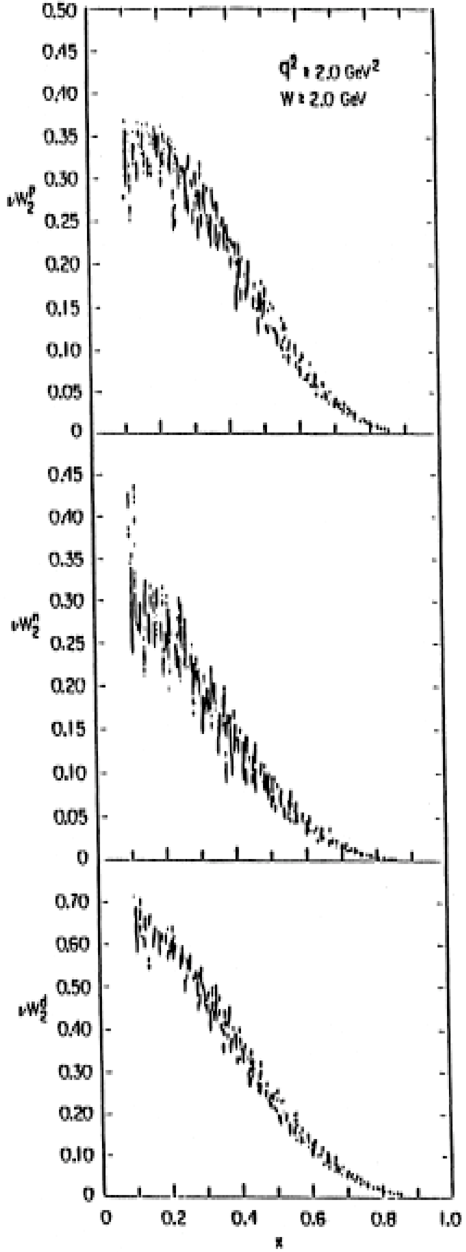
q^2 = 2.0 GeV^2
W = 2.0 GeV

Determination of parton distributions

Parametrise x dep. at low pQCD scale Q_0^2 $\longrightarrow$ $f_i(x, Q_0^2)$

Evolve up in Q^2 using DGLAP eqs. $\longrightarrow$ $f_i(x,\; Q^2 > Q_0^2)$

Global fit to HERA + all related data $\longrightarrow$ f_i's

HERA kinematic domain

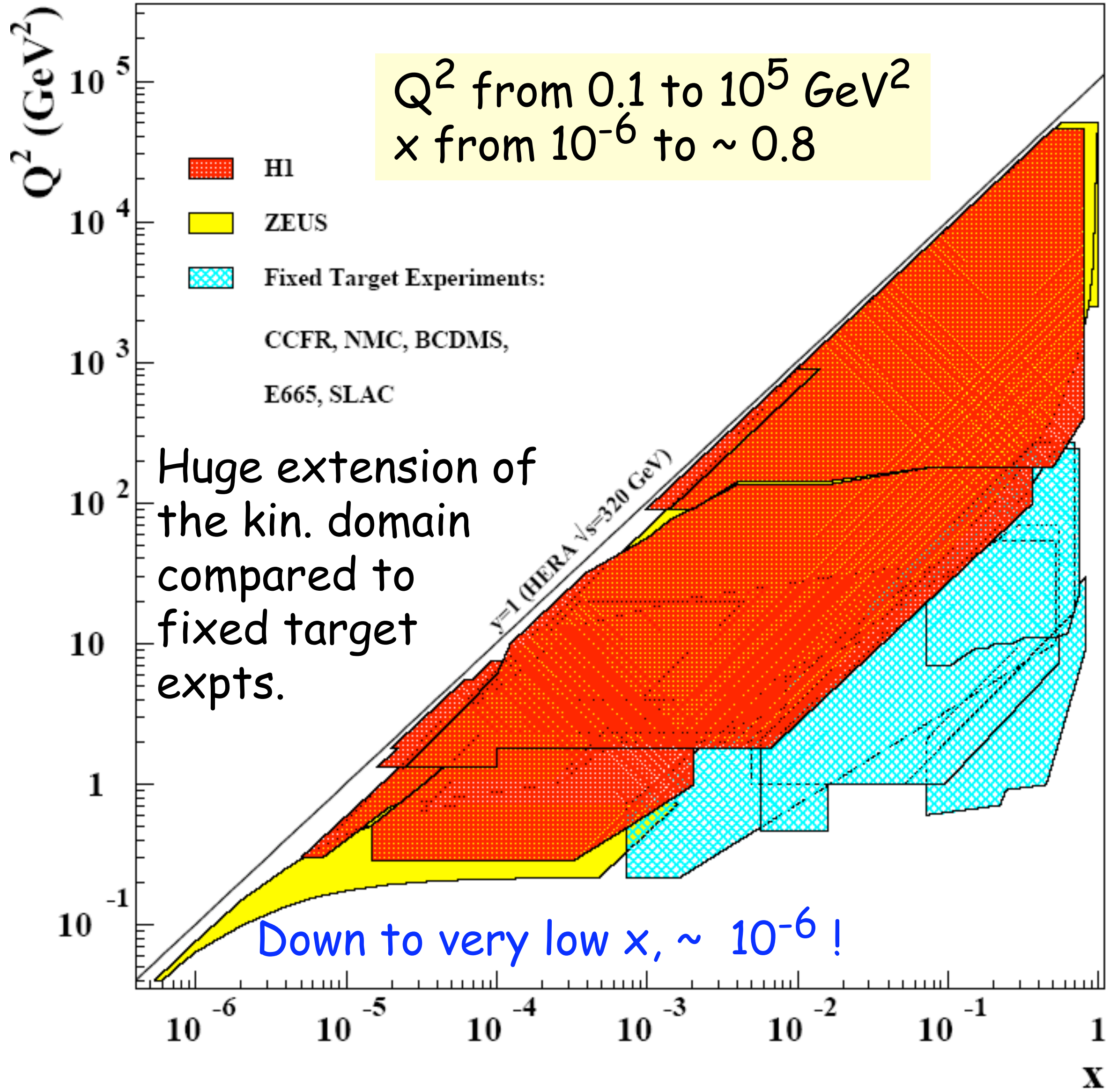

Up to very high Q^2 ~ 10^5 GeV^2

$Q^2 = xyS$ with
$S = (320)^2 \sim 1.2\ 10^5$ GeV^2

For Q^2 above ~ 1 GeV^2 (perturbative regime), x down to ~ 10^{-5}

Very low Q^2 accessible, allow to study the pert – non-pert transition region.

30 GeV e beam against 920 GeV p beam

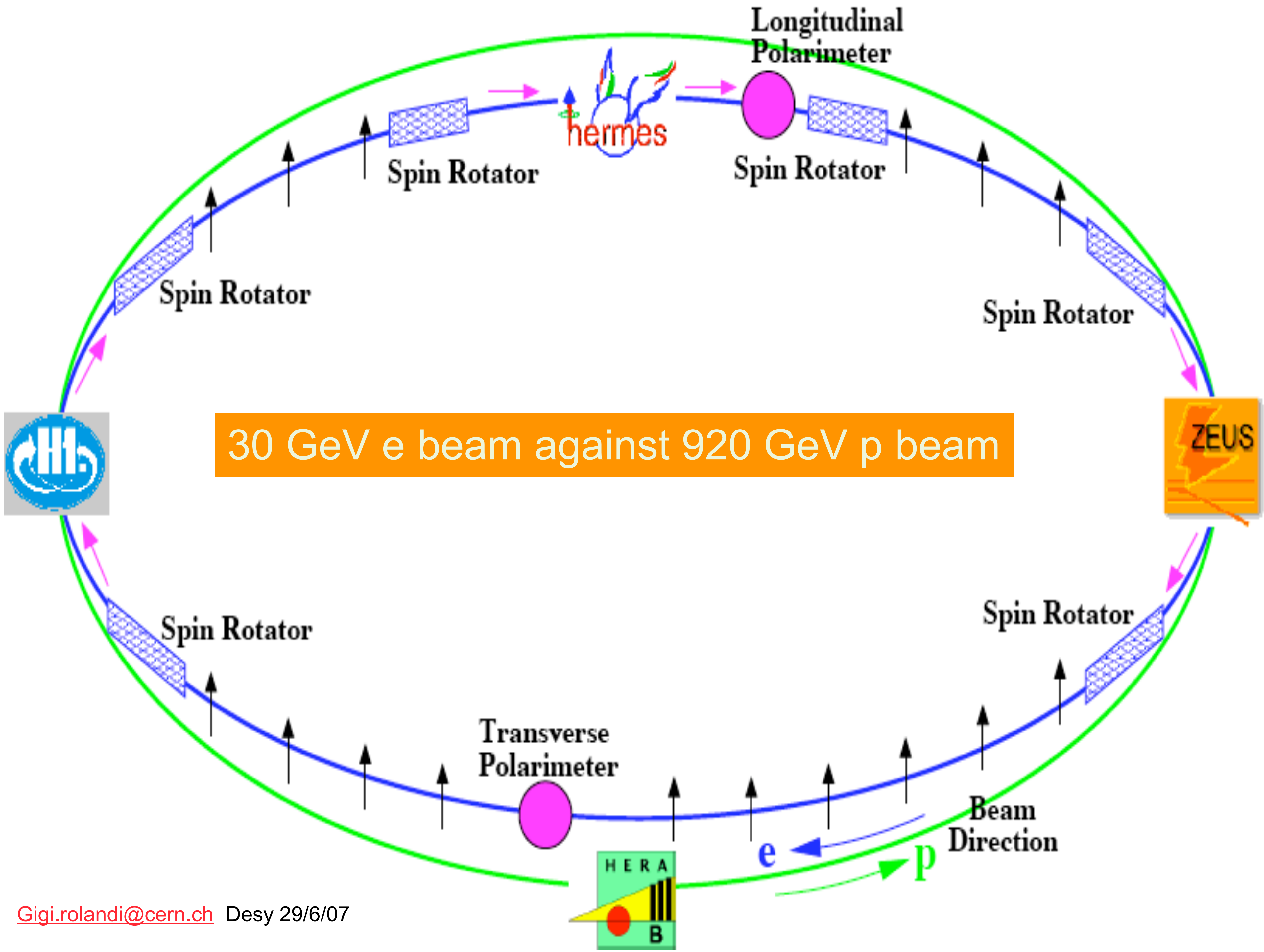

Measurement of the structure of the proton at HERA

The measurement of the structure functions at the high Q^2 values requires calorimetric measurements of the scattered electron and of the hadronic final state formed by the struck proton constituents.

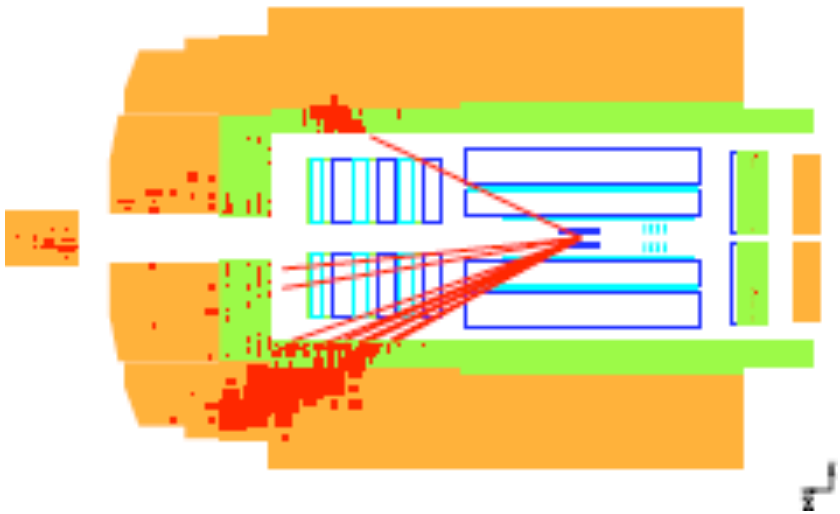

H1

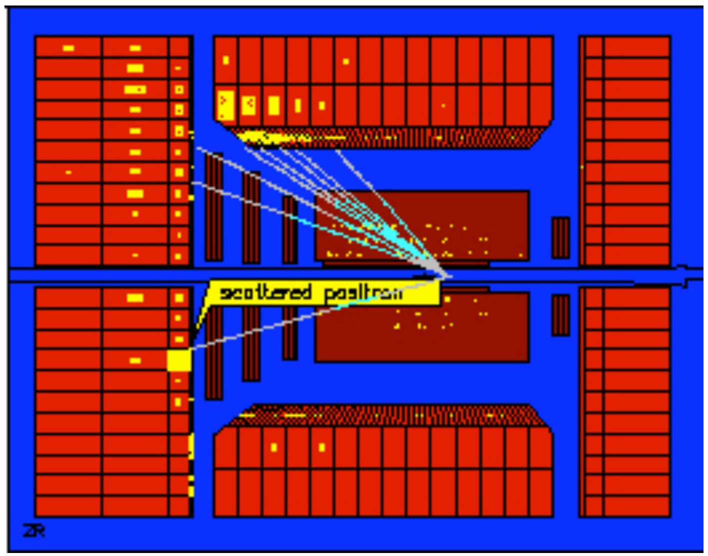

ZEUS

ZEUS Calorimeter

Very hermetic: covering up to $\eta<5$ in the forward direction and Q^2 ~0.1 GeV^2 in the rear direction. Main part is the Depleted Uranium Compensated Sampling Scintillator Calorimeter. Built in e/h ~ 1 tuning U/scintillator thickness. Readout by 12,000 phototubes. Gate time ~ 1 BX.

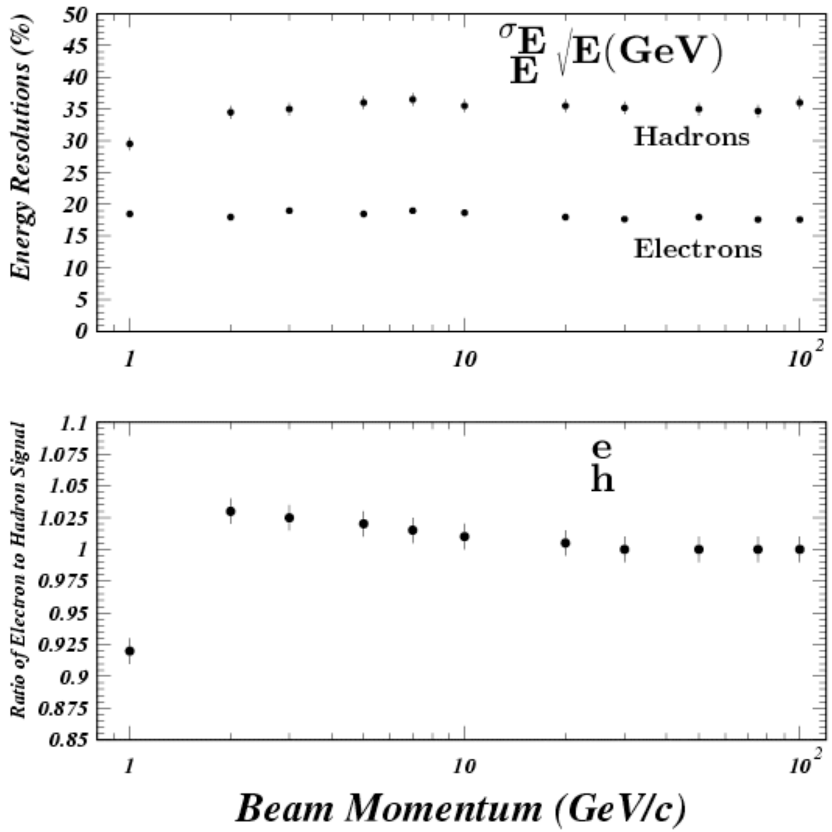

ZEUS Calorimeter

Time information from the sampled signal shape. Very important for background rejection.

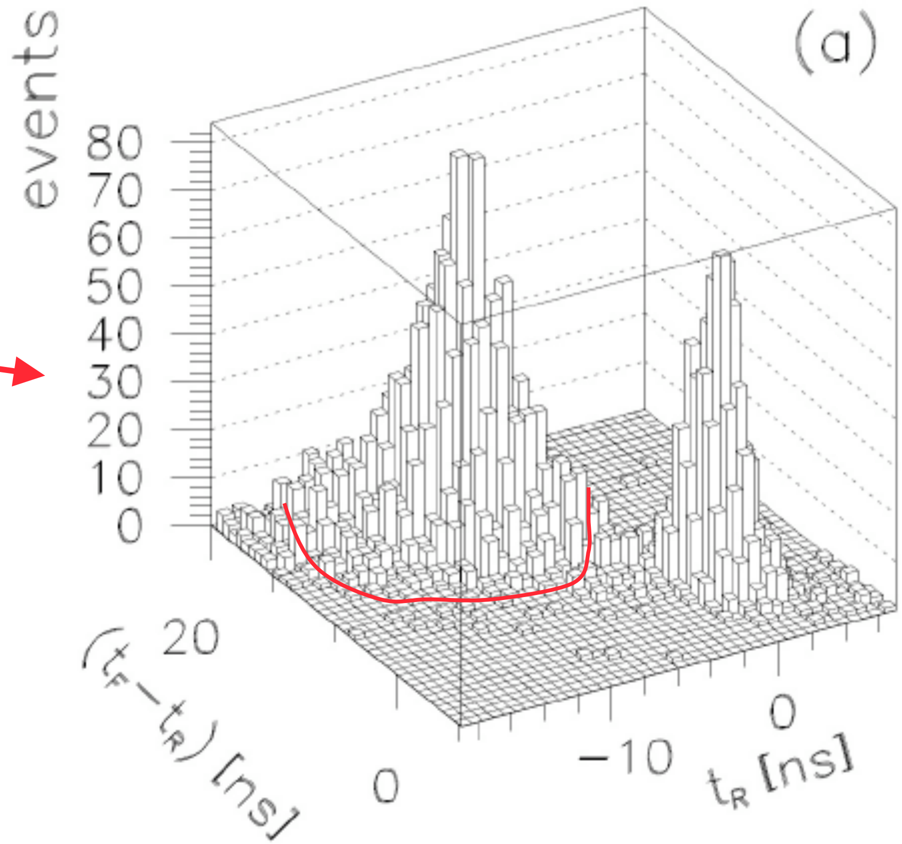

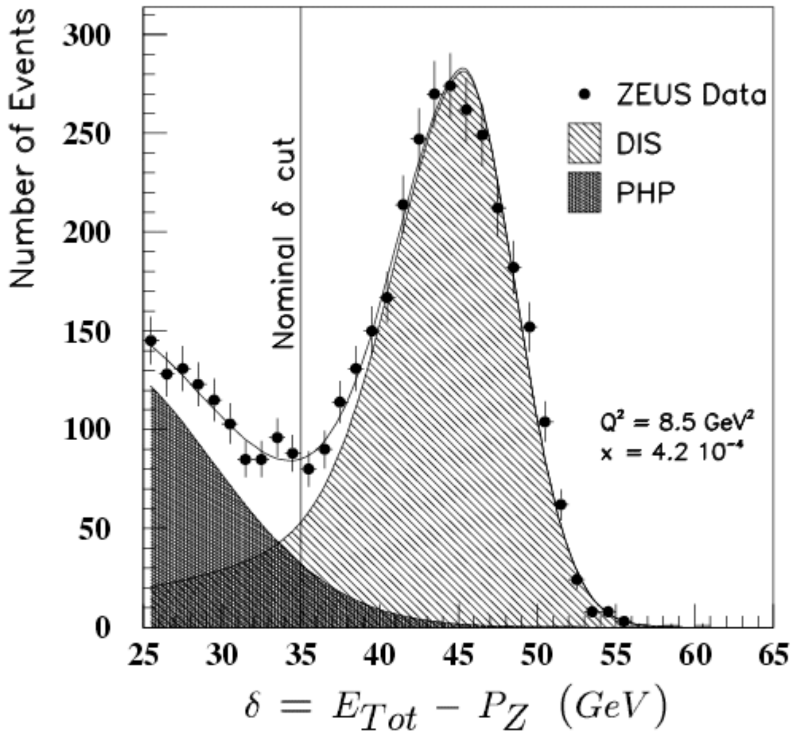

Good calorimeter energy resolution allows to separate efficiently DIS events from photoproduction

H1 Calorimeter

Large coil to minimize the amount of material in front of the Liquid Argon calorimeter.

Easy calibration and fine granularity which allows to separate electrons from pions to high degree. Homogeneity of the response and overall hermiticity are helpful for missing energy detection.

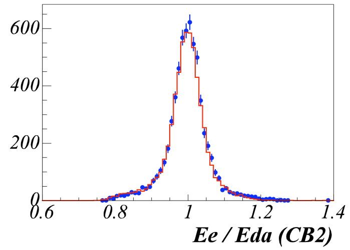

45,000 cells readout. 65,000 electronics channels. 1/3 of the cells readout with two different gains. Shaping time ~ 25 BX

Mean fractional energy shift from absolute energy scale

Syst. uncertainty on energy (0.7% - 3%)

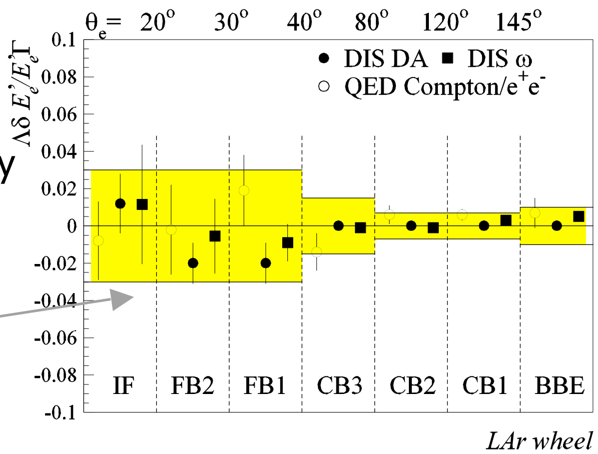

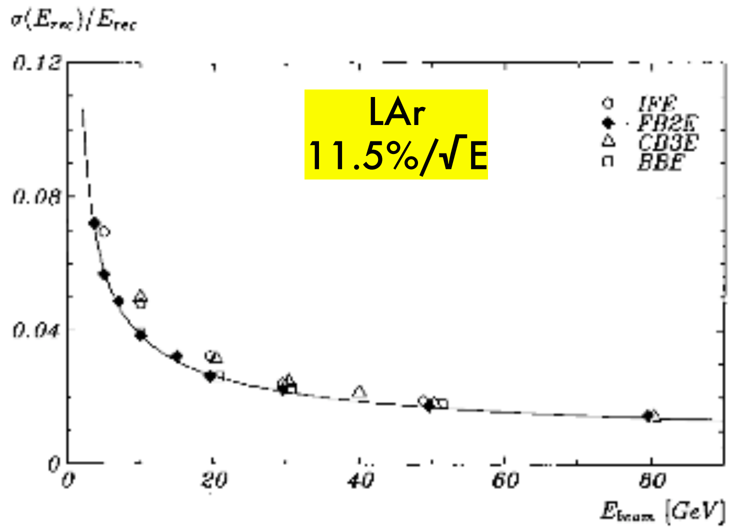

DA : Double Angle method => use only angles of scattered electron and hadronic FS

H1 Calorimeter Software Compensation

Weighting technique for reconstruction of hadrons due to the non compensating calorimetry. High cell signal density indicates electromagnetic signal.

$$E_{tot} = \sum_{cells} w_{cell} E_{cell}$$

Resolution improves to $\frac{50\%}{\sqrt{E(GeV)}}$

Constant term goes from 9% to 3%

This technique is a basis for hadronic calibration of the ATLAS calorimeter

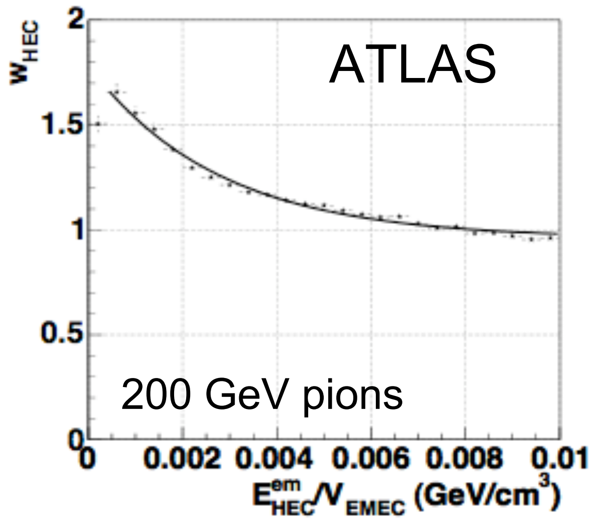

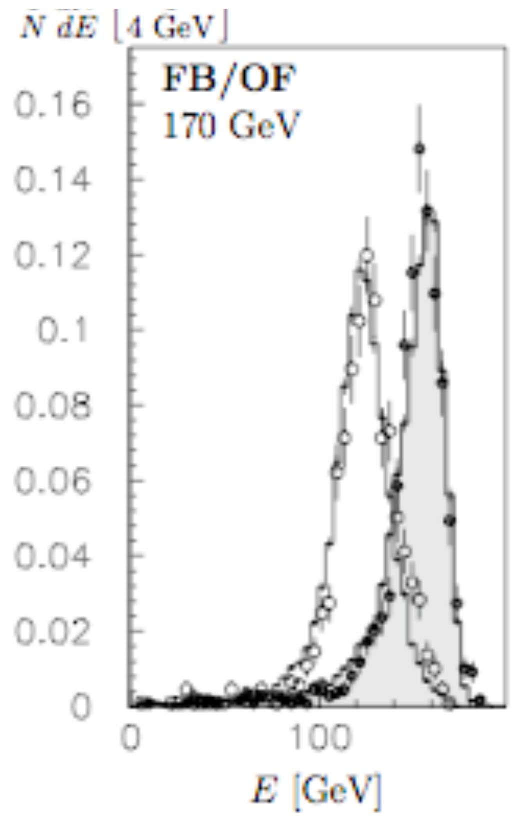

Charged and Neutral current cross sections

$$\frac{d^2\sigma^{\rm NC}(e^\pm p)}{dxdQ^2} = \frac{2\pi\alpha^2}{xQ^4}\left[Y_+ F_2(x,Q^2) - y^2 F_L(x,Q^2) \mp Y_- xF_3(x,Q^2)\right],$$
$$Y_\pm = 1 \pm (1-y)^2$$

$F_2 = \sum e^2_{qi} [q_i(x) + \bar{q}_i(x)]$

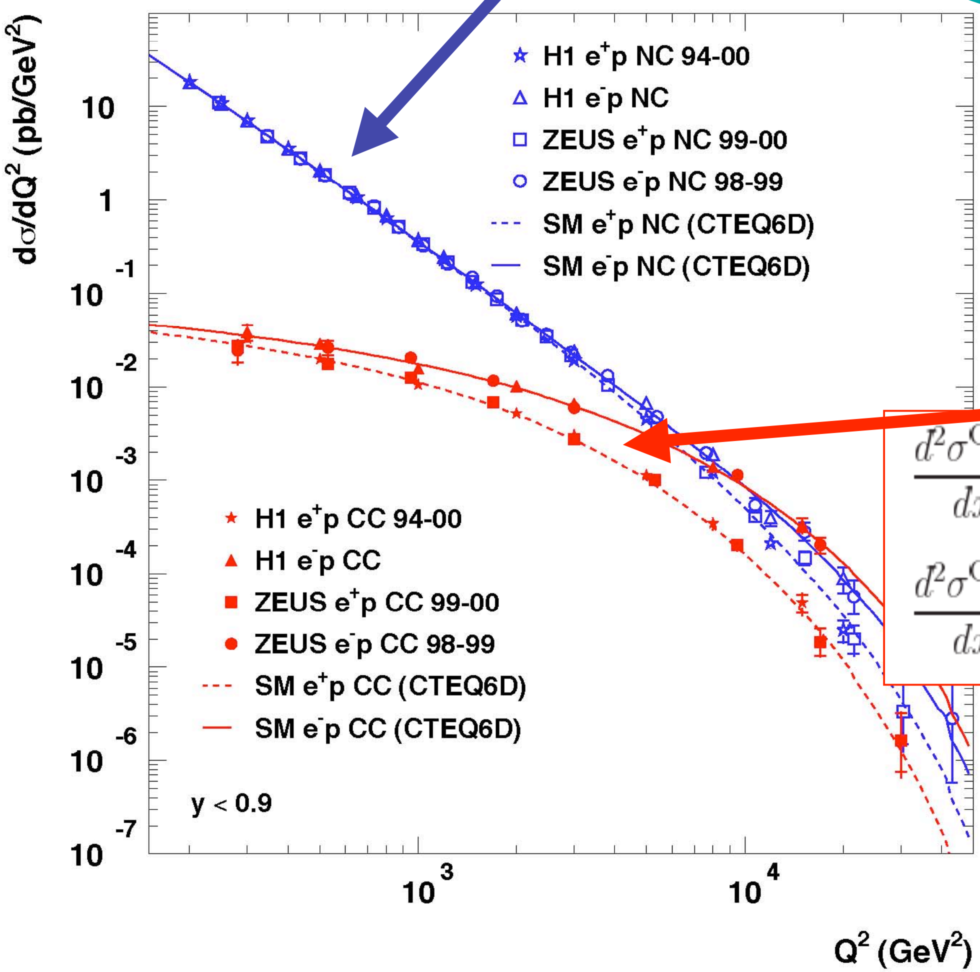

$$\frac{d^2\sigma^{\rm CC}(e^+p)}{dxdQ^2} = \frac{G_F^2 M_W^4}{2\pi x(Q^2+M_W^2)^2}x\left[(\bar{u}+\bar{c}) + (1-y)^2(d+s)\right],$$

$$\frac{d^2\sigma^{\rm CC}(e^-p)}{dxdQ^2} = \frac{G_F^2 M_W^4}{2\pi x(Q^2+M_W^2)^2}x\left[(u+c) + (1-y)^2(\bar{d}+\bar{s})\right],$$

Polarized e+ and e- scattering

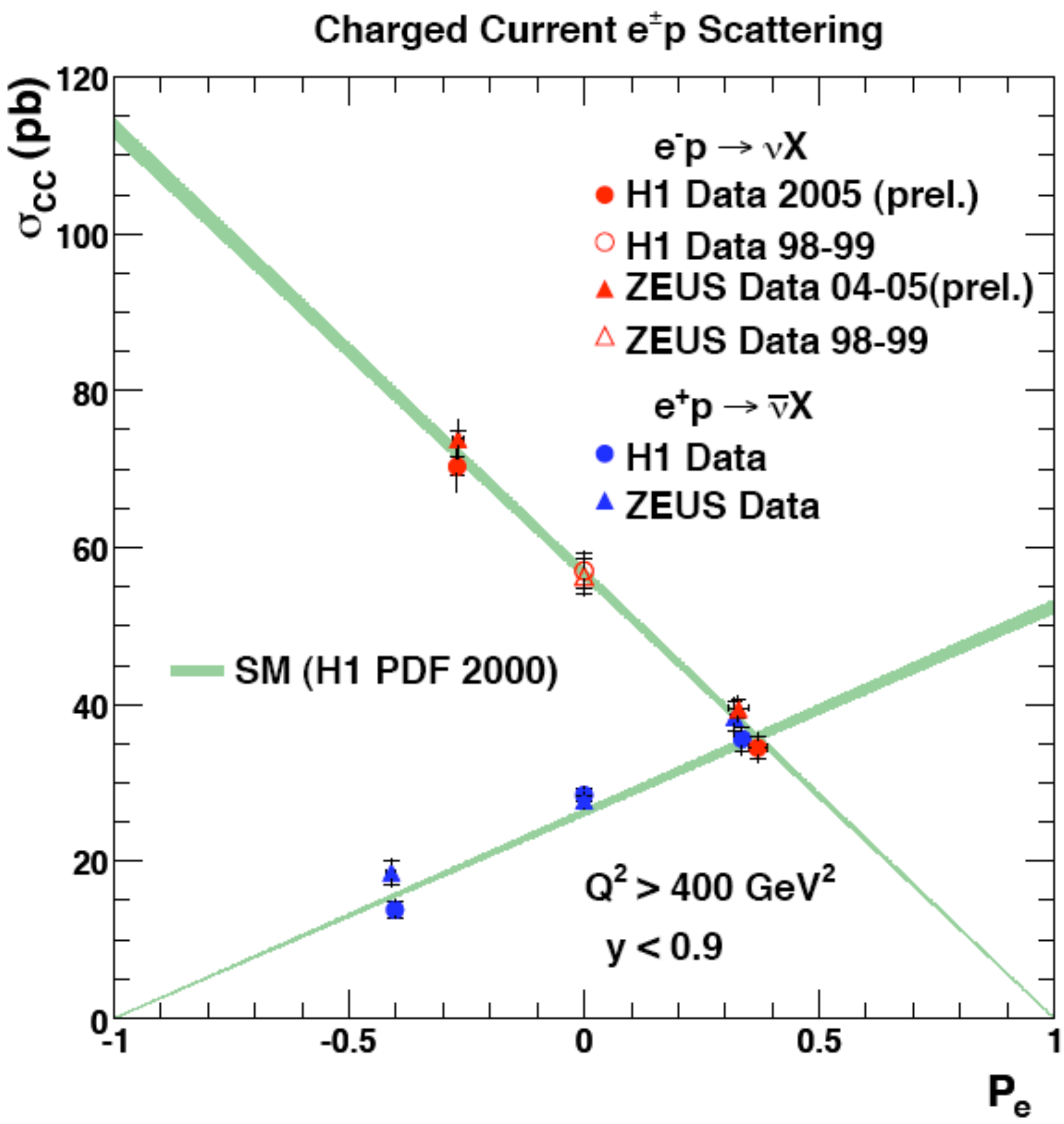

Gluon Density and low x physics

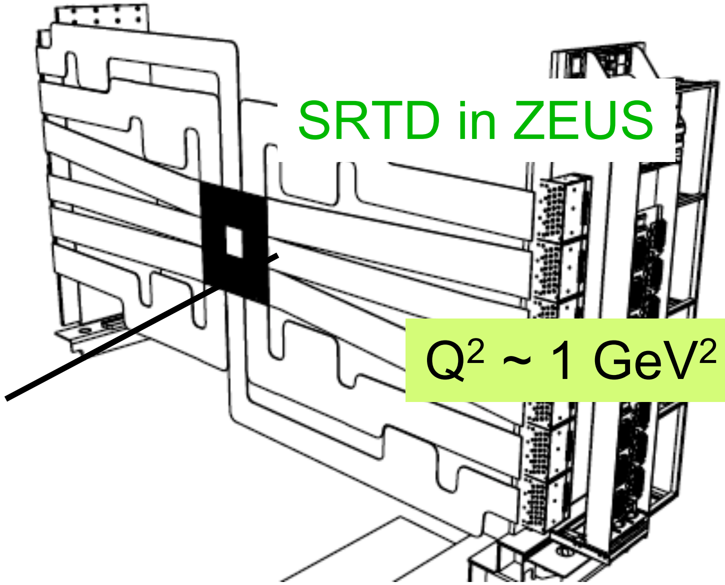

$Q^2 \sim 1\ GeV^2$

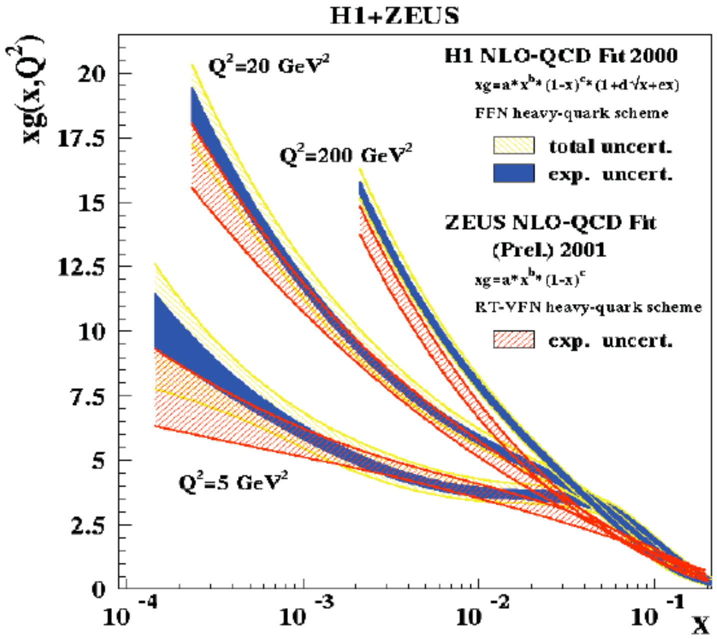

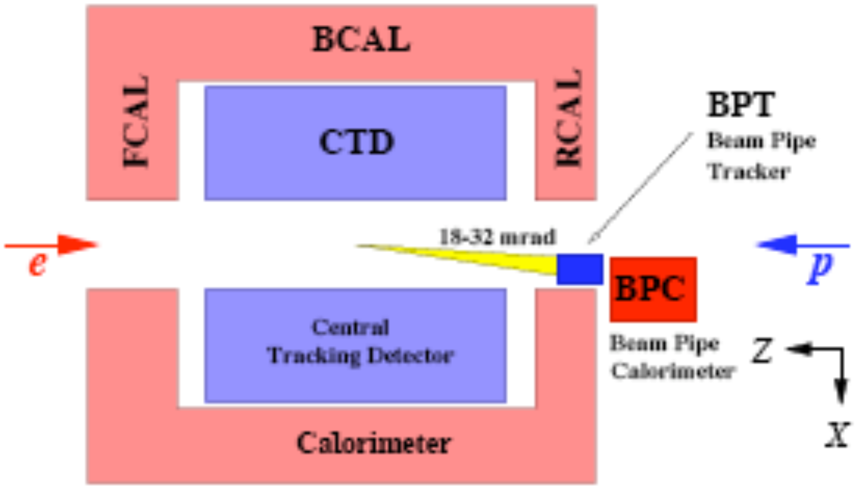

$Q^2 \sim .1\ GeV^2$

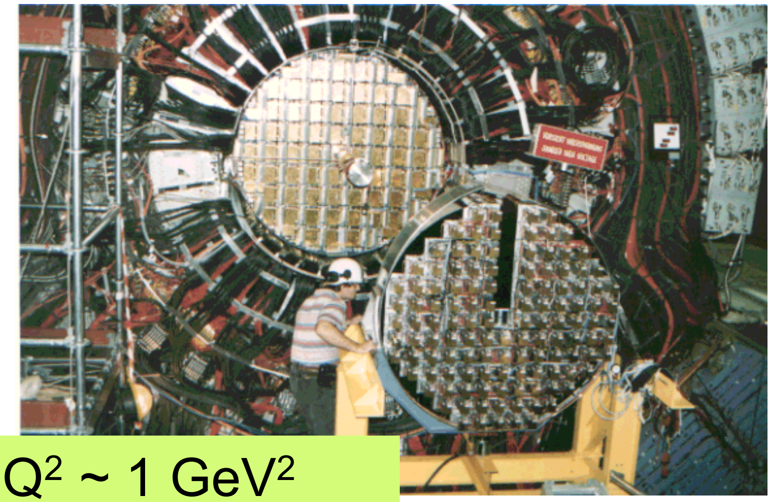

$Q^2 \sim 1\ GeV^2$

Installation of SPACAL in H1

With increasing luminosity, important statistics over the full kinematics domain.

- Good agreement between H1 and ZEUS
- and with fixed target measurements

- Strong scaling violations observed at low x – sign of a large gluon density ($g \to qq$)
- Negative scaling violations at high x ($q \to qg$, a high x quark splits into a gluon and a lower x quark)

Overlaid curves are the results of QCD fits based on the DGLAP equations (see later).

Within DGLAP : via $\partial F_2/\partial \ln Q^2$, access to the gluon density.

Excellent agreement with DGLAP, over 5 orders in magnitude in Q^2 and 4 orders of magnitude in x.

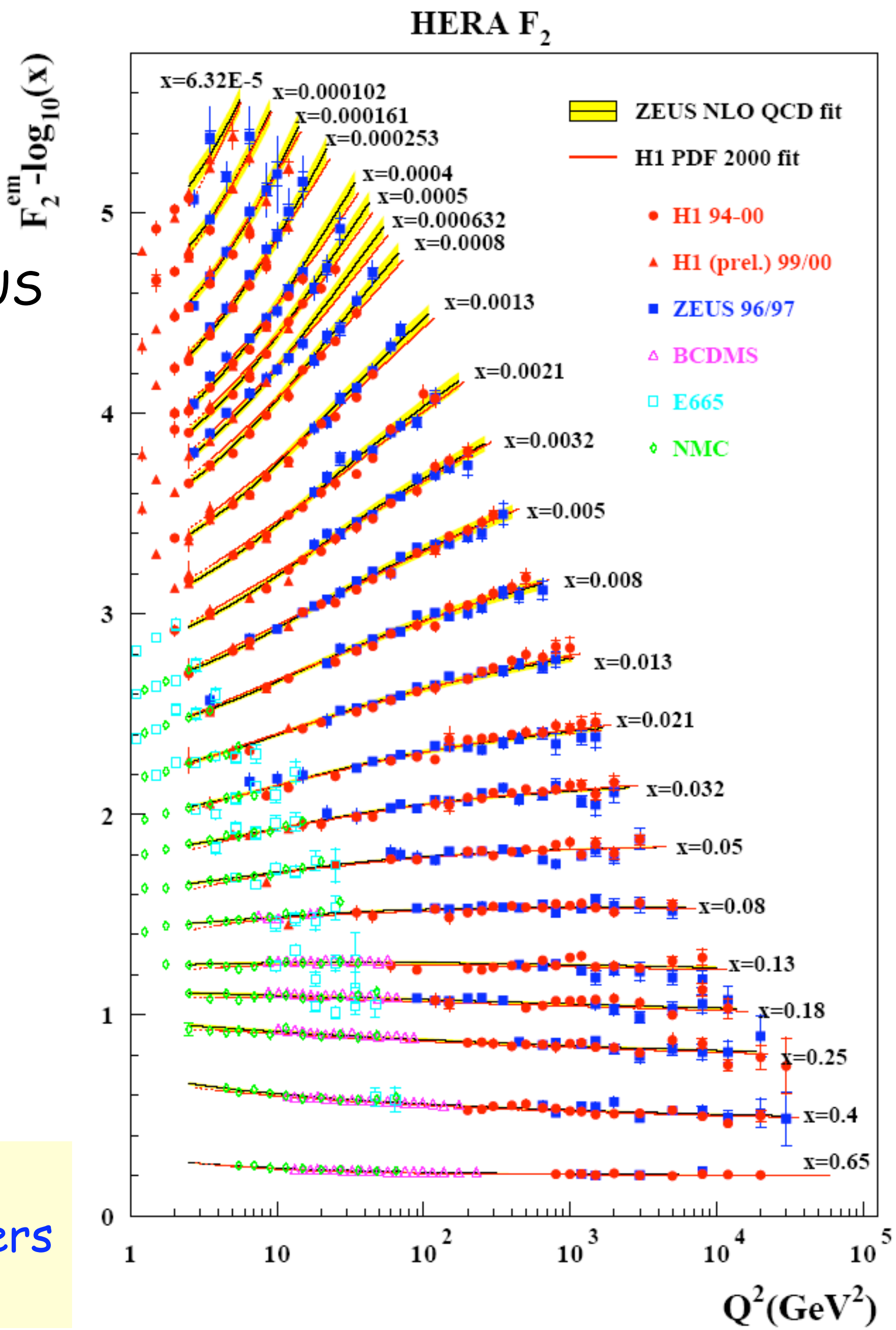

The charm and beauty contents of the proton

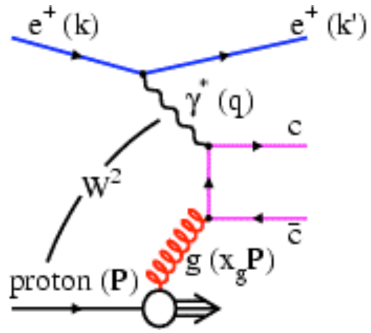

- Exclusive measurements :
  $D^* \rightarrow D^0\, \pi_{slow} \rightarrow K\, \pi\, \pi_{slow}$
  and $b \rightarrow \mu X$, exploiting $P_{T,rel}(\mu)$ and impact parameter

- Semi-inclusive measurements :
  distributions of the significance of track impact parameters are used to fit simultaneously the light q, c and b contributions to F2.
  Use silicon vertex devices around the interaction point.

H1 Central Silicon Tracker

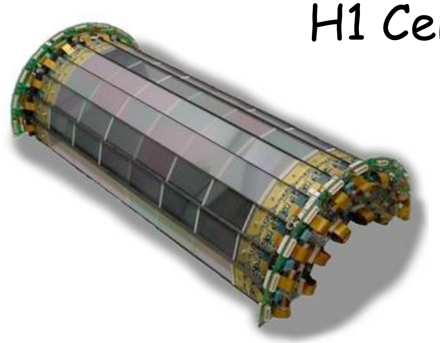

2 cylindrical layers, at radii of ~ 5 cm and ~ 10 cm.
Impact parameter resolution:

$$33\mu m \oplus \frac{90\mu m}{P_T}[GeV]$$

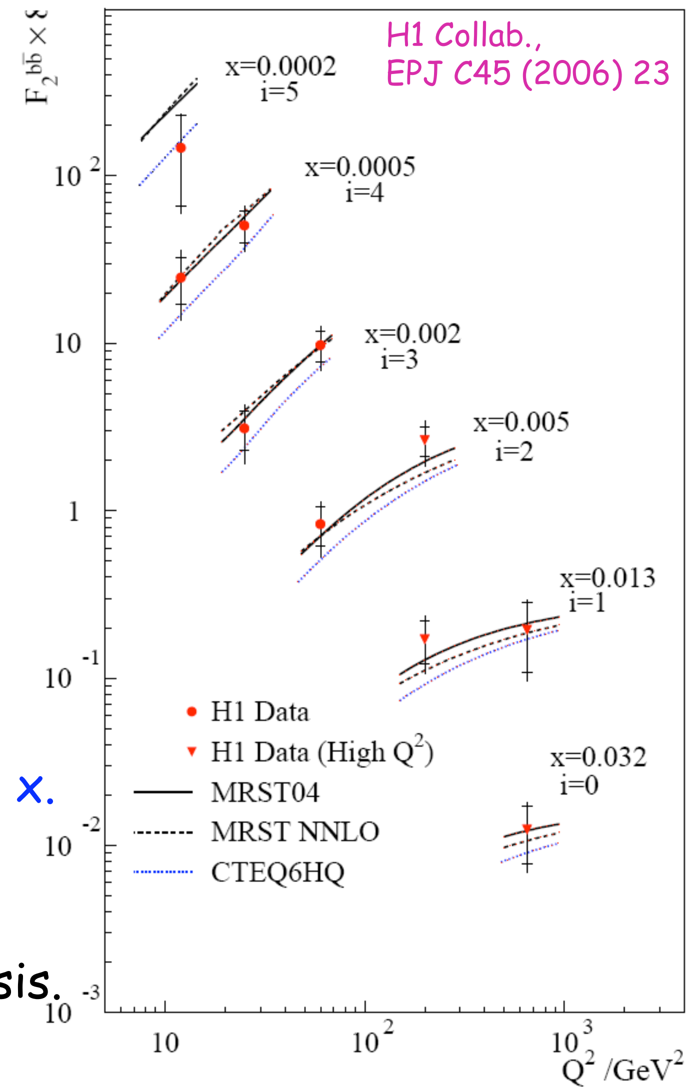

As F_2, $F_2^{bb,cc}$ shows large scaling violations at low x.

Note the difference between the MRST and CTEQ predictions.
Data now included in the most recent CTEQ analysis.

PDFs from Global Fits

Global fits performed mainly by the MRST (now MSTW) and the CTEQ groups.

Non-inclusive DIS data that are usually included :
- Tevatron jet cross-sections → high x gluon
- Drell-Yan measurements pN → $\mu\mu$ → large x sea, $\bar{d} - \bar{u}$
- Dimuon production in νN and $\bar{\nu}$ N ($\nu_\mu s \to \mu c \to \mu\mu X$) → s and $\bar{s}$
- η asymmetry of W production at Tevatron → d/u at medium x

Recent fits also include HERA jet data and F_2^b & F_2^c measurements.

Some data used to be included in global fits, as prompt photon production which in principle brings constraints on the gluon density – but hampered by too large theoretical uncertainties.

Typically this leads to ~ 2000 points in the fits, with a large number of systematic error sources (see later…)

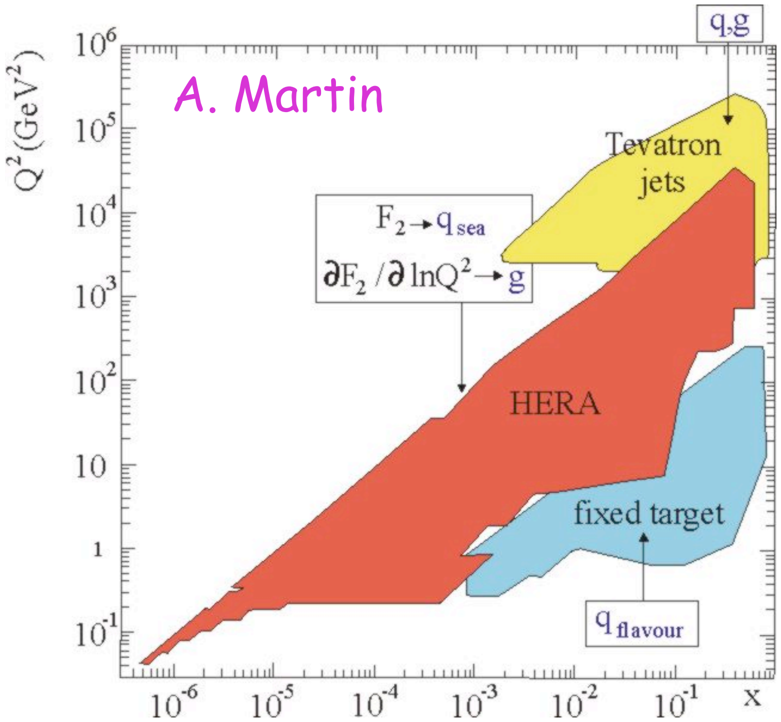

PDFs from Global Fits

Formalism
NLO DGLAP
MSbar factorisation
Q_0^2
functional form @ Q_0^2
sea quark (a)symmetry
etc.

$f_i(x,Q^2) \pm \delta f_i(x,Q^2)$

$\alpha_S(M_Z)$

Data
DIS (SLAC, BCDMS, NMC, E665, CCFR, H1, ZEUS, …)
Drell-Yan (E605, E772, E866, …)
High E_T jets (CDF, D0)
W rapidity asymmetry (CDF)
νN dimuon (CCFR, NuTeV)
etc.

Who?
Alekhin, CTEQ, MRST, GGK, Botje, H1, ZEUS, GRV, BFP, …

http://durpdg.dur.ac.uk/hepdata/pdf.html

LHAPDFv2

CDF: Jet Cross Sections @ NLO pQCD (1)

→ Results $|y^{Jet}| < 2.1$

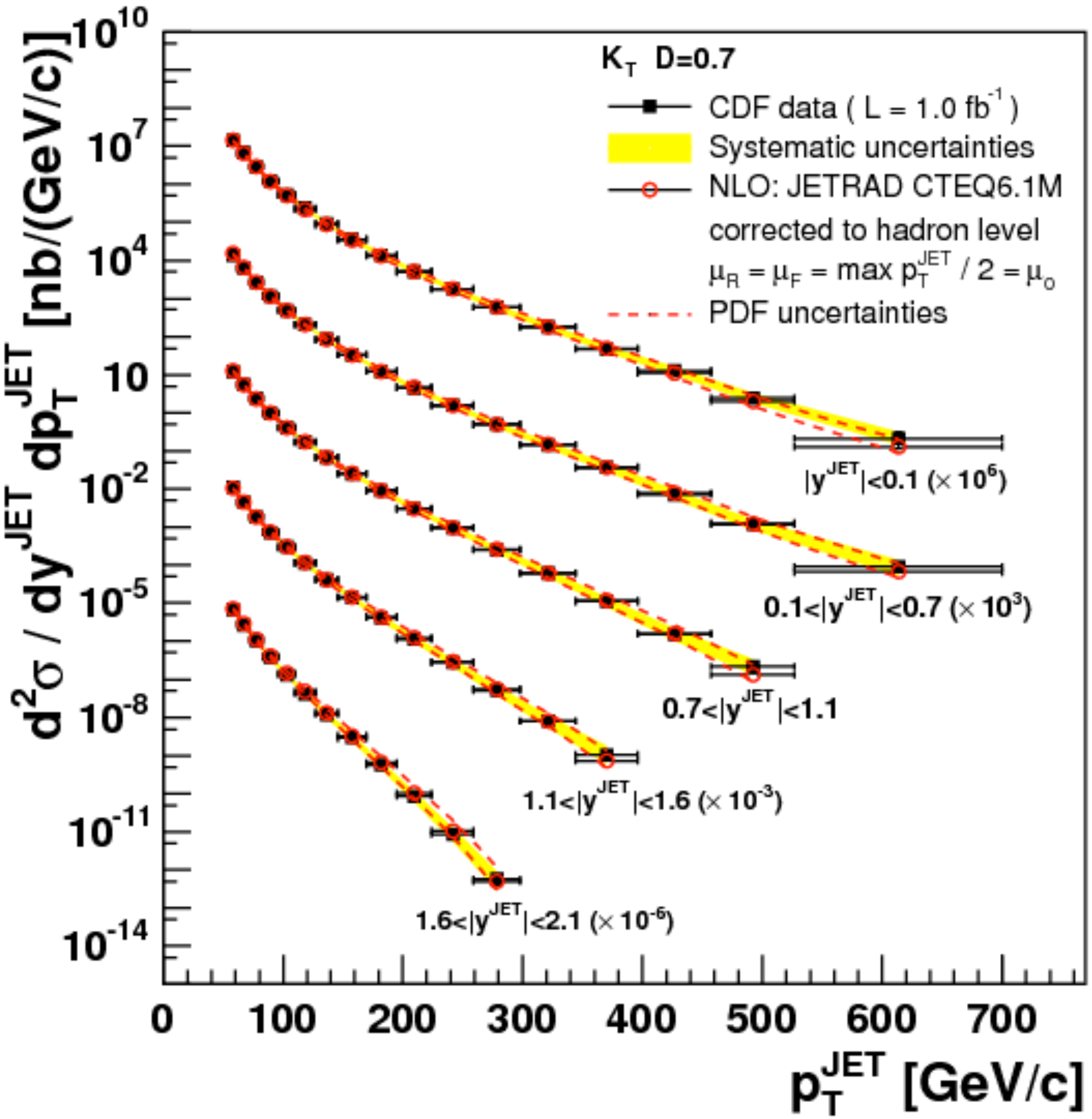

Good agreement with NLO pQCD

CDF: Jet Cross Sections @ NLO pQCD (2)

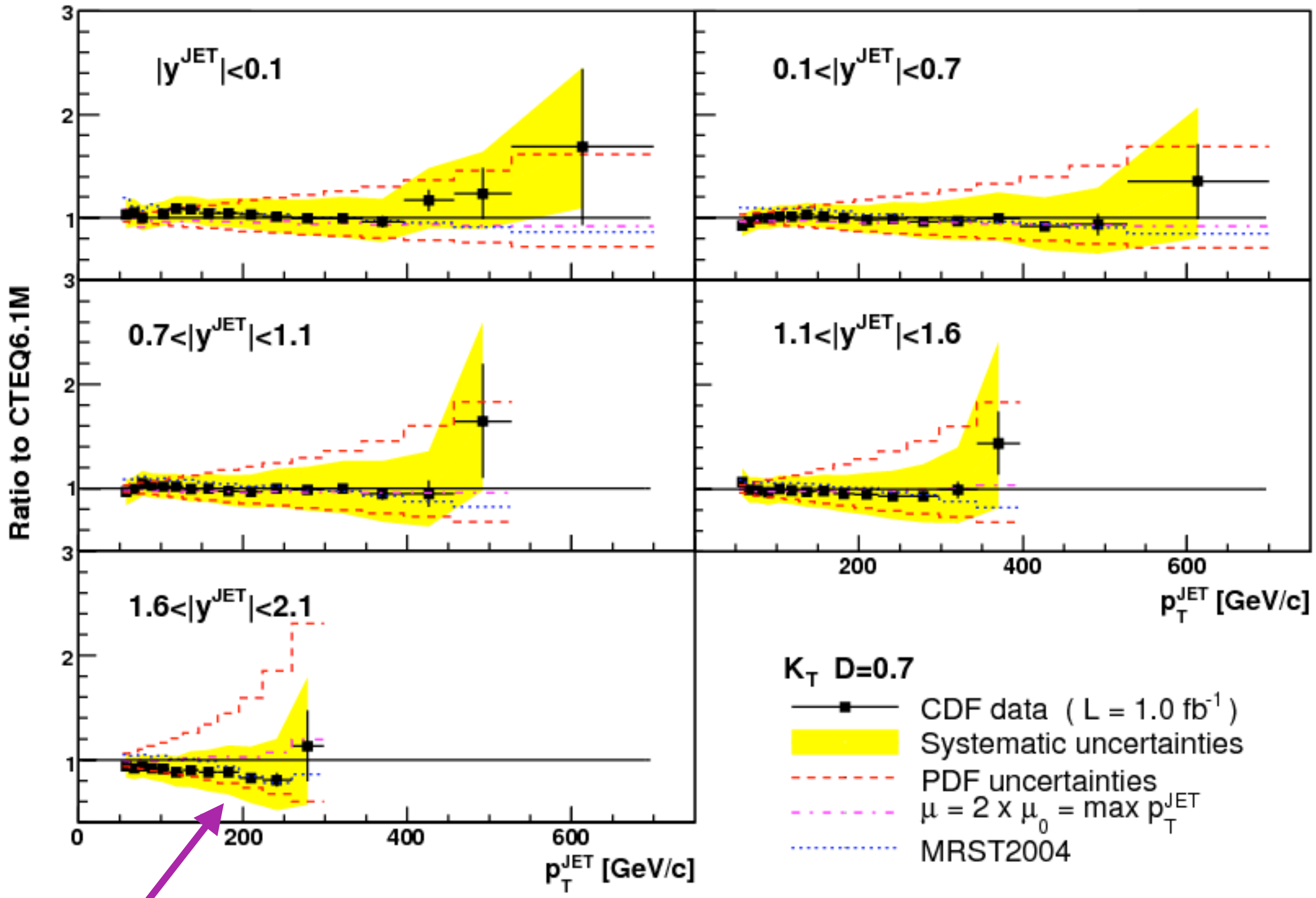

Measurements in the forward region contribute to a better understanding of the gluon PDF

Drell-Yan measurements → constraints on $\bar{d} - \bar{u}$

$\bar{d} = \bar{u}$ was a "natural" assumption in global fits, until the NA51 experiment (CERN) reported that $\bar{d} > \bar{u}$ at x = 0.18 (some hints before from NMC…)

Follow-up by E866 (Fermilab) : fixed target, DY in pp and pd, E_{beam} = 800 GeV.

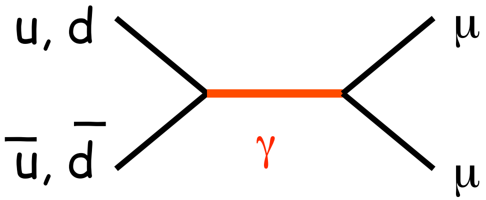

$x_1 = x_{Beam}$, $x_2 = x_{Target}$

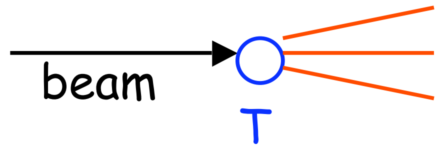

$x_1 > x_2$

For $x_1 \gg x_2$ one has :

$$\sigma_{pp}: \quad \frac{4}{9} u(x_1)\bar{u}(x_2) + \frac{1}{9} d(x_1)\bar{d}(x_2)$$

$$\sigma_{pn}: \quad \frac{4}{9} u(x_1)\bar{d}(x_2) + \frac{1}{9} d(x_1)\bar{u}(x_2)$$

$$\frac{\sigma_{pd}}{2\sigma_{pp}} \sim \frac{1}{2} \frac{\left[1 + \frac{1}{4}\frac{d(x_1)}{u(x_1)}\right]}{\left[1 + \frac{1}{4}\frac{d(x_1)}{u(x_1)}\frac{\bar{d}(x_2)}{\bar{u}(x_2)}\right]} \left[1 + \frac{\bar{d}(x_2)}{\bar{u}(x_2)}\right]$$

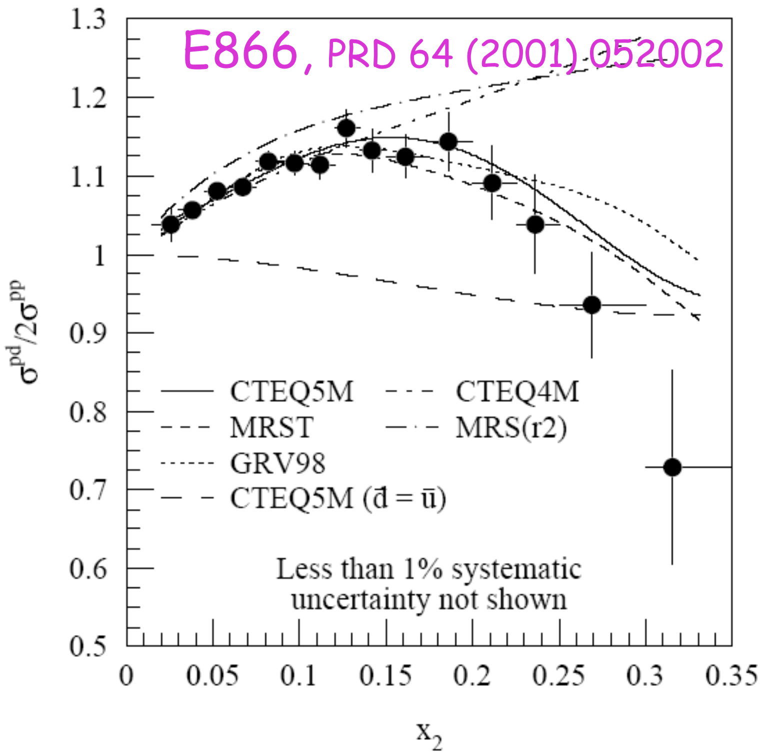

E866 measures this ratio down to < x_2 > ~ 0.03.

Note the spread of the predictions from pdfs before these data were included in the fits.

η asymmetry in W production at the Tevatron

Tevatron : $p\bar{p}$ collider, $\sqrt{s}$ = 1.8 TeV

$$x_{1,2} = (M^2_W / S) \exp(\pm \eta_W)$$

At central rapidity, $x_1 = x_2 \sim 2\ 10^{-3}$
At $\eta \sim 2.5$: $x_1 = 2\ 10^{-2}$, $x_2 \sim 2\ 10^{-4}$

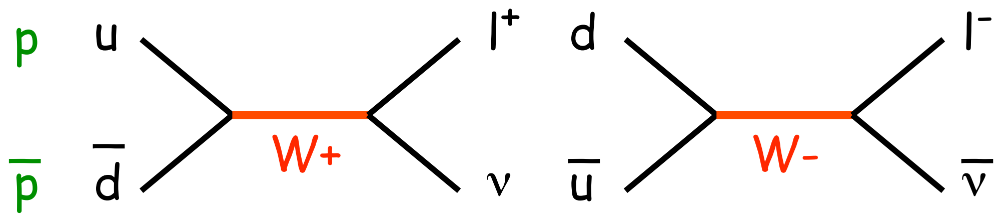

At large η : u(x1) > d(x2) hence W+ (W-) preferably emitted in the direction of the incoming proton (antiproton).

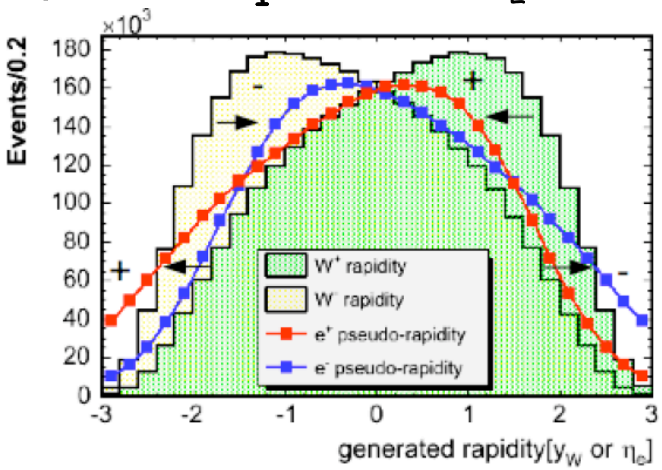

Asym. diluted when looking at η(lepton) :

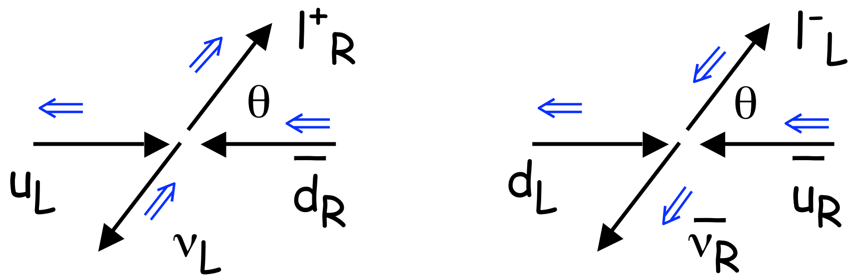

$(1 - \cos\theta^*)^2$ $(1 + \cos\theta^*)^2$

$\sigma(W+) - \sigma(W-) \sim$
$u(x_1)\, d(x_2)\, (1-\cos\theta)^2 - d(x_1) u(x_2) (1+\cos\theta)^2$

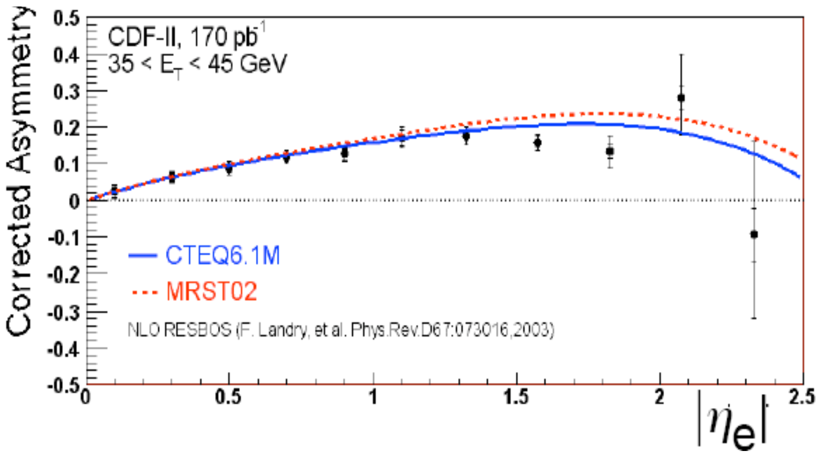

Constraints on the d/u ratio.

Reasonable agreement with e.g. the H1 and the CTEQ fit…

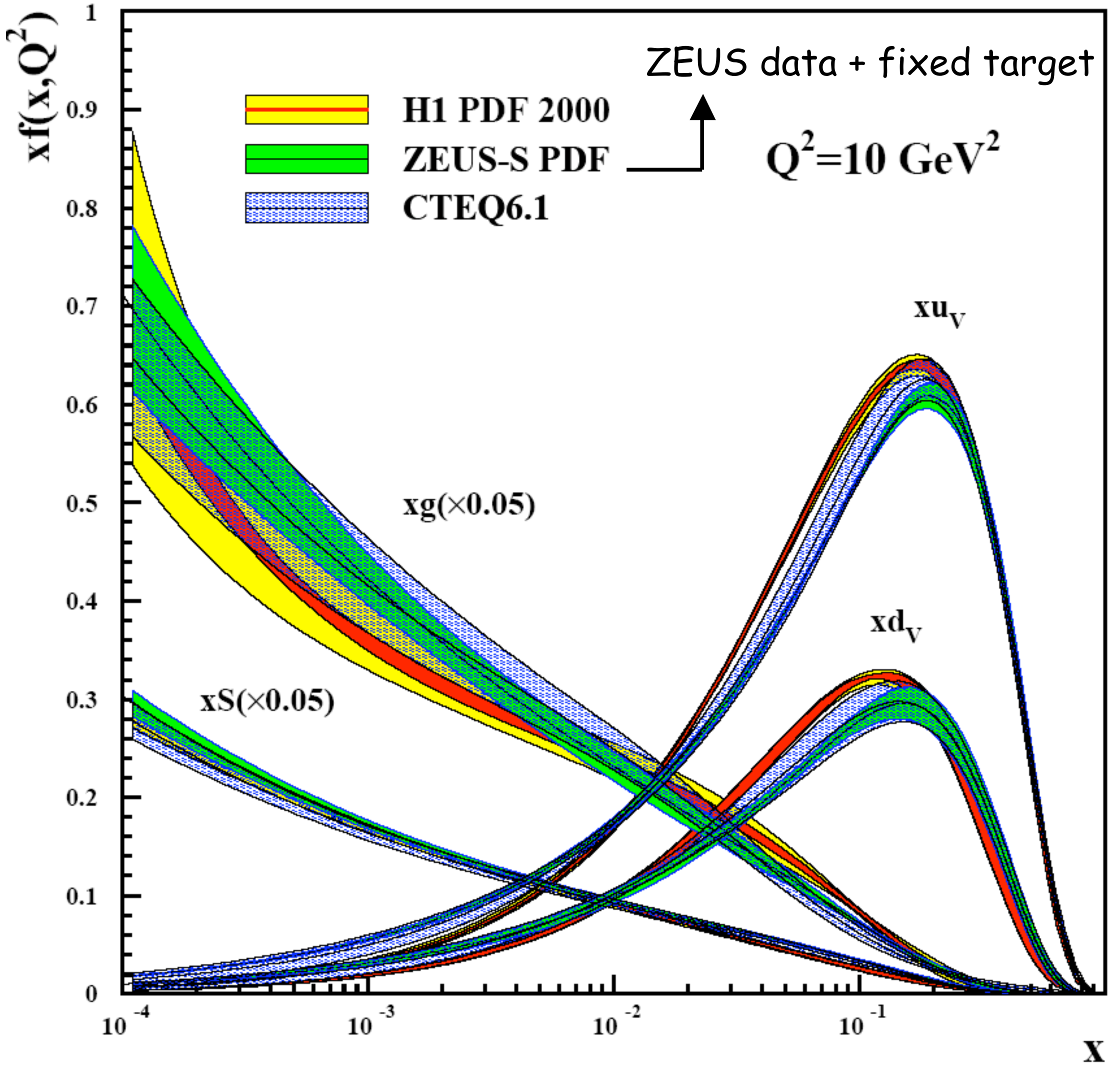

Differences however that are not embedded in the error bands, esp. for the valence distributions.

Sensitivity to those has a different origin in the H1 and ZEUS fits :

- H1 : uses W & Z to do the flavor separation
- ZEUS : this comes mainly from μp vs. μd and xF3 measured in fixed target experiments.

Uncertainties on parton densities

Old days : take many pdf fits available on the market and compare them…

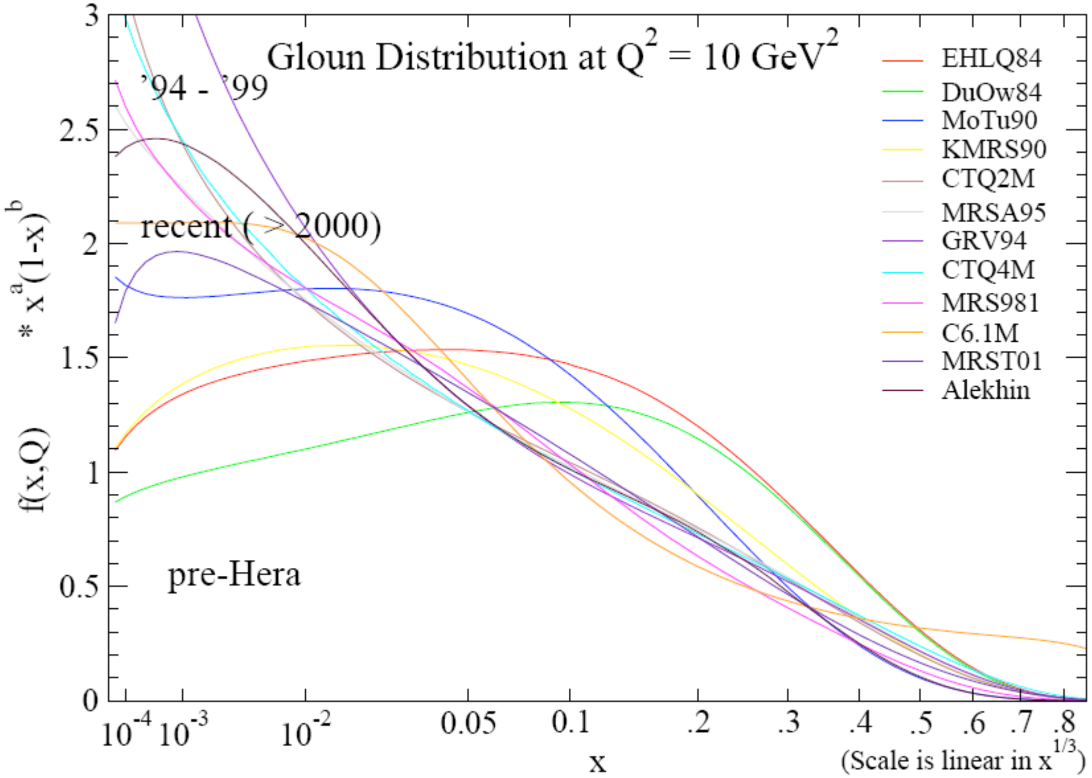

Not correct :

- no statistical interpretation of the spread (what is then the "1σ" error band on xg(x) or on a related quantity ?)
- the envelope is even not "representative" of the true uncertainty, since all fits share the same data – with their exp. errors.

Note : the plot also shows that one should not extrapolate a fit beyond the region where there are data… Before HERA, there was no information on xg(x) at low x !

A lot of work done over the past ~ 5 years to assess rigorously the pdf uncertainties.

The parameters of the QCD fit (i.e. which describe a given set of pdfs at a given starting scale) are usually obtained by minimizing a χ^2 function.

Simplest : if statistical errors >> systematic errors :

$$\chi^2 = \sum_i \frac{(d_i - t_i(p))^2}{\alpha_i^2}$$

Sum runs over data points d_i
α_i = error on d_i
$t_i(p)$ = theoretical prediction for parameters (p)
$\partial\chi^2 / \partial p_k = 0$ gives the parameters p_k

Hessian matrix : $$H_{ij} = \frac{1}{2}\left(\frac{\partial^2\chi^2}{\partial p_i \partial p_j}\right)$$

For a quantity F (a density, or a cross-section) which vary approximately linearly with p around the minimum, the standard formula for error propagation gives :

$$\sigma_F^2 = \Delta\chi^2 \times \sum_{ij} \frac{\partial F}{\partial p_i} H_{ij}^{-1} \frac{\partial F}{\partial p_j}$$

1σ error on F corresponds to $\Delta\chi^2 = 1$.

PDF uncertainties : bottomline

The general trend of PDF uncertainties is that

The u quark is much better known than the d quark

The valence quarks are much better known than the gluon at high-x

The valence quarks are poorly known at small-x but they are not important for physics in this region

The sea and the gluon are well known at medium x

The sea is poorly known at high-x, but the valence quarks are more important in this region

The gluon is poorly known at high-x

Keep in mind that the uncertainties given by the pdf sets do not include those due to :

- Dataset choice and cuts
- parameterization choice
- theory (treatment of HQ, target mass / nuclear corrections, higher twists, low x effects…)

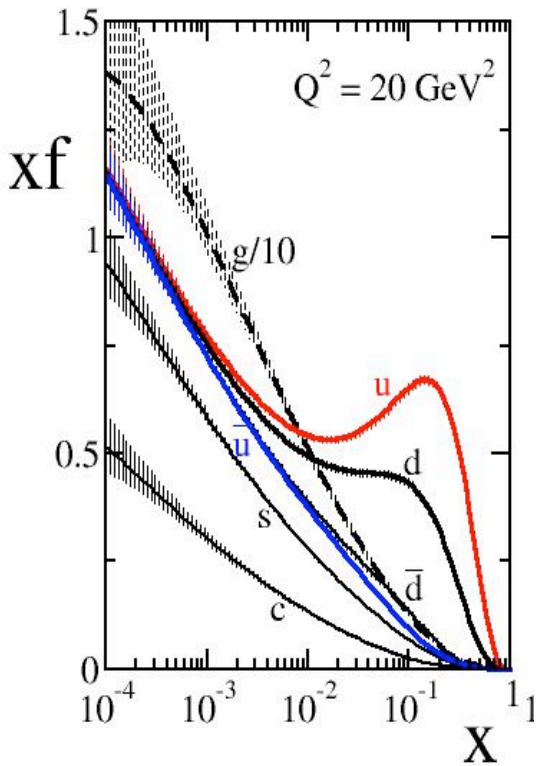

From HERA to LHC

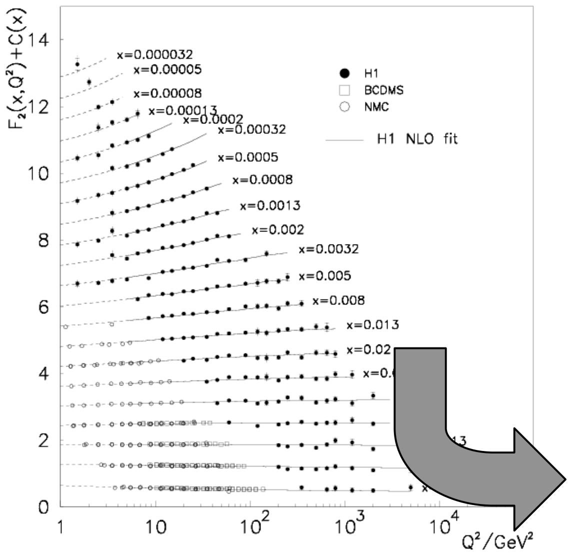

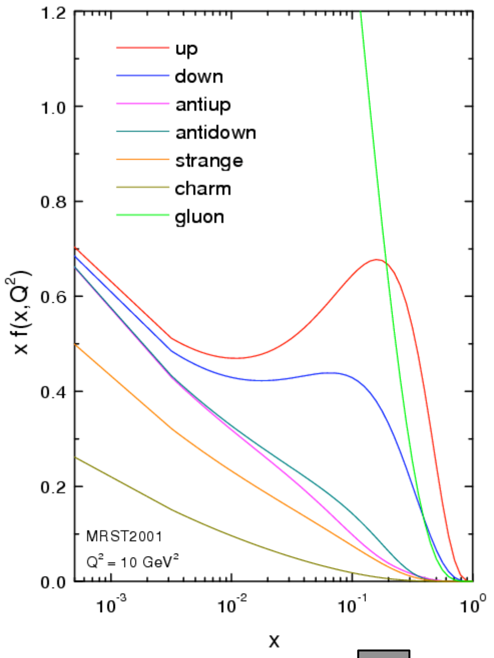

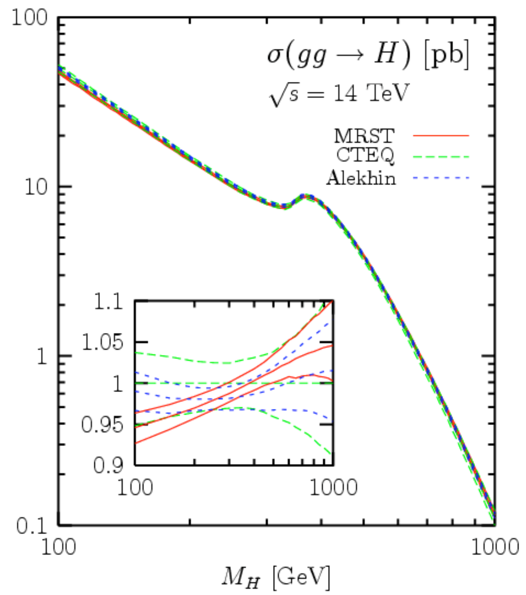

Evolution of the PDFs

momentum fractions x_1 and x_2 determined by mass and rapidity of **X**

$$Q^2 = m_x^2 = s x_1 x_2$$

$$y = \frac{1}{2}\ln\frac{x_1}{x_2}$$

x dependence of $f(x,Q^2)$ determined by fit to data, Q^2 dependence determined by **DGLAP** equations:

$$\frac{\partial q_i(x,Q^2)}{\partial \log Q^2} = \frac{\alpha_S}{2\pi}\int_x^1 \frac{dy}{y}\Big\{P_{q_iq_j}(y,\alpha_S)\, q_j(\frac{x}{y},Q^2) + P_{q_ig}(y,\alpha_S)\, g(\frac{x}{y},Q^2)\Big\}$$

$$\frac{\partial g(x,Q^2)}{\partial \log Q^2} = \frac{\alpha_S}{2\pi}\int_x^1 \frac{dy}{y}\Big\{P_{gq_j}(y,\alpha_S)\, q_j(\frac{x}{y},Q^2) + P_{gg}(y,\alpha_S)\, g(\frac{x}{y},Q^2)\Big\}$$

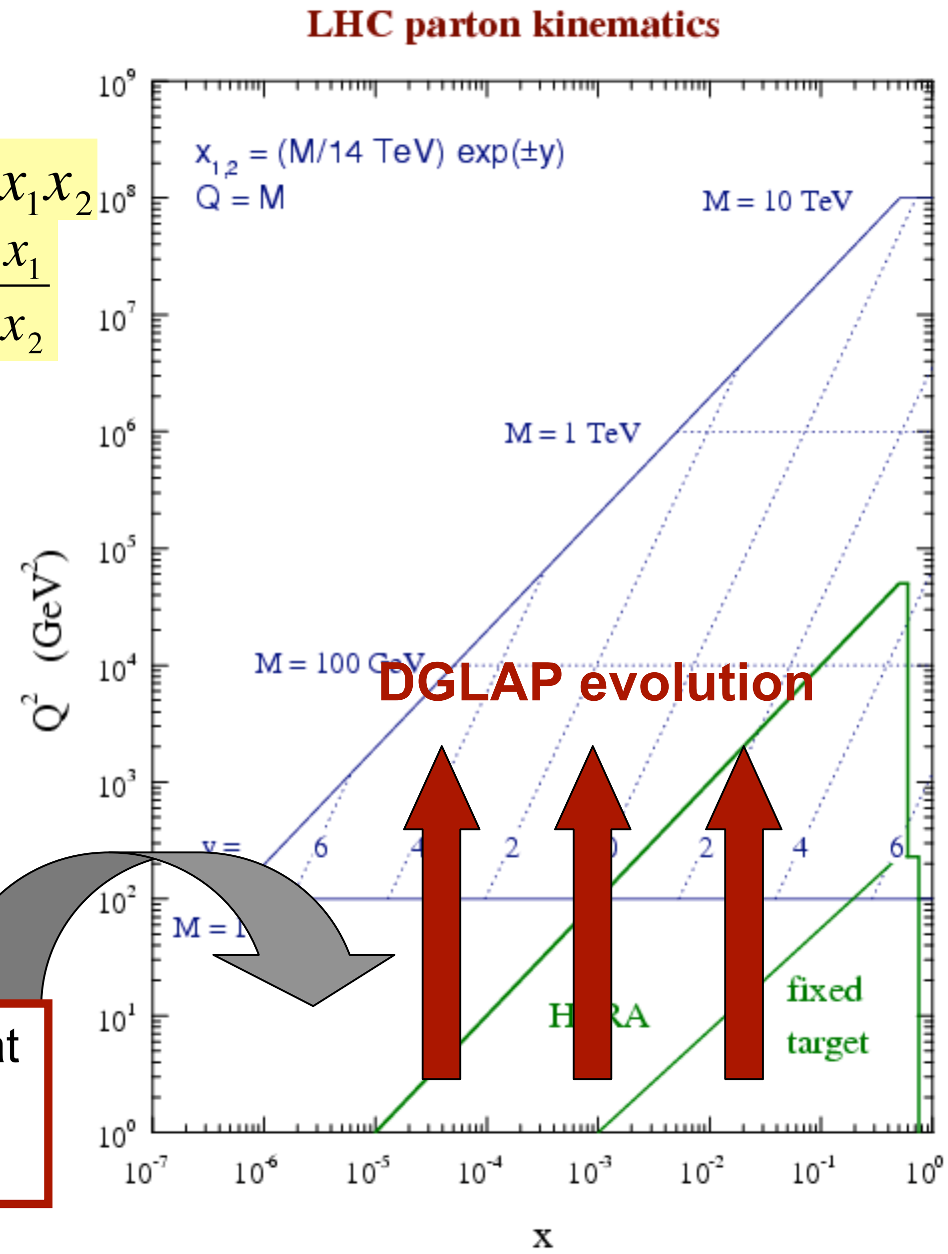

Q. is NLO (or NNLO) DGLAP sufficient at small x? Are higher-orders $\sim \alpha_S^n \log^m x$ important?

J. Stirling

W and Z production at the LHC

Thought of as “standard candles”. Do we know them so well ?

Small theoretical uncertainty :

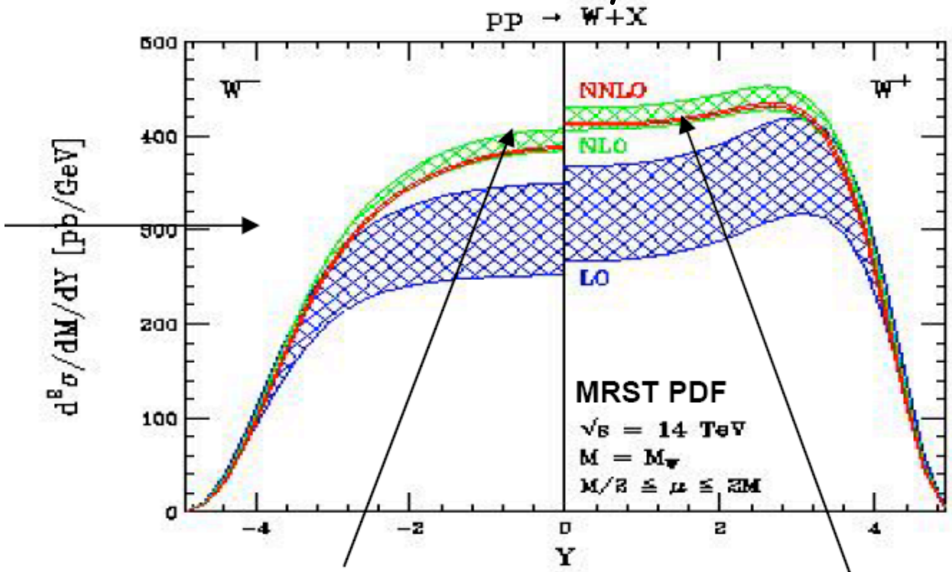

NNLO corrections small ~ few%
NNLO residual scale dependence < 1%

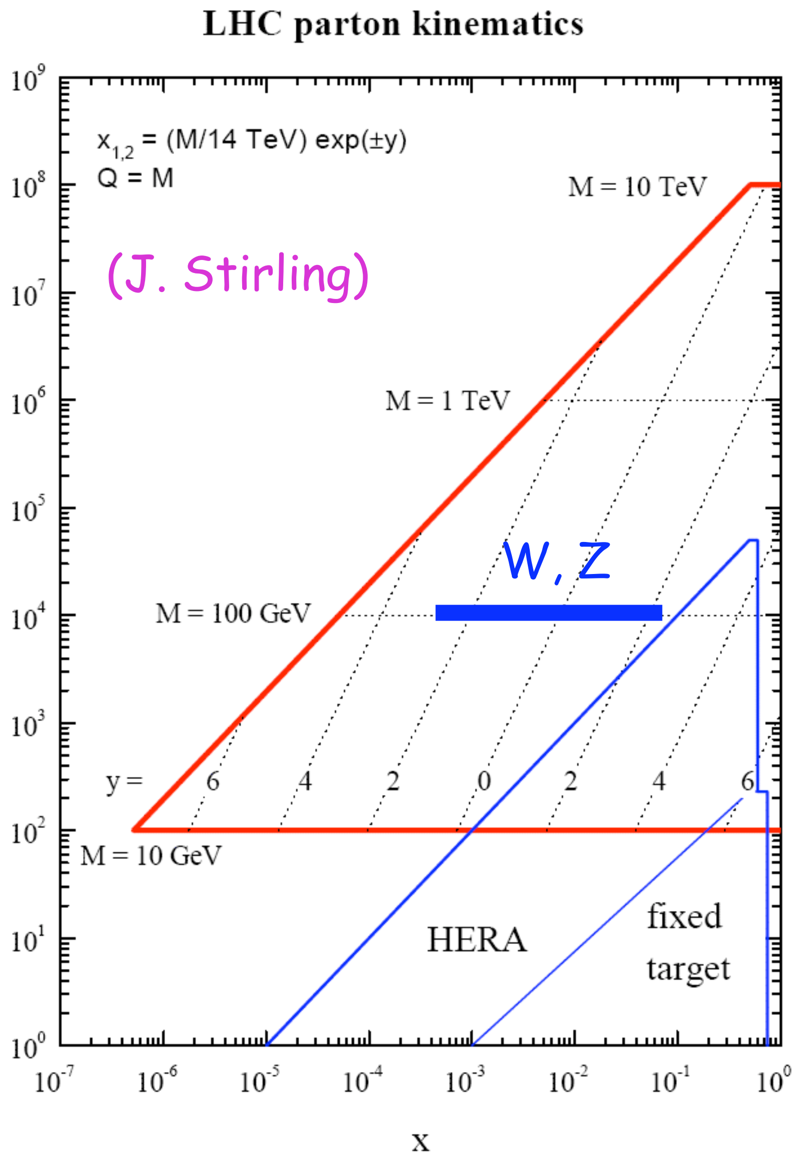

But W & Z at the LHC : <x> ~ 7.10^{-3} at central rapidity. In the measurable range, x between ~ 5.10^{-4} and ~ 5.10^{-2}
i.e. not in the valence region.
i.e. not in the region where quarks are best known…

Uncertainty obtained when using all pdf sets within a given group : usually ~ 5%.

Note by how much the HERA data have allowed this uncertainty to be reduced. This is due to the much improved precision on the gluon density at $x \sim 10^{-3}$.

But the central values from different groups differ by more than 5%, typically 8%.

And $\sigma(W)$ has moved by ~ 8% when going from CTEQ6.1 to CTEQ6.5, mainly due to the new theo. treatment of heavy quarks !

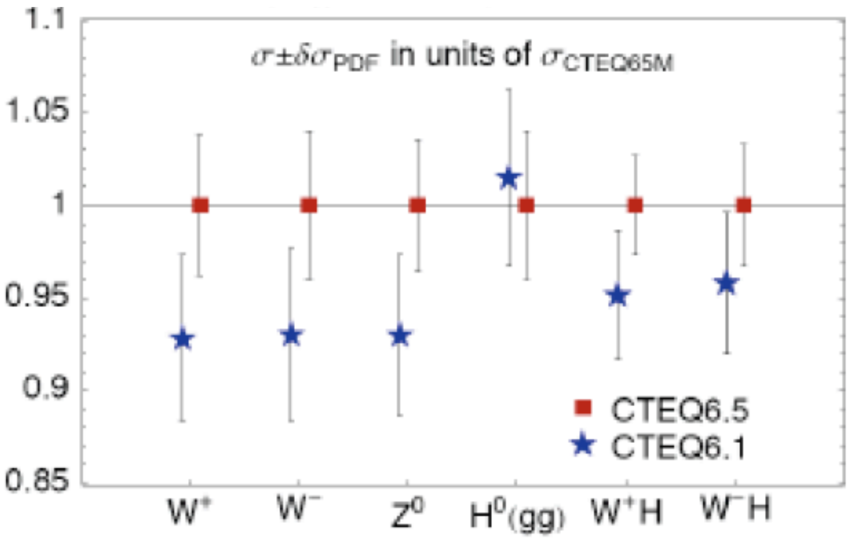

W.K. Tung et al., hep-ph/0611254

i.e. not precise enough yet to be used as a lumi. monitor…

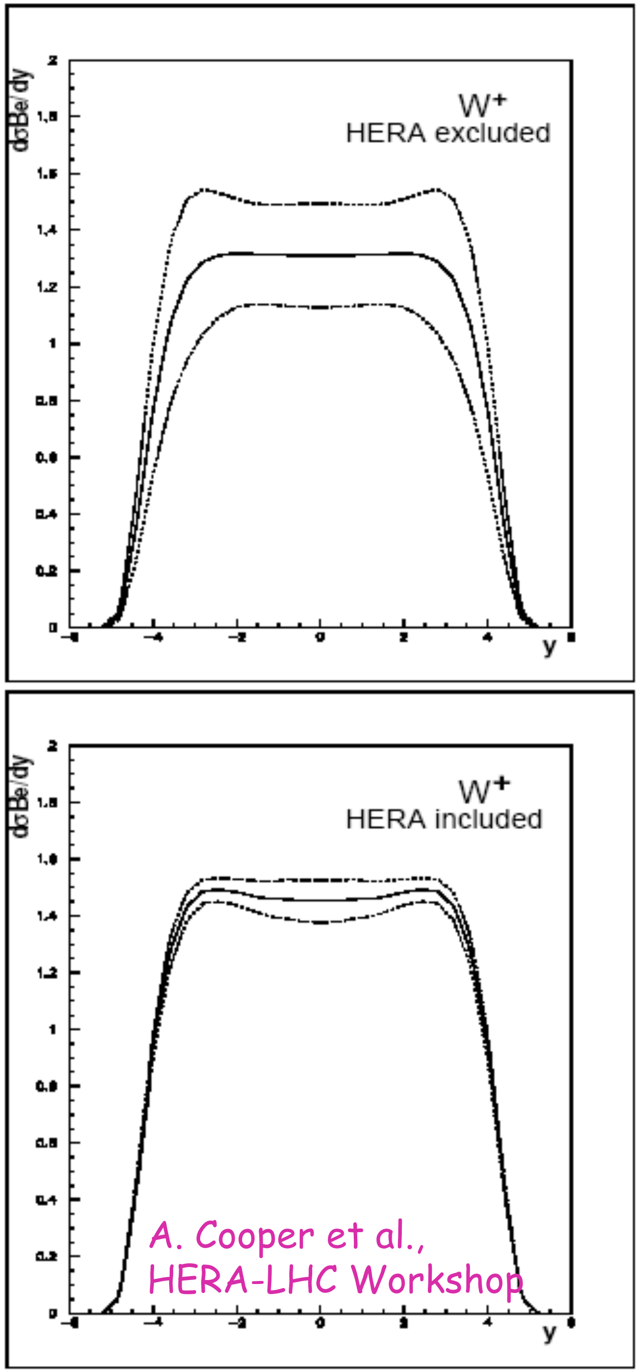

A. Cooper et al., HERA-LHC Workshop

How do pdf uncertainties affect the Higgs discovery potential ?

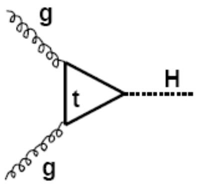

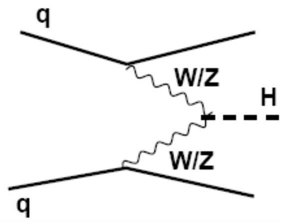

A. Djouadi & S. Ferrag, PLB 586 (2004) 345.

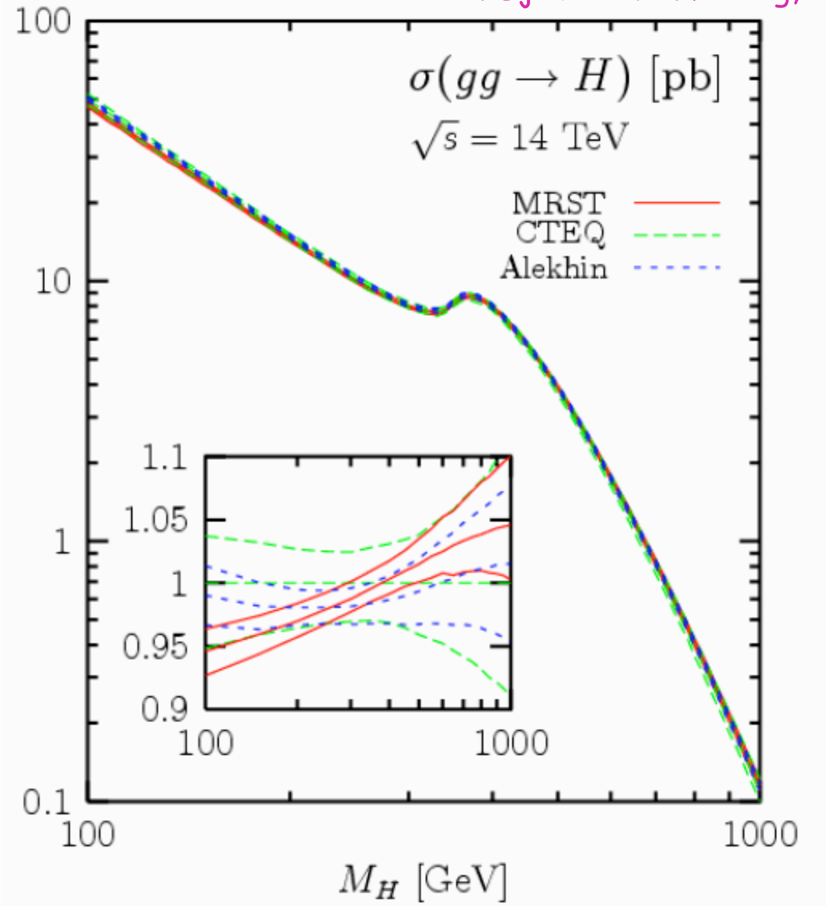

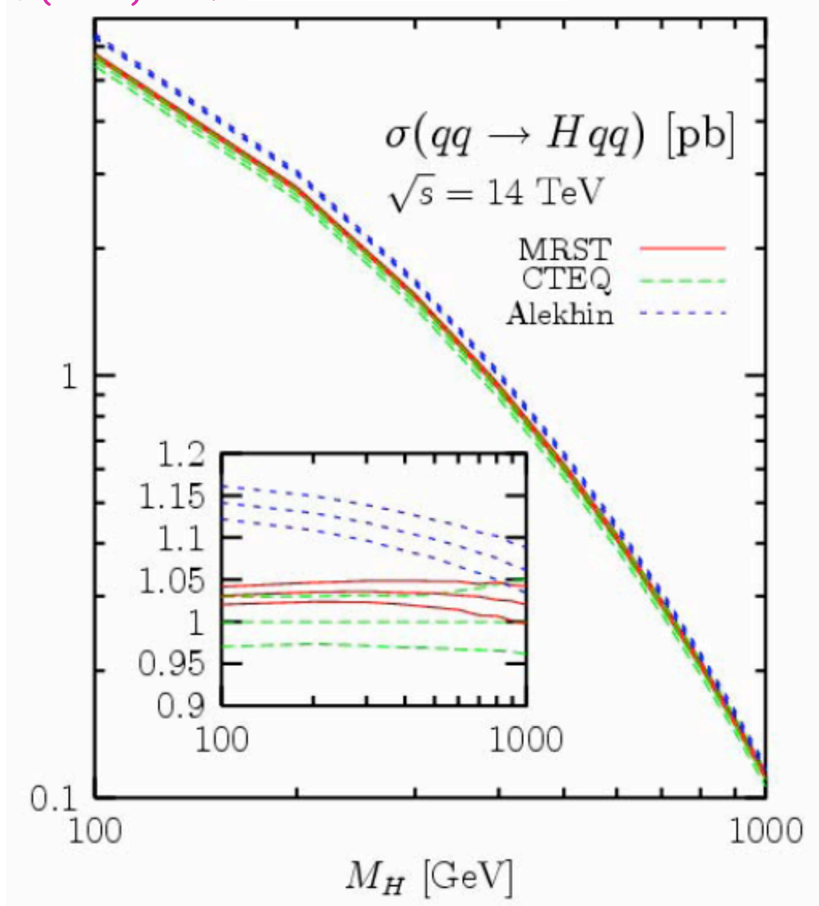

Not too bad… Cross-sections are known to within ~ 10%. Same for backgrounds.

Limited knowledge of proton structure might "fake" a discovery…

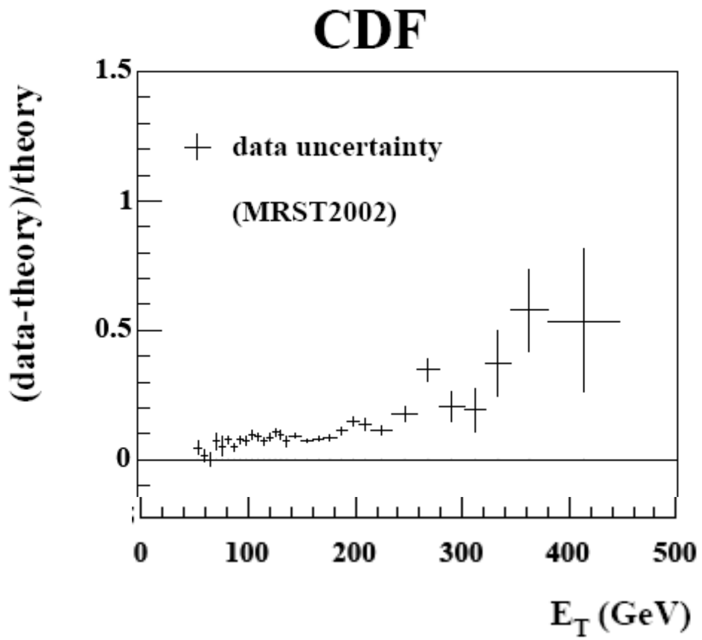

Recall the excess of high Et jets reported by CDF in 1995…

was initially interpreted as new physics (quark substructure ?) until it was realized that a higher gluon density at high x could accommodate these data, while remaining in agreement with other data.

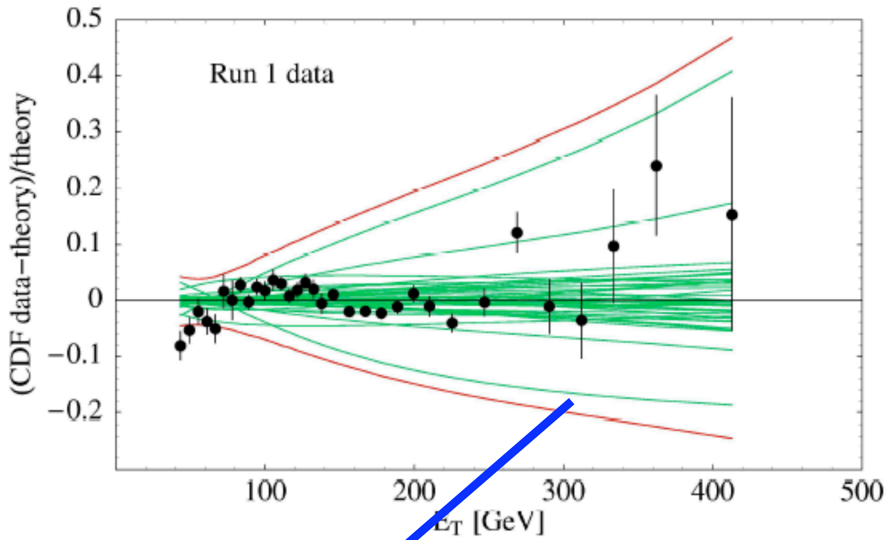

Now we have pdf uncertainties, i.e. better handle even if there might still be some "uncertainty" on these uncertainty bands…

The Tevatron jet data are in reasonable agreement with global fits today, taking into account the large unc. due to the unc. on the high-x gluon.

This eigenvector is dominated by the high-x gluon parameter.

Limited knowledge of proton structure might limit the discovery potential

Some NP models predict deviations in dijet mass spectrum at high mass.
Example : qqqq contact interactions, some extra-dimension models.

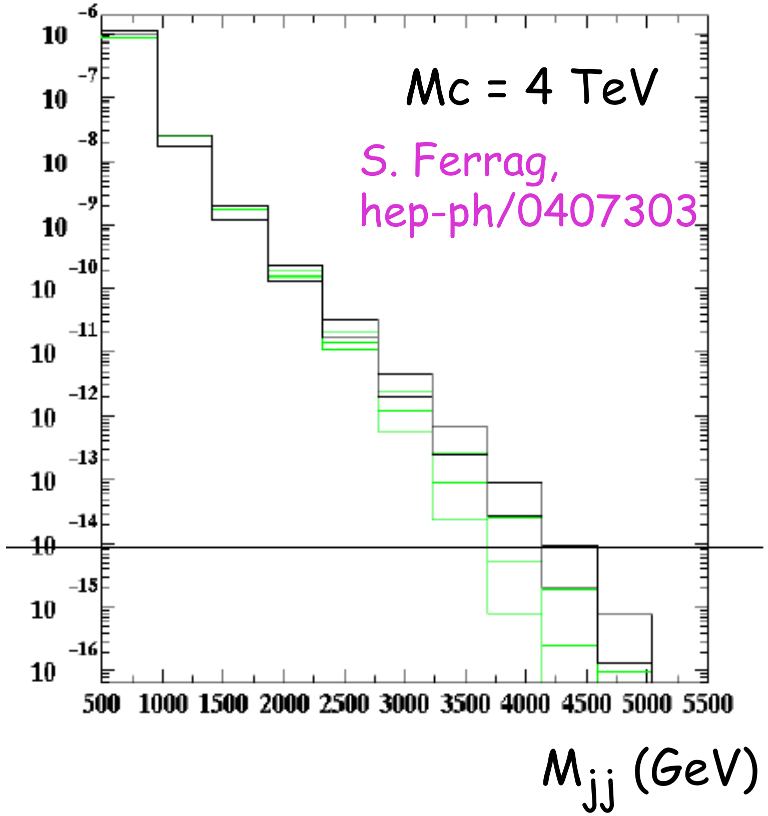

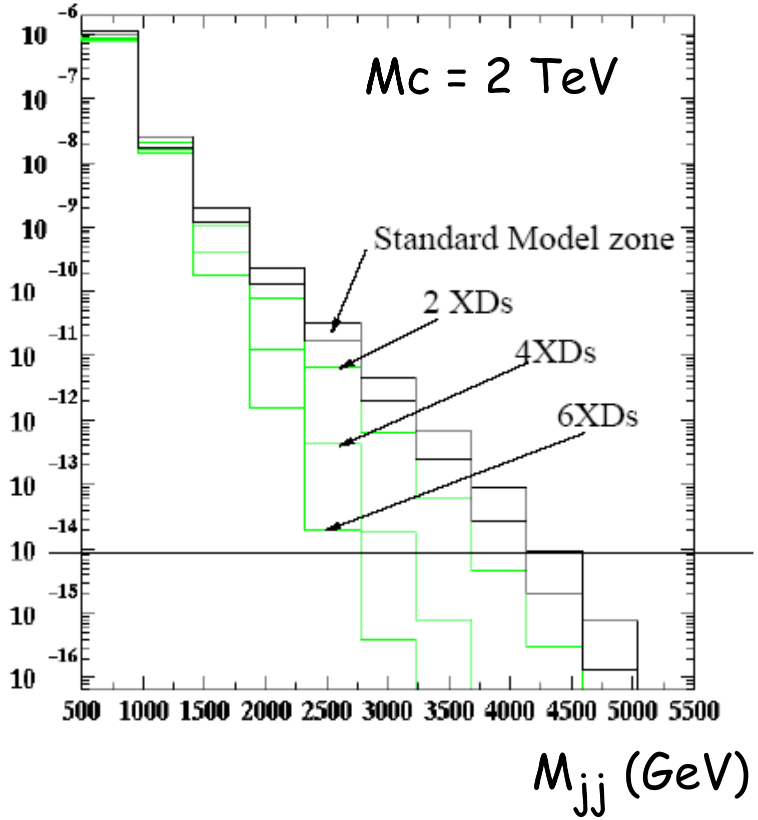

Due to pdf uncertainties, sensitivity to compactification scales reduced from 6 TeV to 2 TeV in this example.
This is due again to the large uncertainty on the high-x gluon.

Improvement of our pdf knowledge from LHC data : jet production

So far our most stringent constraints on the gluon density at high x come from inclusive jet data at the Tevatron.
What about inclusive jet at the LHC ?

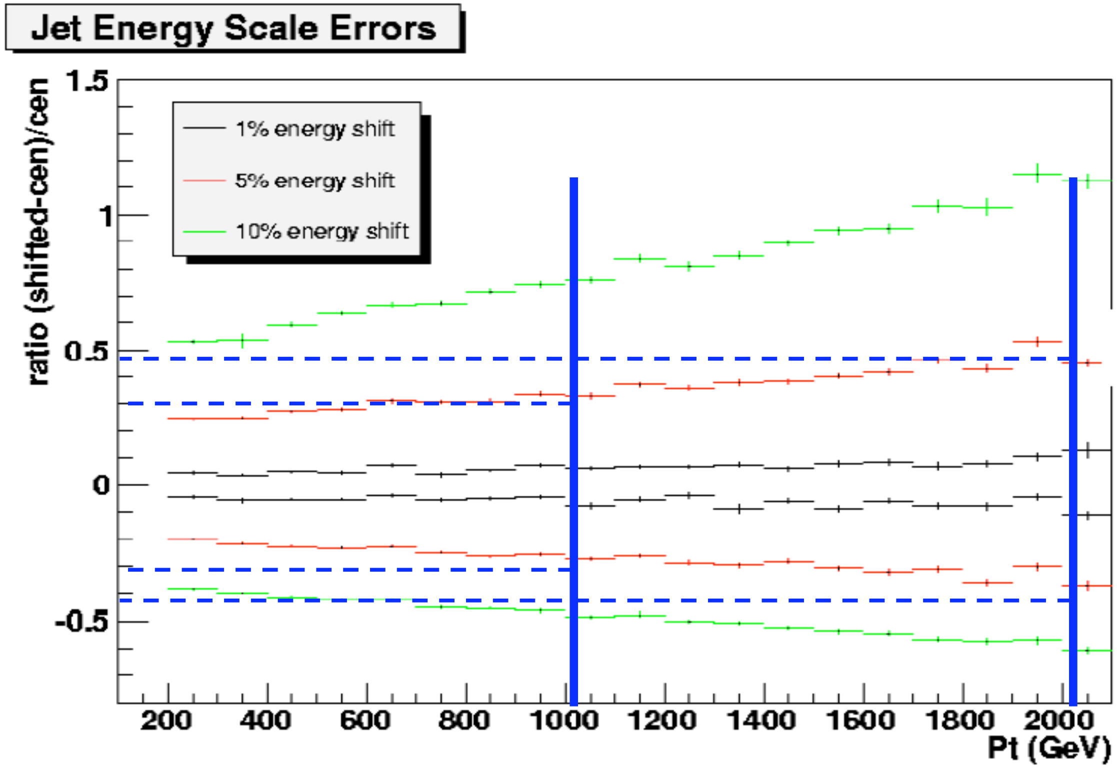

10% JES → 60% on σ

5% JES → 30% on σ

1% JES → 6% on σ

At 1 TeV (2 TeV) , in the range 1 < eta < 2, the pdf uncertainty on the inclusive jet cross-section is about 15% (25%). This means that one must control the jet energy scale very well to bring significant pdf constraints !

Soon we will see the first real events

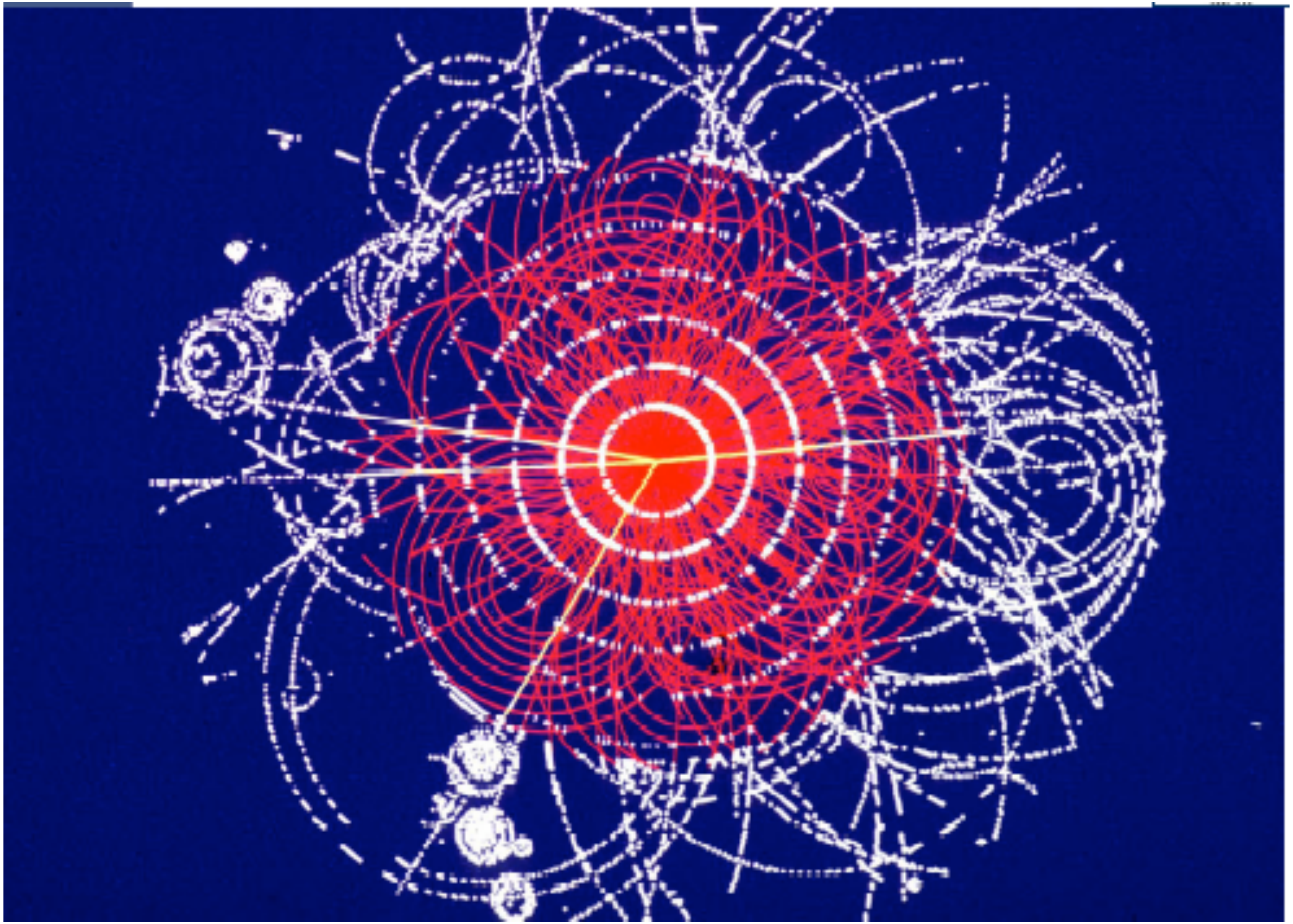

Deep-inelastic scattering

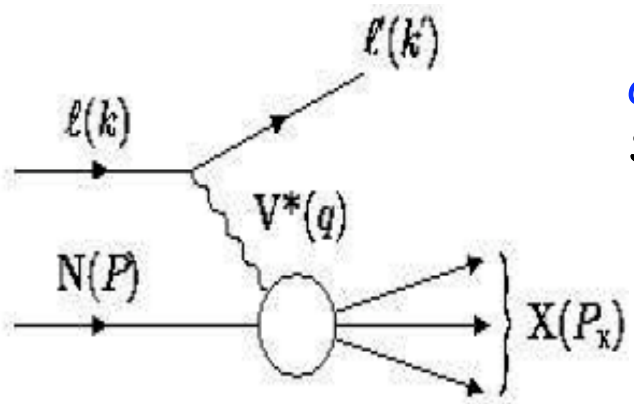

$q = k - k'$, $Q^2 = -q^2$ squared momentum transfer
$S = (p + k)^2$ square of center of mass energy

$$x_{Bjorken} = \frac{Q^2}{2(P.q)}$$

$Q^2 = x\, y\, S$

V can be :
- a γ or Z : Neutral Current DIS
- a W : Charged Current DIS

$$y = \frac{(P.q)}{(P.k)}$$

"inelasticity variable"
In nucleon rest-frame,
$y = (E - E')\, /\, E$

Cross-section depends on 2 variables, generally choose (x, Q^2).

W^2 = squared mass of the hadronic system = $(P + q)^2$ $$W^2 = Q^2 \frac{1-x}{x}$$

Partonic interpretation: $x_{Bjorken}$ is the fraction of the nucleon longitudinal momentum taken by the "struck" quark, in the frame of infinite momentum for the nucleon (light cone variables : $p^+(quark) = x\, P^+(N)$)

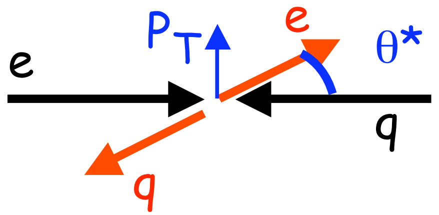

$$y = \frac{1 - \cos\theta^*}{2}$$

$P_T^2 = (1 - y)\, Q^2$

Electron-proton elastic scattering (2)

Since $q_\mu K^{\mu\nu} = 0$ (Exercise)

$$K_4 = \frac{(Mc)^2}{q^2} K_1 + \frac{1}{4} K_2 \quad \text{and} \quad K_5 = \frac{1}{2} K_2$$

$$K^{\mu\nu}_{\text{proton}} = K_1\left(-g^{\mu\nu} + \frac{q^\mu q^\nu}{q^2}\right) + \frac{K_2}{(Mc)^2}\left(p^\mu + \frac{1}{2} q^\mu\right)\left(p^\nu + \frac{1}{2} q^\nu\right)$$

$$\langle|\mathcal{M}|^2\rangle = \left(\frac{2g_e^2}{q^2}\right)^2 \left\{K_1[(p_1 \cdot p_3) - 2(mc)^2] + K_2\left[\frac{(p_1 \cdot p)(p_3 \cdot p)}{(Mc)^2} + \frac{q^2}{4}\right]\right\}$$

Going to the proton rest frame p=(0,0,0,M) and assuming E,E' (electron energies) >>m

Electron-proton elastic scattering

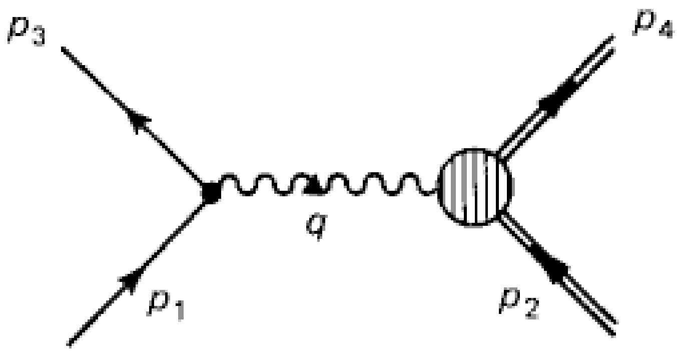

$$L^{\mu\nu}_{\text{electron}} = 2\{p_1^\mu p_3^\nu + p_1^\nu p_3^\mu + g^{\mu\nu}[(mc)^2 - (p_1 \cdot p_3)]\}$$

$$\langle|\mathcal{M}|^2\rangle = \frac{g_e^4}{q^4} L^{\mu\nu}_{\text{electron}} K_{\mu\nu\ \text{proton}}$$

$q=p_4-p_2$; $p\equiv p_2$

$$K^{\mu\nu}_{\text{proton}} = -K_1 g^{\mu\nu} + \frac{K_2}{(Mc)^2} p^\mu p^\nu + \frac{K_4}{(Mc)^2} q^\mu q^\nu + \frac{K_5}{(Mc)^2}(p^\mu q^\nu + p^\nu q^\mu)$$

Where the K_i are function of q^2, the only scalar variable of the problem

($p^2=M^2$ and $pq=-q^2/2$)

Electron-proton elastic scattering (3)

$$\langle |\mathcal{M}|^2 \rangle = \frac{g_e^4 c^2}{4EE' \sin^4(\theta/2)} \left(2K_1 \sin^2\frac{\theta}{2} + K_2 \cos^2\frac{\theta}{2} \right)$$

with
$$E' = \frac{E}{1 + (2E/Mc^2)\sin^2(\theta/2)}$$

$$\frac{d\sigma}{d\Omega} = \left(\frac{\alpha\hbar}{4ME\sin^2(\theta/2)} \right)^2 \frac{E'}{E} \left[2K_1 \sin^2(\theta/2) + K_2 \cos^2(\theta/2) \right]$$

(Rosenbluth)

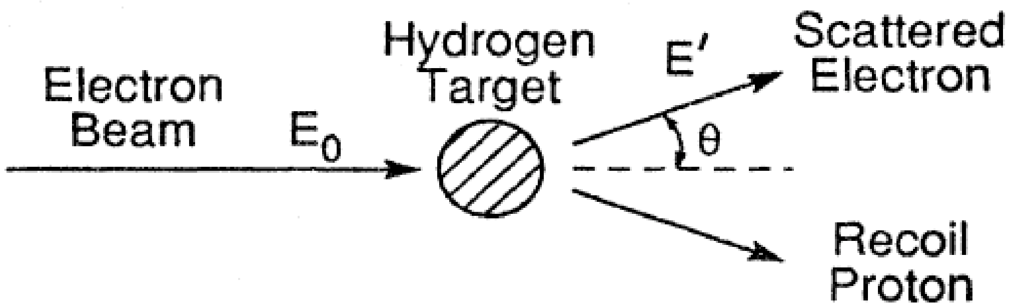

$$Q^2 = 4E_0 E' \sin^2\theta/2$$

$Q^2 \equiv q^2$

$\hbar c$~200 MeV. Fermi

Electron-proton elastic scattering (4)

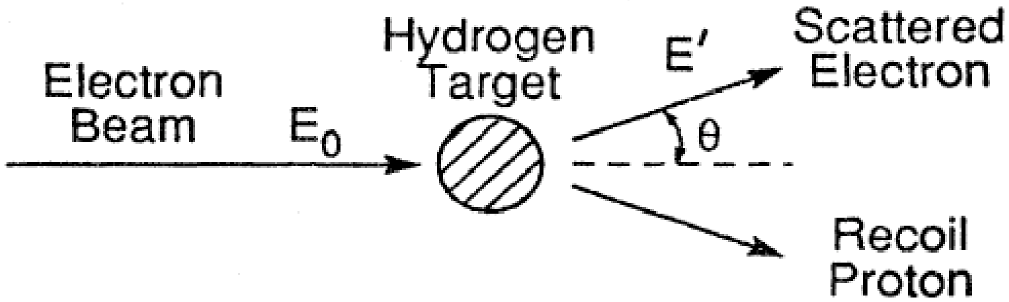

$$Q^2 = 4E_0 E' \sin^2\theta/2$$

$Q^2 \equiv q^2$

$$\frac{d\sigma}{d\Omega} = \frac{\alpha^2}{4E_0^2 \sin^4\theta/2} \cos^2(\theta/2) \frac{E'}{E_0} \left[\frac{G_E^2 + \tau G_M^2}{1+\tau} + 2\tau G_M^2 \tan^2\theta/2 \right]$$

$$\frac{d\sigma}{d\Omega}(E) = \sigma_M(E) \left| \frac{E'}{E} \right| \left[\frac{G_{Ep}^2(q^2) + \tau G_{Mp}^2(q^2)}{1+\tau} + 2\tau G_{Mp}^2 \tan^2(\theta/2) \right]$$

$$\tau = Q^2/4M^2$$

$$G_E = G_E(Q^2)\ , \quad G_M = G_M(Q^2)\ ,$$

$$G_E(0) = 1\ , \quad G_M(0) = \mu_p\ ,$$

σ(arb.un.), Escat and Q2 as a function of st2

Ebeam=0.5 GeV

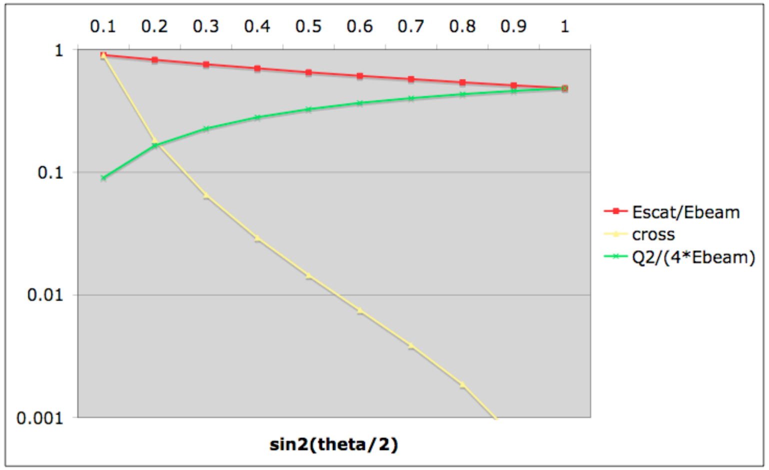

Ebeam= 2 GeV

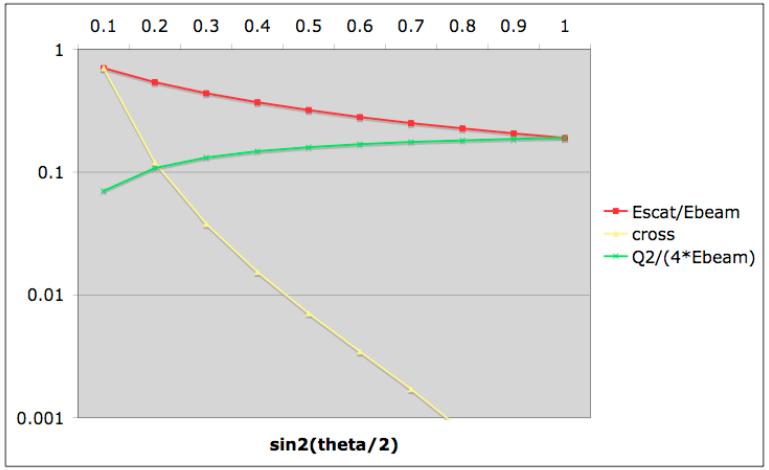

Ebeam=10 GeV

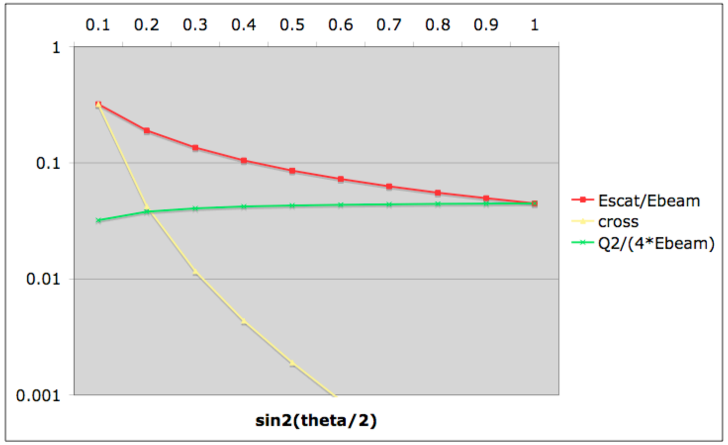

Ebeam=20 GeV

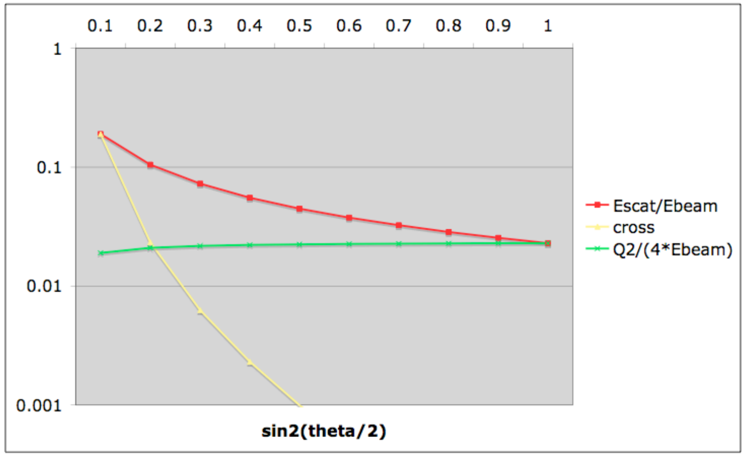

Q2(Gev2) as a function of Ebeam(GeV)

$\sin^2(\theta/2)=0.05$

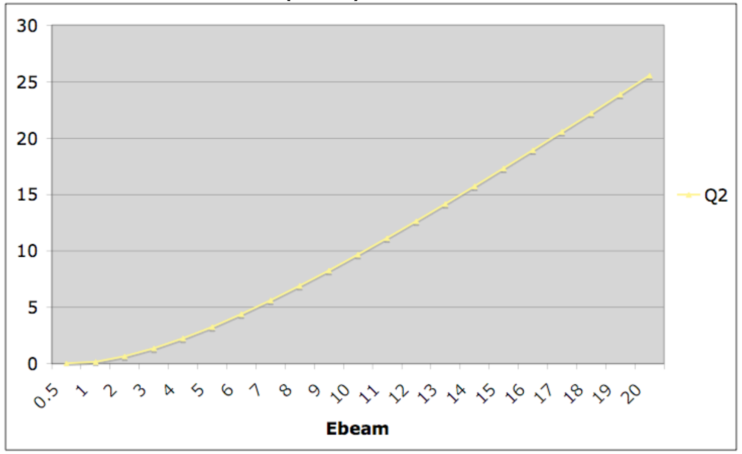

$\sin^2(\theta/2)=0.1$

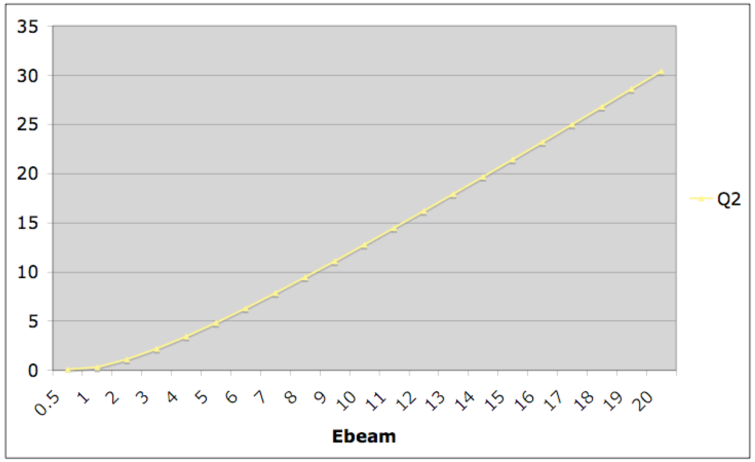

$\sin^2(\theta/2)=0.2$

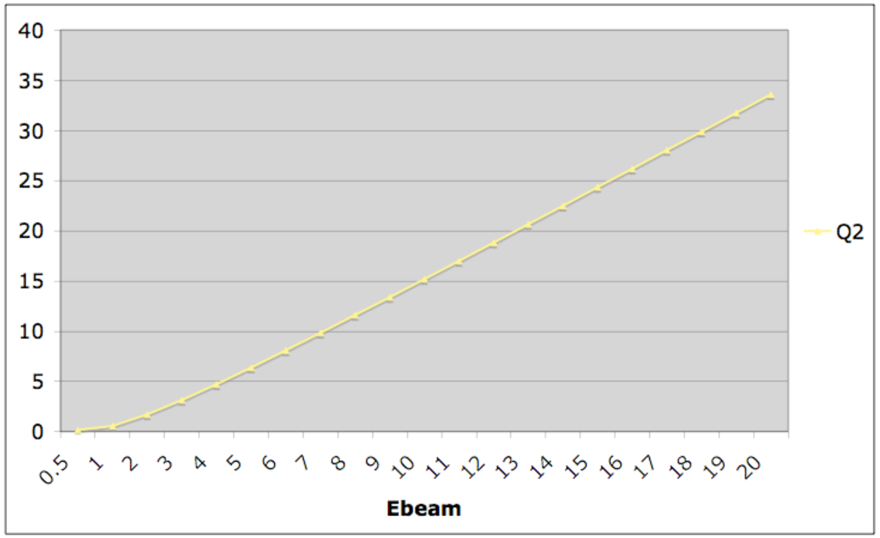

Inelastic e-p and photoproduction (1)

The differential cross section for inelastic electron scattering is related to the total cross section for absorption of transverse (σ_T) and longitudinal (σ_L) virtual photons

$$\frac{d^2\sigma}{d\Omega\, dE'}(E,E',\theta)=\Gamma[\sigma_T(\nu,q^2)+\epsilon\sigma_L(\nu,q^2)]$$

where

$$\Gamma=\frac{\alpha}{4\pi^2}\frac{KE'}{q^2E}\left[\frac{2}{1-\epsilon}\right],$$

$$\epsilon=[1+2(1+\nu^2/q^2)\tan^2(\theta/2)]^{-1},$$

and

$$K=(W^2-M^2)/(2M).$$

The cross sections are related to the structure functions W by

$$W_1(\nu,q^2)=\frac{K}{4\pi^2\alpha}\sigma_T(\nu,q^2),$$

$$W_2(\nu,q^2)=\frac{K}{4\pi^2\alpha}\left[\frac{q^2}{q^2+\nu^2}\right][\sigma_T(\nu,q^2)+\sigma_L(\nu,q^2)].$$

Inelastic e-p and photoproduction (2)

Conversely, the ratio R of the cross sections is related to the structure functions via

$$R(\nu,q_2)\equiv\sigma_L/\sigma_T=(W_2/W_1)(1+\nu^2/q^2)-1 \ .$$

And the structure functions can be related to the measured bi-differential cross section and R

$$W_1=\frac{1}{\sigma_M}\frac{d^2\sigma}{d\Omega\, dE'}\left[(1+R)\left[\frac{q^2}{q^2+\nu^2}\right]+2\tan^2(\theta/2)\right]^{-1},$$

$$W_2=\frac{1}{\sigma_M}\frac{d^2\sigma}{d\Omega\, dE'}\left[1+\left[\frac{2}{1+R}\right]\right.$$

$$\left.\times\left[\frac{q^2+\nu^2}{q^2}\right]\tan^2(\theta/2)\right]^{-1}. \tag{7}$$

What could explain a sea asymmetry ?

- Experimentally : $\bar{d} - \bar{u} > 0.$

  - from DY
  - NMC observed before a violation of the Gottfried sum rule :

    $\int F_2^p - F_2^n = 1/3 \quad (- 2/3 \int x(\bar{d} - \bar{u}))$

Several models… e.g. fluctuation of p in a meson + baryon pair :

(1) $p(uud) \quad \rightarrow \quad \Delta^{++}(uuu) + \pi^{-}(\bar{u}d)$

(2) $p(uud) \quad \rightarrow \quad n(udd) + \pi^{+}(\bar{d}u)$

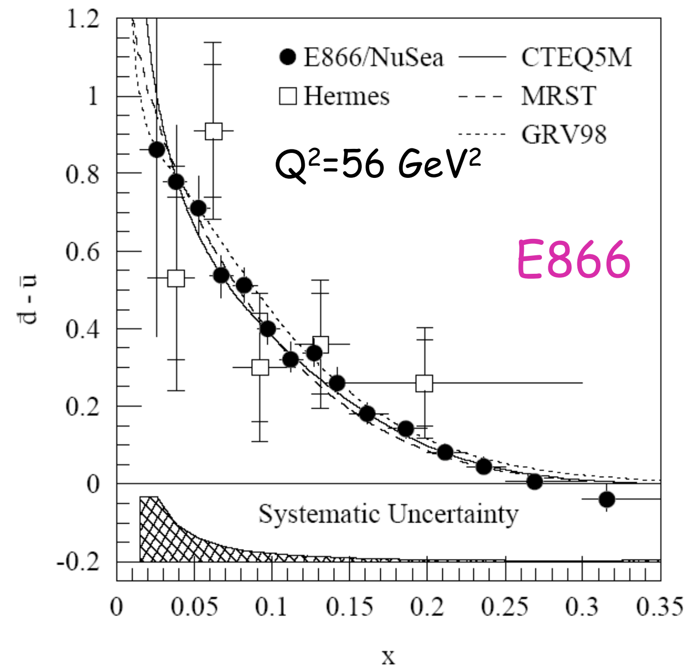

(1) is kinematically disfavored w.r.t. (2), hence the creation of $u\bar{u}$ pair is disfavored.

- strange sea : $\bar{s} = 0.5 (\bar{u} + \bar{d})$? Global fits tell this does not hold.
  - Mass effects
  - indications that $s \neq \bar{s}$. Could be explained by

    $p(uud) \rightarrow \Lambda(uds) + K^{+}(u\bar{s})$

    Λ carries most of the proton momentum hence $s(x) > \bar{s}(x)$ at “high” x.

Experimentally : NuTev, CCFR : $W^+ \, s \rightarrow c \rightarrow \mu^+ X$

$W^- \, \bar{s} \rightarrow \bar{c} \rightarrow \mu^- X$

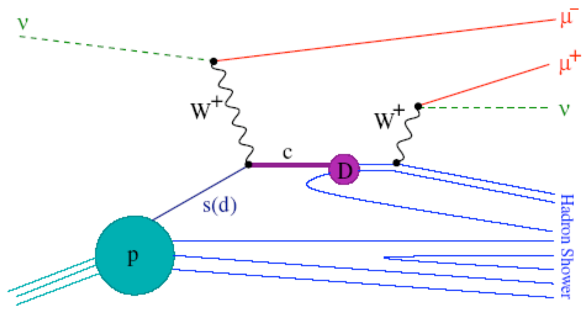

Decomposition of the total Jet Cross section

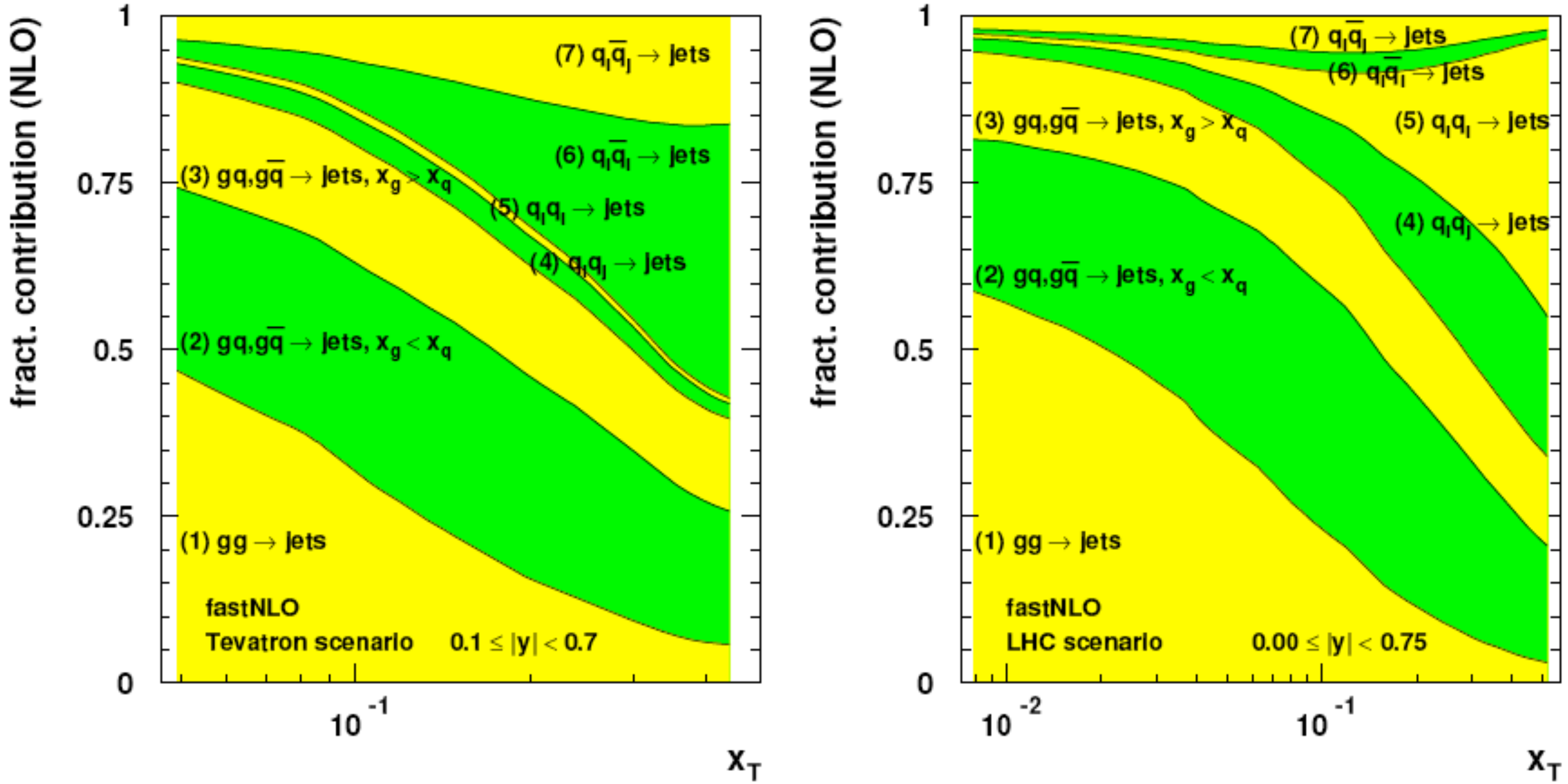

Decomposition of the total jet cross sections into partonic processes as a function of $x_T = 2p_T/\mathrm{sqrt(s)}$